

Coordinated Voltage Control in Electric Power Systems

Mats Larsson



LUND UNIVERSITY

Doctoral Dissertation
Department of Industrial Electrical Engineering
and Automation

Department of
Industrial Electrical Engineering and Automation
Lund Institute of Technology
Lund University
P.O. Box 118
SE-221 00 LUND
SWEDEN

<http://www.iea.lth.se>

ISBN 91-88934-17-9
CODEN:LUTEDX/(TEIE-1025)/1-203/(2000)

© Mats Larsson, 2000
Printed in Sweden by Universitetstryckeriet
Lund University
Lund 2000

Abstract

This thesis deals with various aspects of coordinated voltage control in electric power systems. It consists of an introduction and six papers. The introduction contains a summary of the thesis and tutorials on voltage control and the search methods that have been applied.

The first part deals with the coordination of cascaded tap changers in radial distribution feeders. Poor coordination causes unnecessary operations of the tap changers and consequently unnecessary wear as well as poor voltage quality. A tuning rule for the conventional (local) controllers as well as two new (centralized) schemes are proposed: firstly, an optimal controller based on on-line optimization and secondly, a rule based controller based on a fuzzy inference system. Results from simulations based on load patterns recorded during different seasons indicate that when tuned according to our recommendation, tap changers perform some 10 % fewer operations compared to when the present tuning is in use. The additional reductions with the fuzzy-rule based and optimal controllers are some 36 % and 45 %, respectively. A prototype of the fuzzy-rule based controller has been installed and successfully tested in a distribution feeder in the south of Sweden. The prototype was also used to validate the simulation results presented in the papers.

Another control interaction problem studied is a phenomenon of limit cycles due to load-tap changer interaction. The role of the OLTC deadband in creating a limit cycle phenomenon is addressed. Analytical insights into the behaviour of power systems with continuous and discrete tap models are given using eigenvalue analysis, the describing function method and time simulation. The conditions for occurrence of limit cycles and the identification of key parameters influencing their characteristics are other important aspects of this investigation.

The second part of the thesis describes a coordinated system protection

scheme (SPS) against voltage collapse based on model predictive control. The combinatorial optimization problem that results from the control problem formulation is solved by a search method adapted from the research on artificial intelligence. Using predictions of the system's future behaviour, the SPS optimally coordinates dissimilar and discrete controls such as generator, tap changer and load shedding controls in presence of load dynamics and constraints on controls as well as voltages and currents in the network. The response with the coordinated SPS is compared to a local scheme by simulation of some critical contingencies in the CIGRE Nordic 32 test system. The simulation results indicate that local undervoltage load shedding is near-optimal when coordination with other emergency controls is not necessary. When also other controls such as generator voltage setpoints are considered, the coordinated scheme reduces the amount of load shedding necessary to restore voltage stability by some 35 %. The reduction in the amount of load shed is mainly due to improved utilization of remote generators with excess reactive capacity to spare.

Modelling of power systems has also been addressed. The third part describes a freely available power system library called ObjectStab intended for voltage and transient stability analysis and simulation written in Modelica—a general-purpose object-oriented modelling language. All component models are transparent and can be modified or extended. Power system topology and parameter data are entered in one-line diagram form using a graphical editor. The component library has been validated using comparative simulations with Eurostag.

Acknowledgements

This thesis is a report of my licentiate project on distribution systems (1993–1997) and doctorate project on transmission systems (1998–2001). Over the years, I have had the opportunity to become indebted to many people—at the Department as well as in other places. Thanks to all of you for the enjoyable time I have spent producing this thesis. However, there are some people to whom I am especially grateful.

Gustaf Olsson has been the main supervisor throughout both projects. Despite his busy schedule, he always manages to squeeze in a meeting when there is a need. Thanks to his great engineering intuition, open-mindedness and endless enthusiasm, I have always left those meetings in a happy and illuminated mood. He has co-authored one of the included papers and suggested many improvements to the rest.

Daniel Karlsson has been a great asset during the whole time and has also been my industrial supervisor. Daniel came up with the idea for the licentiate project and besides his co-authoring of two of the included papers, his support, knowledge and contacts have given me plenty of ideas and opportunities.

The included papers are the main part of the thesis. The other co-authors, David J. Hill and Dragana H. Popović, thus also have a large part in the work reported. The opportunity to work with these people gave me a perfect start in the research on voltage stability. David has also organized two research stays at his department at the University of Sydney.

Bo Eliasson, Lars Gertmar, Sture Lindahl, Hans Ottosson, Thomas Pehrson, Jan Rønne-Hansen, György Sárosi and Kenneth Walve have all been part of the project steering committee and provided many interesting comments and suggestions.

Without the support of Sydkraft AB, there could have been no field tests during the work. Daniel Karlsson, who initiated the tests, as well as Curt Lind-

kvist, Alf Larsen, Hans Gjöderum, Lennart Elgemark, Christian Nilsson and Magnus Sommansson were all important assets during these tests. The possibility of these tests has significantly contributed to the credibility of the results of the licentiate project.

The help with proofreading the thesis has been invaluable. Bo Bernhards-son, Sture Lindahl, Gustaf Olsson, Christan Rosén and Olof Samuelsson have all read Part I of the thesis. Their comments and corrections have improved the final product a lot.

Modelling in a new and not completely defined modelling language like Modelica is not always easy. Then it is good to have some experts at hand. Hilding Elmkvist, Sven-Erik Mattsson, Hans Olsson and Hubertus Tummescheit have patiently answered many questions and also helped spread my work to the Modelica-community. Also, Inés Romero Navarro did some early work in her Master's project that were later incorporated in the Modelica library described in this thesis.

Thanks also to Ulf Jeppsson and Morten Hemmingsson, who keep our UNIX system up and running, and Anita Borné, Getachew Darge, Tina Helgeson, Carina Lindström, Lena Somogyi and Olof Strömstedt who have helped out with various practical things around the Department. The sarcasms of my roommate Olof Samuelsson are always a great mood-raiser—thank you for those, and for putting up with mine.

The Sydkraft Research Foundation has been the most important financial contributor. They were the sole financier of the doctorate project and also funded the licentiate project jointly with Elforsk AB. The Royal Swedish Academy of Engineering Sciences (IVA) made a much appreciated research stay in Australia possible through a travel grant from the Hans Werthén Foundation. This financial support is gratefully acknowledged.

Last, but certainly not least, I would like to thank my friends—especially my hiking pals and the running and dining pals in "Kutargänget"—and family for their support over the years.

Lund, December 3, 2000,

Mats Larsson

Contents

| | | |
|-----------|--|-----------|
| I | Introduction | 1 |
| 1 | Introduction | 3 |
| 1.1 | Coordinated Voltage Control in Distribution Systems | 5 |
| 1.2 | Coordinated Voltage Control in Transmission Systems | 11 |
| 1.3 | Modelling of Power Systems with Modelica | 21 |
| 1.4 | Summary and Conclusions | 24 |
| 1.5 | Other Publications | 27 |
| 2 | Voltage and Reactive Power Control | 29 |
| 2.1 | Transfer of Active and Reactive Power | 29 |
| 2.2 | Sources and Sinks of Reactive Power | 34 |
| 2.3 | Voltage Stability | 41 |
| 2.4 | Distribution System Voltage Control | 53 |
| 2.5 | Transmission System Voltage Control | 55 |
| 3 | Solving Problems by Search | 61 |
| 3.1 | Short Introduction to Search | 62 |
| 3.2 | Combinatorial Optimization using Search | 68 |
| II | Included Papers | 71 |
| A | Coordinated Control of Cascaded Tap Changers in a Radial Distribution Network | 73 |
| A.1 | Introduction | 73 |
| A.2 | Power System Model | 75 |
| A.3 | Conventional OLTC Control Systems | 76 |

| | | |
|----------|---|------------|
| A.4 | Multivariable Control | 82 |
| A.5 | Results | 83 |
| A.6 | Discussion | 84 |
| A.7 | Conclusions | 87 |
| A.8 | Acknowledgments | 88 |
| B | Coordination of Cascaded Tap Changers using a Fuzzy-Rule Based Controller | 89 |
| B.1 | Introduction | 90 |
| B.2 | The Österlen Test System | 91 |
| B.3 | Conventional OLTC Controllers | 92 |
| B.4 | Optimal Controller | 92 |
| B.5 | Fuzzy-Rule Based Controller | 93 |
| B.6 | Prototype | 96 |
| B.7 | Simulation and Field Test Results | 96 |
| B.8 | Conclusions | 103 |
| B.9 | Acknowledgements | 103 |
| C | Limit Cycles in Power Supply Systems due to OLTC Deadbands and Load-Voltage Dynamics | 105 |
| C.1 | Introduction | 105 |
| C.2 | Example System | 106 |
| C.3 | Small Signal Stability Analysis | 110 |
| C.4 | Mechanisms in the Limit Cycle Phenomenon | 111 |
| C.5 | Describing Function Analysis | 113 |
| C.6 | Comparison of OLTC Models | 118 |
| C.7 | Discussion | 118 |
| C.8 | Conclusions | 120 |
| C.9 | Acknowledgements | 120 |
| D | Emergency Voltage Control using Search and Predictive Control | 121 |
| D.1 | Introduction | 121 |
| D.2 | Modelling | 123 |
| D.3 | Control Problem Formulation | 126 |
| D.4 | A Tree Search Method | 132 |
| D.5 | Simulation Results | 133 |
| D.6 | Further Work | 136 |

| | | |
|----------------------------|--|------------|
| D.7 | Conclusions | 138 |
| D.8 | Acknowledgements | 138 |
| D.9 | Appendix: Controller Tuning | 138 |
| Addendum to Paper D | | 141 |
| E | Coordinated System Protection Scheme against Voltage Collapse using Heuristic Search and Predictive Control | 145 |
| E.1 | Introduction | 145 |
| E.2 | Coordinated System Protection Scheme | 146 |
| E.3 | Heuristic Tree Search | 148 |
| E.4 | SPS based on Local Measurements | 150 |
| E.5 | The Nordic Test System | 151 |
| E.6 | Scenarios and Simulation Results | 153 |
| E.7 | Conclusions | 160 |
| E.8 | Acknowledgements | 160 |
| F | ObjectStab—A Modelica Library for Power System Stability Studies | 163 |
| F.1 | Introduction | 164 |
| F.2 | The Component Library | 166 |
| F.3 | Extending the Library | 170 |
| F.4 | Case Study: Four-Generator Test System | 171 |
| F.5 | Further Work | 173 |
| F.6 | How To Get ObjectStab Running | 174 |
| F.7 | Conclusions | 174 |
| F.8 | Acknowledgements | 175 |
| III | Bibliography | 177 |

Part I

Introduction

Chapter 1

Introduction

The control of voltage and reactive power is a major issue in power system operation. Because of the topological differences between distribution and transmission systems, different strategies have evolved. This thesis contains contributions of novel voltage control schemes for distribution and transmission systems. Whereas the work on distribution systems is directed at the normal state operation, the work on transmission systems mainly concerns the emergency state. The overall theme of the thesis is to explore and demonstrate how communication and centralized measurements can be used to improve existing voltage control. A particular interest is taken to the development of control schemes to avoid so-called voltage collapse, which can result in widespread outages. The total cost of a widespread outage can be hundreds of millions, or even billions, of (US) dollars (Amin, 2000). Arnborg (1997, and references therein) describe 51 cases of voltage instability or collapse that have occurred in power systems worldwide between 1965 and 1994.

The thesis has three main parts. Part I introduces the field of research on voltage control in power systems. Chapter 1 describes the contributions made in this thesis along with a survey of related work. Chapter 2 contains an introduction to the control of voltage and reactive power intended for readers from outside the power system community, who may want to read this chapter first. Chapter 3 contains an introduction to the search methodology used in some of the included papers.

Part II contains the papers that constitute the main academic contribution. Papers A–C deal with control interaction phenomena related to tap changers in radial distribution systems, and the design of coordinated control schemes

to avoid such control interaction. Papers D–E deal with the design of coordinated schemes for emergency state voltage control in transmission systems, and finally, Paper F introduces a new simulation tool for power system stability analysis based on the general-purpose modelling language Modelica. The relations between the different papers are exemplified in Section 1.4. A few typographical changes and minor corrections have been made to the papers, compared to the versions previously published. Those who reads this introductory chapter prior to the papers can skip the section 'Introduction' of each paper.

Part III contains the bibliography. Since many references are shared by the papers and the introductory part, all references have been collected there.

The following papers are included in the thesis:

- A. Larsson, M. and Karlsson, D. (1995). Coordinated control of cascaded tap changers in a radial distribution network. In *Stockholm Power Tech International Symposium on Electric Power Engineering*, vol. 5, pp. 686–91. IEEE.
- B. Larsson, M. (1999). Coordination of cascaded tap changers using a fuzzy-rule based controller. *Fuzzy Sets and Systems*, vol. 102, no. 1, pp. 113–23.
- C. Larsson, M., Popović, D. H. and Hill, D. J. (1998). Limit cycles in power systems due to OLTC deadbands and load-voltage dynamics. *Electric Power Systems Research*, vol. 47, no. 32, pp. 181–8.
- D. Larsson, M. , Hill, D. J. and Olsson, G. (2000). Emergency voltage control using search and predictive control. *Accepted by International Journal of Power and Energy Systems*.
- E. Larsson, M. and Karlsson, D. (2000). System protection scheme against voltage collapse based on heuristic search and predictive control. *Submitted to IEEE Transactions of Power Systems*.
- F. Larsson, M. (2000). ObjectStab—A Modelica library for power system stability studies. *Modelica Workshop 2000, Lund University, Sweden*.

1.1 Coordinated Voltage Control in Distribution Systems

Background and Motivation

The purpose of voltage control in distribution networks is to compensate for load variations and events in the transmission system, such that customer supply voltages are kept within certain bounds. A number of on-load tap changers (OLTCs), each capable of regulating the voltage of the secondary side of a transformer at one point in the network, are available in the distribution systems for this purpose. The control is discrete-valued, typically with steps of 1-3 %. Figure 1.1 shows the structure of a typical Swedish distribution network. The systems are most often radial, with tap changers cascaded in up to three levels. Therefore, interaction among OLTCs at different voltage levels is possible. OLTC control is presently based on a local voltage measurement in each substation. There is normally no coordination of OLTCs on different voltage levels or in different branches of the network.

Figure 1.2 shows a voltage measurement recorded in an early study (Karls-son, 1993) at a 10 kV substation with the conventional voltage control in operation. The substation is supplied through three cascaded tap changing transformers. There were 24 voltage steps¹ during the 150-minute recording. Nine of the steps are due to local tap operations in the substation (marked ± 1), and the rest are due to tap operations and the connection of capacitor banks higher up in the network. Most of the tap operations made in the substation counteract the effect of tap changers higher up in the network. These operations are preceded by "spikes" in the voltage. The figure clearly shows that there are oscillation and interaction phenomena between OLTCs at different voltage levels.

With coordinated control of tap changers it should be possible to completely eliminate, or at least reduce the number of, counteracting tap operations. Consequently, the total number of operations and the number of voltage spikes due to OLTC interaction would decrease. Wear on the tap changer mechanism is the most common reason for transformer maintenance and therefore a reduction of the number of tap operations is highly desirable. Poor coordination of cascaded tap changers can also be dangerous from a voltage stability point of view. A sudden voltage drop in the feeding network may result in voltage

¹Changes in the voltage of 1 % or more in less than 10 seconds are referred to as voltage steps.

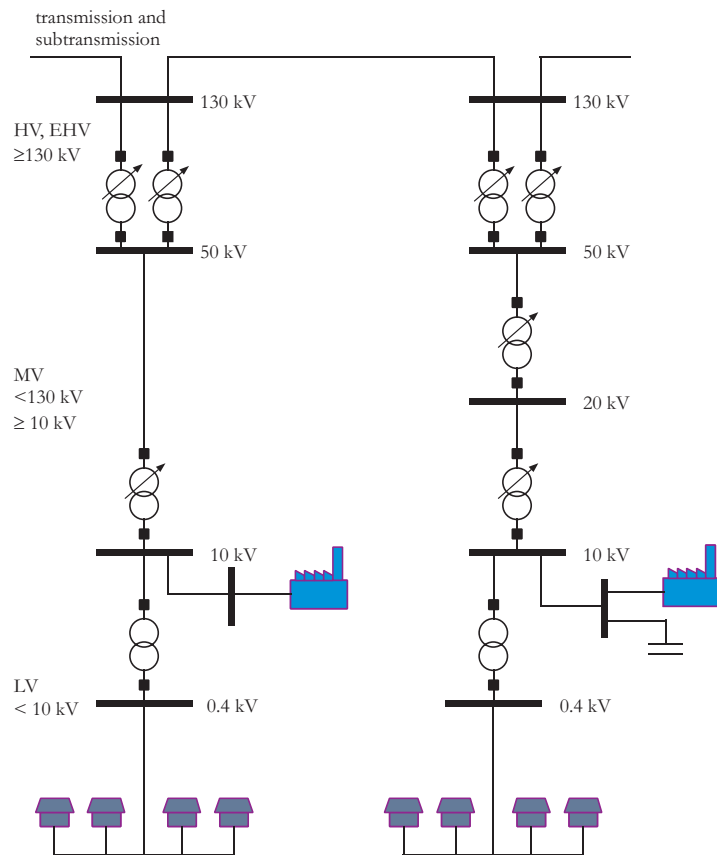


Figure 1.1: Typical structure of a Swedish distribution system. Transformers with OLTCs are marked with an arrow.

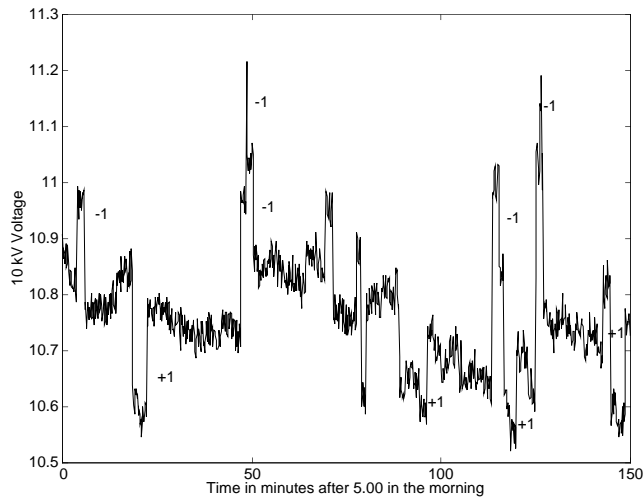


Figure 1.2: Field measurement of the voltage in the 10 kV substation at Östra Tommarp during load pickup. The tap operations made locally are marked with +/-1 (Karlsson, 1993). The large number of voltage spikes is an indication of OLTC interaction.

overshoot at the load level due to OLTC interaction (Karlsson, 1992). Since loads are voltage sensitive, this will increase the loading of the feeding transmission system. Step disturbances are likely to arise during voltage instability incidents as a result of tripped lines or generation units in the transmission system. During such incidents the transmission system is already operating close to its transfer limits and increased loading is highly undesirable. Referring to the role of OLTCs in voltage instability incidents, the new control schemes presented in this thesis can prevent voltage overshoot due to voltage drops in the feeding system. With coordinated OLTC control, it would also be possible to use alternative control strategies during voltage instability incidents.

Contributions of the Thesis

The natural starting point of the work on coordinated OLTC control was to investigate to what extent the problem of OLTC interaction in the normal state operation could be solved by retuning the existing controllers. This resulted in a tuning recommendation that assigns large time delays for lower level OLTCs

and smaller for higher level OLTCs. Tuning according to this recommendation reduces OLTC interaction for step disturbances but not for the disturbances introduced by the daily load variations. Step disturbances occur on a daily basis, for example when capacitor banks are switched in the feeding network. The idea of assigning larger time delays for lower level OLTCs is not new, similar philosophies have for long been used by several network operators around the world. However, the presentation in this thesis provides additional verification of the tuning rule by simulation as well as field measurements.

The next step was to investigate to what degree communication between substations can further improve the control. First, an optimal controller based on on-line tap optimization was developed. This controller eliminates OLTC interaction, but relies on a perfect network model and measurements of the load powers. These drawbacks make it unsuitable for practical implementation unless an accurate network model is available and therefore motivate the development of a simpler scheme that does not have these drawbacks. The work described up to this point is documented in Paper A.

An important aim was also to demonstrate the feasibility of coordinated voltage control as an application of distribution automation. In Paper B, a robust and simple fuzzy-rule based controller was developed for the practical implementation. By simulation of actual load patterns, this controller was shown to offer near-optimal performance without the previously mentioned drawbacks of the optimal controller. A prototype was designed and installed in the distribution system at Österlen in southern Sweden. Using the prototype, a number of load patterns were recorded. The conventional control scheme with conventional as well as revised tuning, the optimal control scheme and the fuzzy-rule based control scheme were then compared by simulation of the recorded load patterns. The prototype was also used to validate these simulation results. Additional details about the implementation of the prototype can be found in the licentiate thesis (Larsson, 1997).

Paper C investigates another potential source of control interactions related to operating states in or close to emergency states. The control system of a single tap changer may interact with controllers in the downstream load and reactive compensation devices causing interaction phenomena or even sustained oscillations. This investigation was motivated by the lack of a well-established practice for OLTC modelling in voltage stability studies. Using a continuous tap changer representation as in Tamura et al. (1989), Hiskens and Hill (1993), Vournas and Van Cutsem (1995), Popović et al. (1996a) in similar studies,

small-disturbance voltage stability analysis indicates that oscillatory voltage instability may arise in highly loaded and reactively compensated systems with recovery loads. It is shown that when a more accurate discrete tap changer model is used, the control system deadband can interact with load dynamics and thereby create a limit cycle phenomenon. The limit cycle can stop the growth in magnitude of the voltage oscillation that would be present in a system model that neglects the deadband. Thus, small-disturbance analysis based on a continuous approximation of the tap changer dynamics that indicates oscillatory voltage instability may be unreliable. On the other hand, small-disturbance analysis indicating monotonous voltage instability appears to be reliable, even with the continuous tap changer approximations. The conditions for existence of limit cycles are obtained using describing function analysis (Hsu and Meyer, 1968). The analysis is restricted to the exponential recovery load characteristics used in the paper and a simplified tap representation incorporating the OLTC deadband, but the results are verified using simulation with a detailed OLTC representation. The conclusions in the paper contradict the popular, but erroneous, assumption that sustained oscillations due to the control system deadband and load-tap interactions can *always* be avoided if the OLTC deadband is appropriately tuned. The results of Papers A, B and C and are given in more detail in the licentiate thesis (Larsson, 1997).

Related Work

Different approaches have been taken to the problem of extending maintenance intervals for tap changers. New designs where the mechanical switches, which are the critical part from a maintenance perspective, are totally replaced by power-electronics have been proposed (Bauer and de Haan, 1998, Larsson et al., 1997). Such tap changers can be used also for rapid compensation of voltage dips and continuous regulation of the voltage. However they are more expensive, less robust to fault currents and have higher power losses than mechanical tap changers. Thyristor-assisted tap changers, which retain the mechanical switches but divert the current through the switches using power-electronics during tap changing, have also been proposed (Cooke and Williams, 1992, Shuttleworth et al., 1996). There is no current through the tap changer during switching and consequently no arcing, and the wear on the tap changer is therefore reduced. Since the current is flowing through the mechanical tap changer between tap changes, no extra power losses are added by the power-electronics

in between tap changes. The capability of fast and continuous control is however lost compared to the designs where the mechanical switches have been completely replaced by power-electronics.

Another way of reducing wear on the tap changers is to improve the control of the existing tap changers as by the tuning rule in Paper A. Carbone et al. (1996) present a tuning rule for the existing controllers similar to that given in Paper A. Yorino et al. (1999) present a decentralized control scheme for the control of cascaded OLTCs based on fuzzy logic and adaptive control to minimize the number of tap operations and load side voltage overshoot.

The problem of coordinating tap changer and capacitor controls in radial distribution systems based on centralized information like the optimal controller and fuzzy controllers in Papers A–B has also been previously treated. Roytelman et al. (1995) employ combinatorial optimization to coordinate tap changer and capacitor bank control based on the full nonlinear power flow formulation. Their approach is similar to the volt/var control problem formulated by Grainger and Civanlar (1985) but with the aspiration of real-time implementation. Results from field tests of the actual implementation are given in Roytelman et al. (1998). Furthermore, Roytelman and Ganesan (2000) discuss modifications of the scheme to account for the effects of remaining local controllers in the controlled distribution system. Another approach by Chang and Huang (1999) employs variable-structure control, a successively linearized system model, and centralized information for the coordination of tap changers.

Referring to the OLTC modelling issues explored in Paper C, the role of OLTCs in combination with aggregate loads has received considerable attention, for example in Abe et al. (1982), Liu and Vu (1989), Medanić et al. (1987), Popović et al. (1996b), Vu and Liu (1992). Voltage instability problems concerned with OLTC dynamics were analyzed by Abe et al. (1982), Tamura et al. (1989), Liu and Vu (1989), Popović et al. (1996b), Vu and Liu (1992) using the continuous state OLTC model, and by Ohtsuki et al. (1991) using a discrete tap representation. Stability conditions for cascaded OLTCs were derived by Medanić et al. (1987), Yorino et al. (1997) using a discrete state tap model. Another type of limit cycles and other oscillatory voltage instability problems created by interaction between cascaded tap changing transformers and/or by load-tap interaction were investigated by Hiskens and Hill (1993), Popović et al. (1996a), Vournas and Van Cutsem (1995) using a continuous tap representation.

Wu et al. (1999a) further investigate the effect of various continuous and discrete OLTC representations on the limit cycle phenomenon first described in Paper C. Wu et al. (1999a) extend the results in Paper C with conditions for existence of limit cycles when the detailed discrete OLTC models presented by Sauer and Pai (1994) are used. Furthermore, the large-disturbance stability properties of a system representation with continuous approximations of the OLTC dynamics are investigated using Lyapunov theory (Kahlil, 1992). Wu et al. (2000) examine the effect of different load characteristics on the existence of the studied limit cycles and shows that for some load characteristics, it is indeed possible to avoid limit cycles by retuning the OLTC control system. This paper also extends some of the results to the multi-tap/multi-load case.

1.2 Coordinated Voltage Control in Transmission Systems

Background and Motivation

Power systems are sometimes referred to as the largest machines built by man. Mature power systems typically cover large areas and often include hundreds of generators, thousands of lines and substations, and millions of customers. Figure 1.3 shows a schematic of the Nordel transmission system that connects Sweden, Norway, Finland, and the eastern part of Denmark (Zealand) by AC connections. The networks of western Denmark (Jutland), eastern and central Europe are connected through DC connections. The system has about 85000 MW of installed generation capacity and the yearly production is about 380 TWh, corresponding to an average yearly utilization of generation capacity of 51 %. More than 75000 km of AC and DC transmission lines with rated voltages between 110 and 400 kV (Nordel, 1999) are present in the interconnected system. The Nordic electricity exchange Nord Pool (Nord Pool, 1999) was formed in 1993, and Norwegian producers could begin trading their energy on the market. Sweden joined the common electricity market in 1996, with Finland following in 1998. The western part of Denmark joined in 1999, with the eastern part following in October 2000. Thus, Scandinavia now constitutes a single power exchange area with the possibility of importing and exporting from/to central and eastern European countries. During 1999, the volume traded on the physical market was 75 TWh, corresponding to about 20 % of the yearly demand. The remaining 80 % was traded using other market mechanisms such as bilateral contracts.



Figure 1.3: The Nordel transmission system (Nordel, 1999). The DC link from Karlshamn to Poland (SwePol Link) is in operation since August 2000.

Although the individual actors on the power market usually have independent goals, such as survival and maximization of profits, the overall goal in the operation of power systems is a reliable energy supply to consumers at a low cost. Seen from the point of view of the engineer, some additional constraints have to be met; for example that the voltage and frequency in all parts of the network should be acceptable, and that operational limits of the individual power system components are not exceeded. Failure to meet such constraints may result in supply interruption or damage to production, transmission or customer equipment. Furthermore, the power system should be robust to the disturbances that sometimes occur in the systems, such that unnecessary blackouts are avoided. The traditional way of ensuring this robustness has been to design the system conservatively such that the system is not utilized to its full physical transfer limits during normal operation. In this way there is some reserve capacity to be used in case of disturbances. However, this is an expensive way of ensuring robustness of the system.

In most mature power systems, the yearly energy demand is increasing but the rate of expansion has decreased, mainly for environmental and economical reasons but sometimes also for political reasons. In Sweden for example, 1155 MW of installed generation was decommissioned whereas only 46 MW of new generation was commissioned during 1999 (Nordel, 1999). The corresponding figures for the entire Nordel area are 2288 MW and 989 MW of decommissioned and commissioned generation capacity, respectively. Only Norway increased its generation capacity during 1999. According to a report (SVK, 2000) from the Swedish transmission system operator Svenska Kraftnät² who is responsible for maintaining frequency control and short-term balance, Sweden is expected to rely on import of about 10% of the Swedish load during the peak load conditions predicted for the winter of 2000-2001. The possibility of import depends on the available excess capacity in the other Nordic countries and central Europe, and the capacity and operational status of the DC links connecting the Nordel system to the central and eastern European systems. If not enough import capacity is available, the system operators may have to disconnect load to ensure the short-term power balance.

The increased import will require transport of more energy across larger distances than before, and therefore the transmission system has to be operated closer to its physical transfer limits. Analysis of severe disturbances has revealed

²Swedish National Grid (<http://www.svk.se/>)

that the consequences of such disturbances are highly dependent on the system loading. When the system is lightly loaded it is inherently robust to disturbances that under high load conditions may trigger cascaded line trippings resulting in widespread power outages. For example, both the disturbance that caused the Swedish voltage collapse in 1983 (Walve, 1986) and the disturbance that caused the voltage collapse on July 2, 1996, in the North American WSCC³ system, would have had much less severe consequences if the system had been under light load conditions. On both occasions, the system was operating under high load, but within normal transfer limits, when a disturbance occurred (WSCC, 1996, Walve, 1986). The faulted components needed then to be disconnected. However, because the systems were highly loaded at the time, when the load of the initially faulted components was transferred to other components these became overloaded and tripped with some time delay, leading to new trippings and so on. These cascaded trippings in combination with insufficient reactive power support eventually resulted in widespread outages. According to the WSCC report, the collapse on July 2 resulted in service interruptions to more than 2 million customers⁴. Arnborg (1997, and references therein) describe 51 cases of voltage instability or collapse that have occurred in power systems worldwide between 1965 and 1994.

On July 3, 1996, the same fault that caused the July 2 outage in the WSCC system occurred again. On this occasion, the operators realized the danger of a cascaded outage similar to the one that occurred the day before and manually interrupted service to some customers. In this way, the load on the system bottlenecks was reduced and cascaded overloading of system components was avoided. The post-disturbance analysis of the events on July 3rd revealed that the well-timed and accurate emergency control indeed did stop a cascading outage from progressing, and the affected area was much smaller than it was on the previous day. However, it is not likely that operators will respond quickly and accurately enough to carry out such emergency control, unless the scenario is fresh in the operators' minds like on July 3, 1996. An automated system that can alert the operators and suggest emergency controls is therefore highly desirable.

New computer and communication technology offer the possibility of implementing decision support tools that continuously monitor the system state

³Western Systems Coordinating Council (<http://www.wsccl.com/>)

⁴Corresponding to about 6 million people.

and suggest preventive and emergency control actions to be taken by the operators, or fully automatic control systems that do not require operator intervention. Such systems would warn operators when stability problems are imminent and suggest emergency control actions to the operators or, if authorized to do so, carry out such actions autonomously. The events described above clearly indicate that such tools could be used to preserve or even increase the robustness of the system, especially when utilized closer to its theoretical transfer limits.

The ultimate countermeasure against voltage collapse is to disconnect customers and thereby reduce the load on critical parts of the network, but this is a control that must be used sparingly to minimize customer inconvenience. Other means of control such as capacitor switching, emergency operation of tap changers in the distribution systems and rescheduling of active and reactive production by generators have been suggested. These means of control are less disruptive to the customers and may be used more freely. In the future, there will be a possibility of trading in "interruptible" power in Sweden. A customer can then, in exchange for a lower electricity rate, accept being considered for disconnection in the event of shortages. However, this is not yet in widespread use but may in future provide a possibility of load disconnection that can be more freely used. By coordinating emergency controls, both in terms of actuators of different types and in different geographical locations, the maximum effect of controls can be ensured.

Contributions of the Thesis

Papers D and E make contributions towards emergency control systems capable of arresting voltage collapse using an optimal combination of dissimilar emergency controls such as generator voltage reference values, load shedding, capacitor switching and tap changer control.

The scheme presented uses a network model and wide-area measurements to account for the actual power flow in the system, load models to account for load recovery dynamics and static generator models to account for generator capability limits. The presented scheme is based on Model Predictive Control (Garcia et al., 1989, Morari and Lee, 1999, Mayne et al., 2000), which is an established control technique in process control. Contrary to what is customary in the literature on process control, the actuators act in a discrete-valued manner, i.e., can assume only a fixed set of values. In model predictive control, the control signal to apply to the controlled system is normally obtained

through the solution of a quadratic programming problem. The additional difficulty that arises from having discrete control variables is represented by integer constraints in the optimization problem. To avoid cascaded outages, inequality constraints are imposed to ensure that voltage and generator current limits are not violated. The resulting combinatorial optimization problem is solved using a search method adapted from the research on artificial intelligence.

The tree search method was first employed in Larsson (1999), using an eigenvalue-shift approach where tree search optimization was used to minimize the real part of the dominant eigenvalue of the dynamic Jacobian matrix. This study highlights some of the problems of using the eigenvalues as a stability measure and proposes a more direct stability criterion in terms of voltage predictions later employed in Papers D–E. Some comments about the applicability of the dominant eigenvalue as a stability measure for the emergency voltage control problem are given in the addendum to Paper D on page 141.

Paper D is a theoretical presentation in which the emergency voltage control problem is formulated as a model predictive control problem, and the search problem is solved using a search method that expands the complete search state space. The approach is similar to that in Larsson (1999), but the study is extended to include a detailed nonlinear predictor based on time simulation as well as simpler ones based on a linearized system representation. The system response with the different predictors is investigated in simulations of a small test system and the simplified predictors are shown to be satisfactory approximations of the more exact, but also more computationally demanding, nonlinear predictor. Furthermore, a tuning procedure that aims to minimize the use of load shedding is presented.

In Paper E, the presented method is applied to the Nordic 32 test system from CIGRE (1995b). This system contains many control variables, and a more sophisticated method is required to solve the search problem. Some of the many search enhancements presented for general single-agent and game tree search (Junghanns, 1999, Schaeffer and Plaat, 2000) are applied to the search problem. These enhancements reduce the computational complexity of the search and thereby make the search problem tractable for real-time implementation. The simulation results in Paper E indicate that undervoltage load shedding relays, which order load shedding if the local voltage decreases below some fixed threshold value, are usually capable of arresting voltage collapse provided enough load is made available for shedding and the relays are properly tuned. Only a small reduction of the load shed can be achieved by the coordinated

scheme compared to the local scheme when load shedding and tap changers are the only controls considered. However, when also generator controls are considered in the control optimization an average reduction of the amount of load shed by about 35 % is achieved, averaged over the contingencies studied. The reduction in the amount of load shed is mainly due to improved utilization of remote generators with excess reactive capacity to spare.

Related Work

The work on emergency control schemes can be divided into approaches using only local measurements and those that rely on centralized measurements. The main advantages of the local schemes are the low installation cost, fast control response and reliability that can be achieved since they do not rely on communication. Fast response is necessary if the system aims at arresting short-term voltage instability. For emergency controllers with the purpose of arresting long-term voltage collapse, response times of up to a minute or so are acceptable. The main drawback of the local schemes is the difficulty of tuning such schemes, and that coordination of emergency controls in different locations is difficult to facilitate using only local measurements.

Emergency control schemes can also be classified as being either of a rule-based or of an algorithmic type. Rule-based schemes are technologically simple to implement but require engineering judgment and specific knowledge of the system in which the system will be installed. The efficiency of a rule-based system may be limited for disturbances that were not foreseen during the design of the system. On the other hand, algorithmic approaches are often theoretically more complicated but do not require specific knowledge about the system, and are applicable to any system as long as a system model is available. Since the algorithmic approaches make their decisions based on a system model, they are better equipped to handle disturbances of kinds not foreseen during the design stage and to coordinate emergency controls of different types and in different locations.

The use of centralized measurements mainly enables better coordination of actuators in different geographic locations compared to schemes using only local measurements. Compared to the rule-based schemes, algorithmic schemes can better assess the effect of emergency controls and also enable better coordination of actuators of different types.

It should be noted that a centralized scheme can coexist with and complement a local scheme. The main task of the centralized scheme is then to steer the system trajectories away from operating points where the local scheme or other protection systems are activated. Since the centralized scheme offers better coordination, this can hopefully be achieved with less drastic emergency controls than would be executed by a standalone local scheme. Because of the longer response time of the centralized systems, they are presently better suited for protection in the long-term time frame than the short-term. Note, however, that fast wide-area communication systems (WAMS) are becoming available (Samuelsson, 2000), which will make the use of centralized strategies feasible also for schemes aimed at short-term voltage collapse. In the Nordic system, which contains a significant amount of heating loads, the risk of long-term voltage collapse is considered greater than that of its short-term counterpart.

A brief overview of the research on emergency voltage control schemes and some implementations are given in the next section.

Local and Rule-based Approaches

The simplest load shedding schemes are of the undervoltage type, that is, load shedding orders are issued if the local voltage decreases below some fixed threshold value, usually after some time delay. One undervoltage load shedding relay of this type is described in Vu et al. (1995). While such relays are most often reliable in the sense that they can arrest a collapse, they can at least in theory misoperate. Misoperation here means situations where the relay issues load shedding orders in situations where shedding is not needed.

The tuning of such local schemes is most often based on engineering judgment and the knowledge obtained from off-line simulation of credible disturbances. This approach is tedious and requires good knowledge of the system in which the load shedding scheme is to be implemented. Moors et al. (2000) present an automated method of tuning load shedding schemes, where optimization by a genetic algorithm is used to determine a set of parameters that is optimal for a training set of credible contingencies. The design of the training set is however a non-trivial task.

Vu et al. (1995) describe the load shedding system that has been in use since 1992 in the Puget Sound Area (WA, USA). The system makes in total 1800 MW of load available for shedding through about 50 local undervoltage relays. The paper also reports that until 1995, no misoperations had been de-

tected and that the operation of the undervoltage relays at least on one occasion has prevented a serious incident. After the voltage collapses of July 2 and July 3, 1996, the WSCC reviewed their voltage security strategy and now require their members to review the need for undervoltage load shedding schemes in their systems (Abed, 1999).

Local and Algorithmic Approach

Another approach is to use "adaptive" relays that estimate the stability margin using time-series analysis of local measurements (Vu et al., 1997, Balanathan et al., 1998a). As of yet, there has been no system study presented that indicates the relative benefit of using this type of adaptive relays over the conventional relays described in the previous section. The simulation results in Paper E indicate that the conventional relays perform quite well, when coordination with other types of emergency controls are not needed. However before any firm conclusions can be drawn, also other systems and contingencies should be studied. The adaptive relays may also be easier to tune than conventional relays.

Centralized and Rule-based Approaches

Since 1996, there has been a protection scheme against voltage collapse present in the southern region of Sweden (Ingelsson et al., 1997). The rule-based scheme can order load shedding, switching of shunt reactors and request emergency power from DC links and gas turbine generators. The scheme operates on the basis of centralized measurements taken from the SCADA system. At the time of publication of this thesis, the system was out of service and under revision following the transfer of the operational responsibility from Sydkraft AB to Svenska Kraftnät. This transfer of responsibility is an effect of the deregulation of the Swedish power system.

Kolluri et al. (2000) describe the rule-based protection scheme installed in the system operated by Entergy Inc. in New Orleans (LA, USA). The system monitors voltage, unit current limiter and tripping signals, and the system load level through the SCADA system, and it can order load shedding.

CIGRE (1998) describes some other schemes developed by various system operators. A system for automatic blocking of tap changers has been installed in the French system. The system is regional and operates if the voltage of a pilot node of the region stays below a fixed threshold value for a prescribed duration of time. The tap changers of the entire region are then blocked. In

blocked mode, tap changers are however allowed to lower their ratio to avoid overvoltages. A similar system has been installed in Belgium. In this scheme, the reference voltages of distribution tap changers are reduced to provide a load reduction. Operational experience with the system indicates that a 5 % load side voltage decrease normally corresponds to a load reduction of about 2-3 %. BC Hydro in Canada has developed a rule-based load shedding scheme based on centralized measurements of voltage and the var reserves of generators. Ontario Hydro has an emergency control scheme using load shedding, tap locking, re-closing of disconnected lines and capacitor switching. The system is rule-based and employs regional measurements.

Centralized and Algorithmic Approaches

Since the proper coordination of emergency controls is highly dependent on the system loading and state, algorithmic approaches that employ detailed network models to account for the current power flow in the system and thereby the effect of controls, can better coordinate and minimize the usage of emergency controls than the local or rule-based schemes.

From a static viewpoint, the existence of a solution to the power flow equations (Glover and Sarma, 1994) guarantees the existence of an equilibrium point. Emergency control schemes utilizing the static approach aims to restore a lost equilibrium by applying the necessary controls. Some examples of the work using static approaches are Granville et al. (1996), Popović et al. (1997), Wang et al. (1998), Feng et al. (1998) who employ various optimization or sensitivity techniques in order to calculate the minimum load shedding necessary for restoration of an equilibrium point. Popović et al. (1997) present a method of coordination of secondary voltage control and load shedding based on optimization and a linearized system model. Similar work has also been carried out using various quantitative stability measures—so-called voltage stability indices or proximity indicators (CIGRE, 1995a). The approach is then to use sensitivity or optimization techniques to optimize the index. Such work have been presented for example by Tuan et al. (1994), Nanba et al. (1998), Berizzi et al. (1998). Methods that use only static considerations can only guarantee existence of a stable operating point created by the countermeasures. Whether or not the system trajectories are attracted to the new stable equilibrium may also depend on the timing of the countermeasures (see page 52). This drawback of the static approach motivates also methods considering the system dynamics

in the determination of emergency controls.

Methods based on dynamic approaches deal with the actual attraction or non-attraction to a stable equilibrium point created by emergency measures. Approaches based on dynamic system models have previously been presented by for example Van Cutsem (1995) and Makarov et al. (1998). These references use the dominant eigenvalue of the dynamic Jacobian matrix as a stability measure and determine the optimal control direction from eigenvector and sensitivity analysis. Larsson (1999) also attempts an eigenvalue-shift approach, but with less success than the two previous references (see page 141). In Overbye and Klump (1998), emergency control actions are determined through analysis of the sensitivities of an energy function stability measure to controls. A method based on differential dynamic programming and a security measure as the distance to the closest bifurcation has been derived in Popović et al. (1998) and applied to a system model representing the main grid of New South Wales, Australia, in Wu et al. (1999b).

1.3 Modelling of Power Systems with Modelica

Background and Motivation

The simulation of power systems using special-purpose tools is now a well-established area and several commercial tools are available, e.g., PSS/E⁵, Eurostag⁶ and Simpow⁷. While these tools are computationally very efficient and reasonably user-friendly, they have a closed architecture, and it is difficult to view or change most of the component models. The implementation of new network component models requires special skills⁸, although it is normally possible to enter new controller blocks such as governing and excitation systems in block diagram form.

Modelica (ModelicaDef, 1999, ModelicaTut, 1999) is an object-oriented general-purpose modelling language that is under development in an international effort to define a unified language for modelling of physical systems. Modelica supports object-oriented modelling using inheritance concepts taken from computer languages such as Simula and C++ to allow proper structuring

⁵Power Technologies (<http://www.pti-us.com/>)

⁶Tractebel (<http://www.eurostag.be/>)

⁷ABB Power Systems (<http://www.abb.com/powersystems>)

⁸With Eurostag this is presently impossible, with PSS/E this requires editing of the FORTRAN source code and with Simpow this can be done using a tool-specific modelling language.

of models. It also supports acausal modelling, meaning that a model's terminals do not necessarily have to be assigned an input or output role at the modelling stage. This simplifies modelling and model reuse since each component can be modelled independently. Since the input or output role of terminals is dependent on the environment in which the component is connected, this issue is resolved by the simulation tool when a system model is compiled (ModelicaTut, 1999).

There is already a number of Modelica libraries for other application domains such as 3-dimensional multibody systems, rotational and translational mechanics, hydraulics, magnetics, thermodynamical systems and chemical processes. Components from different domain libraries can be freely mixed.

One problem with the domain-specific tools is that the component models do not perfectly agree in different simulators. When transferring from one tool to another, not only need the data files be converted, but some tuning of the parameter values is often necessary before the same results can be obtained in two different programs. These disparities may be due to differences in the component modelling or due to differences in the integration methods. Another problem is that while the domain-specific tools have good models for the power system components, they lack support for models from other application domains. For example, modelling relay controls using state graphs or Petri-nets is not possible using most of these tools. Modelling wind power plants may require a more detailed representation of the mechanical system than is available in a standard generator model, for example including a gearbox or stochastic wind variations. With a Modelica library for power systems, such components could be taken from Modelica libraries for other application domains, and be interfaced to the components provided by the power system library. The Modelica language will soon be proposed as an ISO-standard, and can then be used to interchange models between users of different simulation tools, as long as both tools comply with the Modelica standard. At present, there are two simulation tools supporting the Modelica language⁹, however this number is likely to increase in the future.

Contributions of the Thesis

Paper F presents a Modelica library of power system components called *ObjectStab* for the analysis of electromechanical transients. The aim has been to

⁹Dymola (<http://www.dynasim.se>) and MathModelica (<http://www.mathcore.se>).

provide a basic framework within which individual users can define models according to their specific requirements, rather than trying to provide all the models that the domain-specific tools usually provide. Using the components from the library, the power system can be drawn in one-line diagram form using a graphical editor or entered in a textual format. The library has an open structure and all models can be modified or extended using various Modelica constructs, such as state machines, block diagrams or plain algebraic or differential equations. The models also have reasonable default parameter values defined such that users can play around with the models even before they have full understanding of all component parameters. Since the library has been used primarily for voltage stability studies in this thesis, the library content is somewhat biased towards this type of studies. The component library however contains models suitable also for frequency and angle stability studies.

Related Work

Modelling of power systems using a general-purpose simulation tool have been previously demonstrated in the form of the Power System Toolbox (Chow and Cheung, 1992), which is a set of Matlab program files capable of simulation of electromechanical transients in power systems. Here, the component models are accessible, but the modification of these requires a proper understanding of the interaction of the model files in this specific environment. Graphical editing of the models is not possible. The use of causal modelling to model power systems, as required by Simulink that does not have the capability of automatically determining the causality of connectors, is illustrated in Hiyama et al. (1999) where a model for transient stability simulation is described. With this approach, the network has to be modelled using the traditional admittance matrix method and the power system topology cannot be visualized in the graphical editor.

Object-oriented modelling of power systems using general-purpose simulation languages has previously been described in Mattsson (1992), where a block library was developed using the modelling language Omola. However, the Omola project is now discontinued and the experiences from this have been brought into the Modelica project. Some of the models in the ObjectStab library are based on models developed in a Master's project (Romero Navarro, 1999) using the tool-specific modelling language previously used by Dymola. Another Modelica implementation of power system models has been described

by Bachmann and Wiesmann (2000). This implementation unifies the analysis of electromagnetic and electromechanical transients in a single tool. However, these models are proprietary and not accessible to the public.

1.4 Summary and Conclusions

In Papers A–B the problem of OLTC control system interaction has been described and three means of improved control have been proposed, each one with its own merits:

- a tuning rule for the conventional controllers;
- a centralized controller based on on-line tap optimization;
- a centralized controller based on a fuzzy inference system.

The first solution obviously has the merit that the existing controllers are preserved, so that no new investments are necessary. Therefore, this is suitable as a first step before a centralized controller is implemented. The simulation and field measurement results in Paper A indicate about a 20 % reduction of the number of tap operations compared to the conventional tuning.

The two new controllers rely on communication between substations. The simulation results indicate a reduction of the total number of tap operations by about 36 % compared to conventional scheme with the new tuning, with the fuzzy-rule based controller. The additional reduction with the optimal controller is about 45 % compared to the conventional controllers and 14 % compared to the rule-based controller. The optimal controller relies also on a network model and is suitable for implementation as part of a distribution automation system that can provide an up-to-date network model, whereas the fuzzy rule-based controller is conveniently implemented on its own. The optimal controller was also used as a benchmark during the design of the rule-based controller. The fuzzy-rule based controller was used in a prototype that has been tested in the rural distribution system at Österlen, Sweden. Note that the simulation results in Paper B are based on actual load patterns recorded using the prototype, whereas those in Paper A are based on assumed load patterns. Consequently, the simulation results in Paper B are more reliable than those in Paper A.

In Paper C the phenomenon of limit cycle behaviour due to tap changer deadbands and load-tap interaction has been investigated. Also, the effect of

tap dynamics modelling on system behaviour has been illustrated. It has been shown that the results from small-disturbance analysis based on a continuous OLTC model are unreliable, especially in a heavily loaded power system. Under heavy load conditions, the system with a detailed OLTC model exhibits a limit cycle that can arrest oscillatory voltage instability predicted by small-disturbance analysis. The key parameters in creating/avoiding this kind of limit cycles are identified as the system load level, degree of reactive compensation and the load-voltage dependency. In certain loading conditions, adjusting OLTC control system parameters such as time delays or deadband size is shown not to have any effect on the existence of the limit cycles.

Paper D demonstrates the application of model predictive control to emergency voltage control. The proposed controller optimally coordinates capacitor switching, tap changer operation, and load shedding in different geographic locations, ensuring minimum usage of emergency controls such as load shedding. A search method is employed to minimize a cost function based on predictions of the system's future behaviour. A detailed predictor based on time simulation as well as less computationally demanding ones based on a linearized system model have been presented, and the properties of the different predictors are discussed and illustrated using time simulation.

Paper E demonstrates the application of the method to a model of the Swedish power system and the monitoring of generator capabilities by constraints in the controller. A heuristic tree search method is used to enhance the efficiency of the search. Eight scenarios, some of which lead to voltage collapse unless emergency control measures are taken, have been used to evaluate system protection schemes based on local as well as centralized measurements. Simulation results indicate that load shedding based on local measurements is near optimal when load shedding is the only emergency control considered. Another conclusion is that the reactive capability of generators is somewhat better utilized when generators use line-drop compensation. On the other hand, the results indicate that the protection scheme based on centralized measurements can use remote generators to support a weak region as an alternative to load shedding. The reduction in the required amount of load shedding is about 35 % compared to the best local strategy. Also, the centralized scheme maintains a more even voltage profile than the local schemes and may therefore avoid short-term voltage instability that occurs with the local scheme, even though the short-term dynamics are not explicitly modelled.

Paper F presents a Modelica library for power system stability studies called ObjectStab. Using the library, users can quickly enter their power system in one-line diagram form using a graphical editor, without having to type cryptic data files in text format or entering parameter data in countless dialog windows. It is primarily intended as an educational tool, which can be used to experiment with and observe the effect of the different levels of modelling detail or to try out new types of controllers. The library has an open structure and all models can be modified or extended using various Modelica constructs, such as state machines, block diagrams or plain algebraic or differential equations. The models also have reasonable default parameter values defined such that students can play around with the models even before they have full understanding of the meaning of all system parameters. The flexibility of the library makes it easy to modify the models and export the system representation to other tools for further analysis. Since there is not yet a simulation tool that both supports Modelica and can exploit the sparse structure of the equation system describing a large power system model, it cannot yet compete with the special-purpose tools in terms of computational efficiency for large systems. It is therefore at present most suitable for analysis of small systems.

The relations between the different papers in the thesis can be exemplified as follows: The control interaction phenomena described in Papers A–C were motivated mainly from the transformer maintenance and voltage quality perspective. However, a beneficial side-effect is that the absence of voltage oscillations that can be achieved by coordinated voltage control makes the distribution systems more well-behaved in case of outages in the feeding transmission system. Furthermore, with coordinated voltage control in distribution systems, these can be used as actuators by an emergency control system such as that described in Papers D–E. The Modelica library ObjectStab has been used for all simulations in Papers D–F and would have greatly simplified the work described in papers A–C if it had been available at the time.

1.5 Other Publications

Apart from the papers included in the thesis, the results of the project have also been reported in the following publications:

Larsson, M. (1996), Coordinated control of cascaded tap changers in a radial distribution network, *Preprints from Reglermötet, University of Technology, Luleå, Sweden*.

Larsson, M. (1997). *Coordinated tap changer control - Theory and Practice*. Department of Industrial Electrical Engineering and Automation, Lund University, Sweden. Licentiate Thesis, ISBN 91-88934-07-1.

Larsson, M. and Karlsson, D. (1998). Reduce tap changer wear and tear. *Transmission & Distribution World*, vol. 50, no. 4, pp. 51–3, 56–8.

Larsson, M. (1999). Emergency state voltage control using a tree search method. In *Power Engineering Society Summer Meeting*, vol. 2, pp. 1312–17. IEEE.

Wu, Q., Popović, D. H., Hill, D. J. and Larsson, M. (1999). Tap changing dynamic models for power systems voltage behaviour analysis. In *1999 Power Systems Computation Conference, Trondheim, Norway*.

Romero Navarro, I., Larsson, M. and Olsson, G. (2000). Object-oriented modelling and simulation of power systems using Modelica. In *Power Engineering Society 2000 Winter Meeting*, vol. 1, pp. 790 –795, IEEE.

Chapter 2

Voltage and Reactive Power Control

This chapter outlines some of the fundamentals of voltage control and stability and highlights the aspects most important to the papers in Part II. Readers requiring more detailed descriptions are recommended to consult the textbooks by Taylor (1994) and Van Cutsem and Vournas (1998), or the summaries by Vu et al. (1995) and Van Cutsem (2000).

2.1 Transfer of Active and Reactive Power

Consider the circuit in Figure 2.1. A strong source with voltage E supplies a remote load through a transmission line modelled as a series reactance. The receiving end voltage V and angle δ depend on the active and reactive power transmitted through the line. The active and reactive power received at the load end can be written (Van Cutsem and Vournas, 1998)

$$P = -\frac{EV}{X} \sin \delta \quad (2.1)$$

$$Q = \frac{EV}{X} \cos \delta - \frac{V^2}{X} \quad (2.2)$$

After eliminating δ using the trigonometric identity we get

$$\left(Q + \frac{V^2}{X}\right)^2 + P^2 = \left(\frac{EV}{X}\right)^2 \quad (2.3)$$

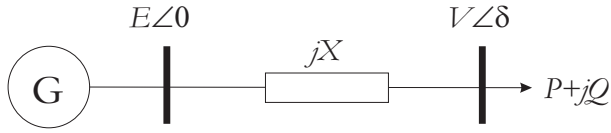


Figure 2.1: Single line diagram of a simple radial power system.

Solving for V^2 yields

$$V^2 = \frac{E^2}{2} - QX \pm X \sqrt{\frac{E^4}{4X^2} - P^2 - Q \frac{E^2}{X}} \quad (2.4)$$

Thus, the problem has real positive solutions if

$$P^2 + Q \frac{E^2}{X} \leq \frac{E^4}{4X^2} \quad (2.5)$$

This inequality shows which combinations of active and reactive power that the line can supply to the load. Substituting the short-circuit power at the receiving end, $S_{sc} = E^2/X$, we get

$$P^2 + QS_{sc} \leq \left(\frac{S_{sc}}{2}\right)^2 \quad (2.6)$$

Some preliminary observations that can be made from the condition (2.6) are:

- The maximum possible active power transport is $S_{sc}/2$ for $Q = 0$.
- The maximum possible reactive power transport is $S_{sc}/4$ for $P = 0$.
- An injection of reactive power at the load end, i.e., $Q < 0$ increases the transfer limit for active power.
- The transfer limits are proportional to the line admittance and to the square of the feeding voltage E .

Thus, it appears more difficult to transfer reactive than active power over the inductive line, and it seems that reactive power transfer can influence the ability of the line to carry active load. Furthermore, assume for now that the load has

admittance characteristics, that is, the active and reactive power received by the load can be written

$$P + jQ = V^2 G(1 + j \tan(\phi)) \quad (2.7)$$

Thus, the load produces reactive power for leading power factor ($\tan(\phi) < 0$) and absorbs reactive power for lagging power ($\tan(\phi) > 0$). After normalizing equations (2.4) and (2.7) using

$$p = P/S_{sc}, \quad q = Q/S_{sc} \quad (2.8)$$

$$v = V/E, \quad g = G/(1/X) \quad (2.9)$$

Using normalized quantities, the positive solution to (2.4) can be written

$$v = \frac{1}{\sqrt{g^2 + (1 + g \tan(\phi))^2}} \quad (2.10)$$

Not surprisingly, there is no voltage drop over the line when the load admittance is zero and the load voltage approaches zero as the load admittance increases towards infinity. Figure 2.2 shows the so-called onion surface (Van Cutsem and Vournas, 1998) given by (2.10) drawn in the pqv -space. It illustrates the relationship between receiving end voltage and transferred active and reactive power, and each point on the surface corresponds to a feasible operating point. The surface visualizes the set of operating points that the combined generation and transmission system can sustain. The actual operating point is determined by the apparent load admittance, and the stability of this operating point is determined jointly by the slope of the surface and the load characteristics. The stability of operating points will be dealt with in Section 2.3. The solid lines drawn on the surface correspond to operating points with varying g and constant $\tan(\phi)$ (shown by the number beside each line). The dashed line around the "equator" of the surface corresponds to the transfer limit according to the condition (2.6).

Figure 2.3 shows so-called pv -curves (Taylor, 1994), which are projections of the solid lines drawn on the onion surface onto the pv -plane. The right-most point of each pv -curve marks the maximum active power transfer for a particular power factor. The corresponding voltage shown by the dashed curve is therefore often referred to as the *critical* voltage and the active loading as the *theoretical transfer limit*. The critical voltage and theoretical transfer limit

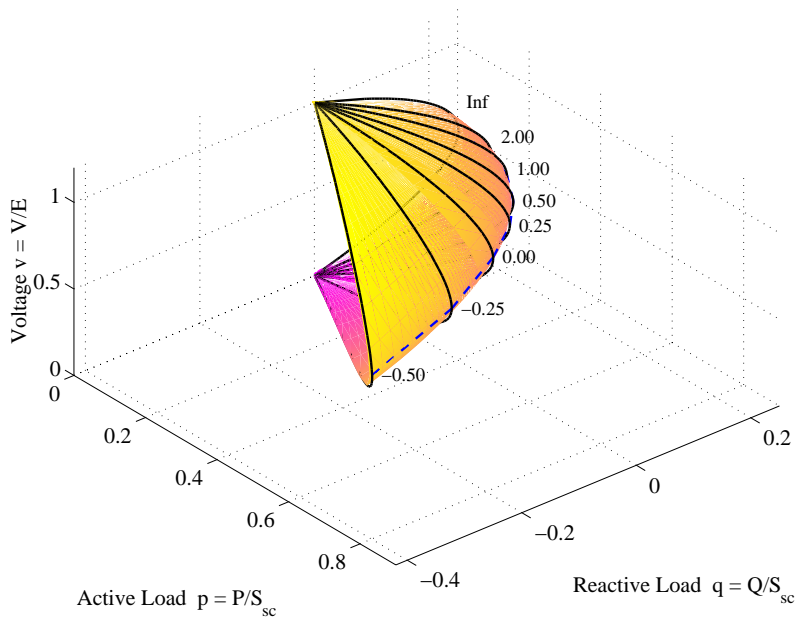


Figure 2.2: The so-called onion surface (Van Cutsem and Vournas, 1998) as given by Equation (2.10) drawn using normalized load quantities.

increase with decreasing $\tan(\phi)$. As will later be demonstrated in Section 2.3, only operating points on the upper half of the pv -curve are stable when the load has constant power characteristics.

According to the condition (2.6), the maximum power a purely active load can theoretically receive through the line is half the short-circuit power at the load bus, given that no reactive power is received at the load end. The shaded region indicates normal operation of a line—the voltage of both ends of the line is normally kept close to the rated voltage of the line. Typical limits are $\pm 5\%$ deviation from nominal voltage. The receiving end voltage at the theoretical transfer limit with a purely active load is $1/\sqrt{2} \approx 0.71$, which is normally considered unacceptable. The *practical transfer limit* is therefore about 35% of the short-circuit power or even lower when the load has a lagging power factor¹. Capacitor banks connected at the load end are often used to increase the load end voltage and thereby the practical transfer limit. Reactive power is

¹The limit referred to here is the voltage-drop limit.

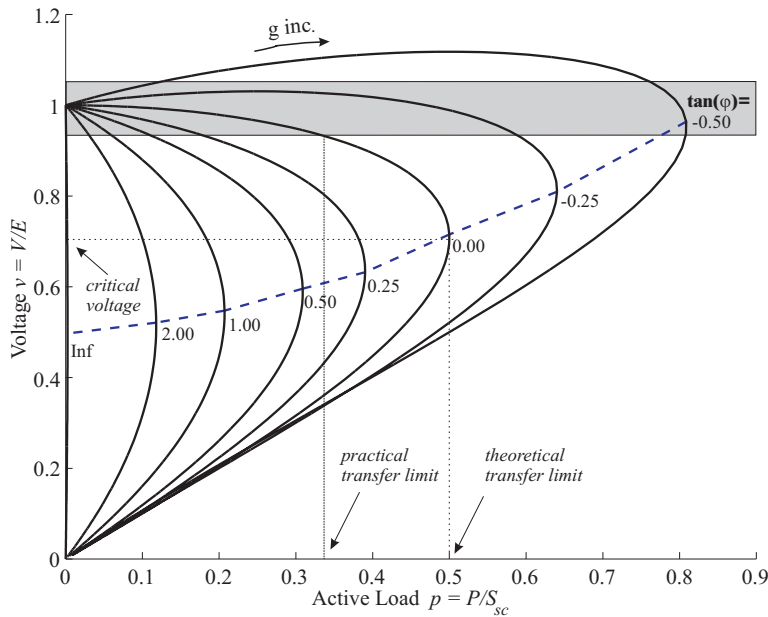


Figure 2.3: The onion surface projected onto the pv -plane. The practical and theoretical transfer limits and the critical voltage is given for $\tan(\phi) = 0$. The shaded region indicates normal operation of the line.

then being produced locally instead of transferred by the line, and the apparent power factor of the load (as seen from the transmission system) is enhanced. The operating point then shifts to another pv -curve corresponding to a lower value of $\tan(\phi)$. When the operating point is on the upper part of the pv -curve, which is the case under normal operation, this corresponds to higher voltage.

The pv -curves also indicate the *stiffness* of system with respect to active power load variations. By overcompensating the load, such that the apparent $\tan(\phi)$ becomes negative, transfer beyond half the short-circuit power with voltage close to nominal levels can theoretically be accommodated. Note however that the sensitivity to load variations, which corresponds to the steepness of the pv -curve within the shaded region, is much larger in an overcompensated system. Another important aspect is that the critical voltage is brought closer to nominal voltage. It will be shown in Section 2.3 that for constant power load characteristics, the theoretical transfer limit coincides with the voltage stability

limit. Thus, the difference between the critical voltage and the voltage of the current operating point can be used as a robustness measure in terms of voltage. Similarly, the difference between the current loading and the theoretical transfer limit can be used as a robustness measure in terms of active power.

2.2 Sources and Sinks of Reactive Power

The previous section showed that the voltage at the receiving end is highly dependent on the absorption or injection of reactive power by the load. The control of voltage is in fact closely related to the control of reactive power. An injection of reactive power at a bus that is not directly voltage regulated will in general increase the voltage of that bus and its surrounding network.

The most important sources and sinks of reactive power in power systems are listed below.

- Overhead (AC) lines generate reactive power under light load since their production due to the line shunt capacitance exceeds the reactive losses in the line due to the line impedance. Under heavy load, lines absorb more reactive power than they produce.
- Underground (AC) cables always produce reactive power since the reactive losses never exceed the production because of their high shunt capacitance.
- Transformers always absorb reactive power because of their reactive losses. In addition, transformers with adjustable ratio can shift reactive power between their primary and secondary sides.
- Shunt capacitors generate reactive power.
- Shunt reactors absorb reactive power.
- Loads seen from the transmission system are usually inductive and therefore absorb reactive power.
- Synchronous generators, synchronous condensers and static VAR compensators can be controlled to regulate the voltage of a bus and then generate or absorb reactive power depending on the need of the surrounding network.

- Series capacitors are connected in series with highly loaded lines and thereby reduce their reactive losses.

Controllable components are generally classified as either *static* or *dynamic*. Static components such as shunt capacitors and reactors can be regulated in fixed discrete steps and with some time delay. They can therefore not be used to improve system response to short-term phenomena such as those related to the generator mechanical or flux dynamics. Hunting phenomena involving such discrete compensation devices may occur in heavily compensated systems (Yorino et al., 1997, Larsson et al., 1998), which have poor voltage stiffness properties. They are however very reliable and cost-effective for reactive compensation in the long term as long as they are used in moderate amounts. On the other hand, dynamic compensation devices, such as synchronous condensers and generators, and static var compensators, can be controlled rapidly and continuously. Thanks to their short response time, they can be used to improve short-term as well as long-term response of the power system. The drawback is that dynamic compensation is 5-10 times more expensive per Mvar of compensation (Taylor, 2000b). Some loads, for example arc furnaces, create fast voltage fluctuations with frequencies of about 2-10 Hz. Such voltage variations require dynamic compensation by for example a static var compensator (Kundur, 1994). The reactive demand from loads close to generation areas is often supplied by the generators and by the less expensive static devices, such as shunt capacitor banks and reactors, in load areas far from generators. It is however not unusual to install capacitor banks in combination with dynamic devices to increase the effective control range of these devices.

Steady-state Characteristics of Compensation Devices

Referring to the $p-v$ -curves shown in Figure 2.4, the effect of the control measures will be discussed in terms of their effect on the system stiffness, critical voltage and the theoretical and practical transfer limits as defined in Section 2.1. Increased stiffness is beneficial for the robustness of the system since it implies a smaller voltage change for a certain change in the load. Increasing the critical voltage is generally detrimental to system robustness since it increases the voltage at which voltage instability occurs². The separation of the theoretical

²Assuming constant power load characteristics (Pal, 1992)—the system may still be stable for other load characteristics.

and practical transfer limits can be used as a measure of the system robustness against load change.

The shape of the p - v -curve of the uncompensated system depends on the power factor of the load as well as the impedance of the line and the feeding end voltage. The load is now supplied through an ideal tap changing transformer and shunt compensation is connected at the load bus, below the transformer, where applicable. Series compensation is inserted in series with the line impedance. The base case with no compensation corresponds to the system studied in Section 2.1 with $E = 1$, $X = 1$ and $\tan(\phi) = 0$.

Shunt capacitors act by adding capacitive admittance to the load and can thereby adjust the power factor of the load as seen from the transmission system. The amount of reactive power generated by a capacitor is quadratically dependent on the voltage so it will provide less support at low voltages. Compensation by capacitor banks increases the practical transfer limit but also increases the critical voltage and decreases the stiffness of the system. The theoretical and practical transfer limits are brought closer together. The injection of a fixed amount of reactive power at the load bus, for example by a generator, increases the critical voltage less than the corresponding amount of shunt capacitor and is less detrimental to the stiffness of the system. In addition, the injection of a fixed amount of reactive power increases the theoretical and practical transfer limits more than the corresponding amount of capacitor compensation. Shunt reactors have the opposite effect compared to capacitor banks and are sometimes used to absorb excess reactive power produced by lightly loaded lines and cables.

Generators normally operate in voltage control mode in which an *automatic voltage regulator* (AVR) acts on the exciter of a synchronous machine. The exciter supplies the field voltage and consequently the current in the field winding. Within the capability limits of the machine, it can thereby regulate the voltage of the bus where it is connected. The response time of the primary controllers is short, typically fractions of a second, for generators with modern excitation systems. The amount of reactive power that a generator must produce to regulate the voltage depends on the structure and load situation of the surrounding transmission system.

Series capacitances are connected in series with the line inductance and can lower the apparent reactance of a line and thereby scale the p - v -curve along the p -axis. This increases the maximum transfer capability of the line without increasing the critical voltage and thereby keeps the theoretical and practical trans-

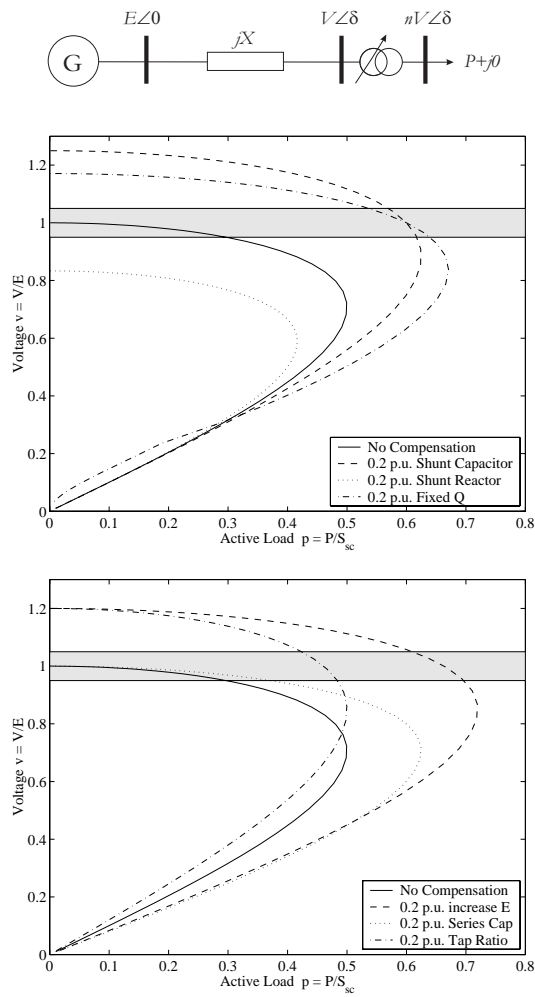


Figure 2.4: The effect of various compensation devices in the pv -plane.

fer limits separated. The stiffness of the system is improved and series capacitors would appear to be the ideal compensation device. They have however, a reputation of causing subsynchronous resonance and need complicated protection equipment to protect them from fault currents (Kundur, 1994). They are therefore not in widespread use for the purpose of alleviating voltage problems, since voltage problems are often less expensively solved using shunt compensation. Although the installation of series capacitors most often has been motivated by other types of stability problems, they do however contribute to improved voltage control where they have been installed.

Power transformers with on-load tap changers can scale the pv -curve along the v -axis and thereby increase the practical but not the theoretical transfer limit. Transformers equipped with tap changers can shift reactive power between their primary and secondary sides and thereby regulate the voltage of their low voltage side. The regulation of the low side voltage however affects the voltage at the high voltage side in the opposite direction. This effect is small under normal operation but may be a significant factor in voltage instability incidents such as described in Section 2.3. When the tap ratio is increased, stiffness of the system is sacrificed and the practical transfer limit moves closer to the theoretical limit.

An increase of the feeding voltage E scales the pv -curve along both axes and thereby increases the practical and theoretical transfer limits. The stiffness is slightly decreased and the practical and theoretical transfer limits are brought closer together. Note however that the control range of the feeding voltage is usually limited since both line ends must comply with the practical voltage limit.

Similarly to the production of reactive power by shunt capacitor banks, the generation by cables and overhead lines is quadratically dependent on the voltage and has a similar detrimental effect on the system stiffness.

Voltage Sensitivity of Loads

So far, we have assumed that the apparent admittance of the load is constant. However, the admittance of many loads varies with the supply voltage—either by their inherent design or by control loops connected to the load devices. Typical examples of such loads are motor drives equipped with power-electronic converters and thermostatically controlled heating devices, which adjust their apparent admittance in order to consume constant power. The composite load

seen from the transmission level often contains a significant amount of induction motor loads, which exhibit potentially very complex voltage behaviour. However, for small voltage excursions, say less than 10 %, the active power drawn by induction motors can in the long term be approximated as constant and the reactive power as proportional to an exponential of the voltage. The dynamic response of loads to voltage changes plays a major role in the analysis and evolution of voltage instability. Simplifying matters somewhat, the load as seen from the transmission level can normally be considered as constant power in the long term since it is connected through tap changers that keep the load voltages close to their nominal values.

There are two fundamentally different approaches to the modelling of voltage dependency of the aggregate load at a high-voltage bus. One method is to start from models of the individual load devices and aggregate them according to the load composition below a certain point in the network. The main advantage of this approach is that the load parameters have a physical meaning. Since each load device is physically modelled, it is reasonable to assume that these aggregated models are appropriate for large disturbances, provided that the individual component models and their parameter values are appropriate. Drawbacks of this method are the difficulty of knowing the true load composition and the large computational complexity when these models are used for simulation. A survey on this type of load modelling is given in IEEE (1995).

The other approach, referred to as generic load modelling, employs parameter estimation methods and black-box modelling. Parameter values in a nominal model structure can be mathematically extracted from a recorded load response to a known disturbance. A disadvantage with these models is that they can usually only be trusted to be reliable under the same loading conditions and for the same type of disturbance as were applied when the recordings were done. Control design on the basis of this type of model would require on-line parameter estimation or a conservative choice of parameter values based on extensive field measurements. The load model used throughout this thesis was proposed by Karlsson (1992) through the parameter estimation approach to load modelling. Load parameter values obtained over a wide range of operating conditions were also given. The model is based on the assumption that most load devices have an instantaneous voltage dependency resulting in an instantaneous load relief if the supply voltage decreases, and a steady-state voltage dependency that gives a lasting load relief. The instantaneous dependency is generally stronger than the

steady-state dependency. The load model structure is:

$$T_p \frac{dx_p}{dt} = -x_p + P_s(V) - P_t(V) \quad (2.11)$$

$$P_d = x_p + P_t(V) \quad (2.12)$$

where x_p is an internal state modelling the load recovery dynamics. The active power load model is parameterized by the steady-state voltage dependency $P_s(V) = P_0 V^{\alpha_s}$, the transient (instantaneous) voltage dependency $P_t(V) = P_0 V^{\alpha_t}$ and a recovery time constant T_p . P_d is the actual active power load and P_0 is the sum of the rated power of the loads connected. A similar model is used for the reactive power, with corresponding characteristics $Q_s(V) = Q_0 V^{\beta_s}$, $Q_t(V) = Q_0 V^{\beta_t}$ and recovery time constant T_q . The voltage V is here normalized using the nominal voltage of the bus where the load is modelled. Typical parameter values are shown in Table 2.1.

When the load dynamics are fully recovered and the load is supplied at nominal voltage, the actual load demand is equal to the sum of the ratings of all connected load devices. This model is a special case of the generalized framework for black-box load models presented in Karlsson and Hill (1994). A generic model that includes also the effects of varying voltage phase angle has been presented by Ju et al. (1996). Results from field measurements on the BC Hydro system were presented by Xu et al. (1997), based on a generic load model structure presented in Xu and Mansour (1994). More recent work has used higher-order load models to account for the effect of cascaded tap changers in the downstream load (Lind and Karlsson, 1996, le Dous, 1999).

The response of a power system model to critical disturbances is highly dependent on the load representation used. Borghetti et al. (1997) make a comparison between the responses of detailed induction motor load models and a generic exponential recovery load model, and conclude that a detailed representation of induction motors is required in voltage stability studies of systems with a significant amount of induction motor load. Arnborg et al. (1998) compare the system response with different types of generic dynamic load models and conclude that the type of load representation used can affect the qualitative behaviour of the system, even if the load models exhibit the same response to a nominal disturbance, such as the one applied when the load recordings were done. Despite this potential drawback of the generic load models, they are often the best choice available since the values of their parameters can be

| T_p | T_q | α_s | α_t | β_s | β_t |
|----------|----------|------------|------------|-----------|-----------|
| 60-300 s | 30-200 s | 0-2 | 1-3 | 2-5 | 4-6 |

Table 2.1: Typical parameter values for the load model given by Equations (2.11)-(2.12). Adapted from Karlsson and Hill (1994).

extracted from off-line experiments or even by on-line estimation. The discrepancies found when comparing generic load models and detailed induction motor models present themselves mainly at very low voltages, say at less than 90 % of rated voltage. If the voltage is kept higher than that by appropriate emergency control, the generic load models can be expected to be accurate as long as the choice of parameter values is appropriate. An early approach to on-line estimation of load parameter values was presented by Dovan et al. (1987).

2.3 Voltage Stability

The *voltage stability* of power systems basically implies its capability of reaching and sustaining an operating point in a controllable way following a disturbance, and that the steady-state post-disturbance system voltages are acceptable. More formal definitions can be found for example in Van Cutsem and Vournas (1998). Furthermore, the term *voltage instability* denotes the absence of voltage stability and *voltage collapse* the transition phase during which a power system progresses towards an unacceptable operating point due to voltage problems, often resulting in blackouts or separation of the system into separate unsynchronized islands.

The dynamics of voltage phenomena can be divided into the two main groups: short- and long-term dynamics. Short-term phenomena act on a time scale of seconds or shorter and include, for example, the effect of generator excitation controls, induction motor recovery/stalling dynamics and FACTS³ devices. The long-term dynamic phenomena act on a time scale of minutes and include, for example, the effect of recovery dynamics in heating load and the effect of generator overcurrent protection systems. A detailed categorization of phenomena into the short- and long-term categories is given in Van Cutsem and Vournas (1998).

³Flexible AC Transmission System

As discussed in the previous section, many loads respond to a voltage drop by increasing their apparent admittance. Assume that the load supplied by the network in Figure 2.1 has such a recovery mechanism according to the normalized model

$$T \frac{dg}{dt} = p_0 - p \quad (2.13)$$

$$p = g v^2 \quad (2.14)$$

Thus, the load has instantaneous admittance characteristics but also an internal controller that aims to restore the power drawn to constant power p_0 with the time constant T s. Furthermore, assuming that the load is purely active ($\tan(\phi)=0$) and combining (2.10) and (2.13)-(2.14), the full model can be written in the differential-algebraic form

$$T \frac{dg}{dt} = p_0 - g v^2 \quad (2.15)$$

$$v = \frac{1}{\sqrt{g^2 + 1}} \quad (2.16)$$

Substituting (2.16) in (2.15) yields

$$f(g) = \frac{dg}{dt} = \frac{1}{T} \left(p_0 - \frac{g}{1 + g^2} \right) \quad (2.17)$$

Solving for stationary points yields the two solutions

$$g^* = \frac{1}{2p_0} \pm \sqrt{\frac{1}{4p_0^2} - 1} \quad (2.18)$$

Thus, we can conclude that there are two separate equilibria if $p_0 < 0.5$ that coalesce for $p_0 = 0.5$. For $p_0 > 0.5$ there appears to be two separate equilibrium points with complex g . But g is real-valued since we have defined it as the real part of the admittance phasor in equation (2.7). Thus, we can conclude that there are no equilibria for $p_0 > 0.5$ and that a *loss of equilibrium* occurs when p_0 increases beyond 0.5. Since (2.17) is always positive for $p_0 > 0.5$, the admittance will increase towards infinity (or an internal limit in the load device) and the load voltage will approach zero. Small-disturbance stability analysis (Kahlil, 1992) can be used to determine that for $p_0 < 0.5$, the low admittance solution

corresponding to the upper half of the pv -curve is asymptotically stable and the high admittance solution on the lower half is unstable.

Figure 2.5 shows simulation results with the initial state at the stable and unstable equilibria for $p_0 = 0.3448$, respectively. At simulation time 20 s, the load setpoint is increased to $p_0 = 0.4$. From (2.18) we see that for the given initial value of the active power load, there are two possible solutions:

- The load operates in the stable equilibrium (a) on the upper part of the pv -curve. When the load setpoint is increased, the load increases its admittance and the operating point moves toward (a') to the right on the pv -curve. This corresponds to higher active power transfer on the line and the load settles at the new equilibrium point (a') with a slightly lower voltage and the load consumption at its new setpoint. The combined load and transmission system is thus stable.
- The load operates in point (b) on the lower part of the pv -curve. When the load setpoint is increased, the load increases its admittance and the operating point moves to the left on the pv -curve. This corresponds to even lower load consumption and the load increases its admittance further, moving the operating point further to the left and so on. Thus, the operating point is unstable and the system will approach the point (0,0) in the pv -plane.

Assuming constant power load characteristics as above, the theoretical transfer limit marked by the dashed curve in Figures 2.2–2.3 therefore also becomes a steady-state voltage stability limit. However, note that the operating point may transiently move to the unstable lower part and back again to the stable equilibrium on the upper part of the pv -curve. Analogously, there is no guarantee that the system will reach a stable operating point simply because such an operating point exists. A trajectory will only approach the stable equilibrium as long as it remains within the *region of attraction* of the stable equilibrium. Such regions of attraction can be approximately computed using a Lyapunov-method for general dynamical systems, but the problems of finding a good Lyapunov-function may make the results conservative (Kahlil, 1992). Vu and Liu (1992) present other analytical methods for computation of such stability regions. In the simple case studied here, the region of attraction can be found exactly, and is bounded by point (b) on the pv -curve in Figure 2.5. That is, for all initial conditions with an admittance value smaller than that corresponding to the

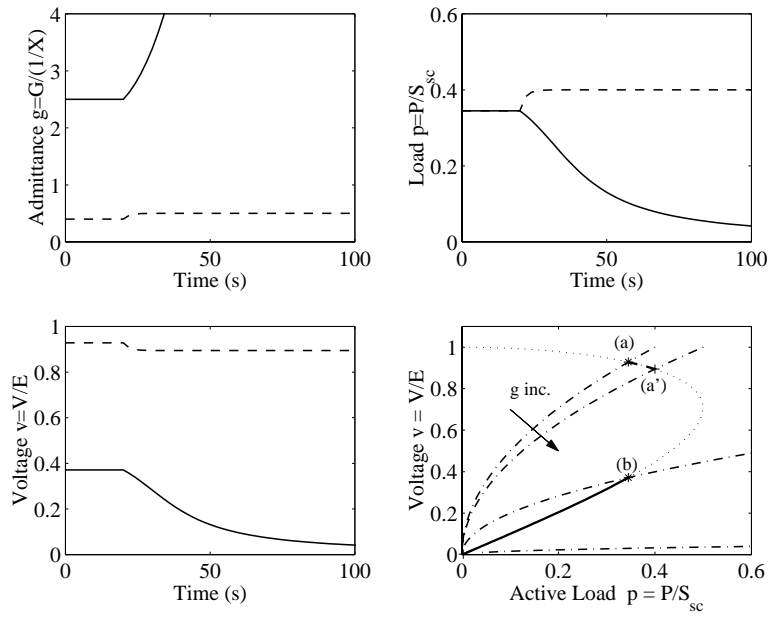


Figure 2.5: Illustration of voltage instability due to load recovery dynamics. Dashed curves correspond to the stable case, and the solid curves to the unstable case. The dotted line is the $p-v$ -curve and the dash-dotted lines correspond to (transient) load characteristics for different g .

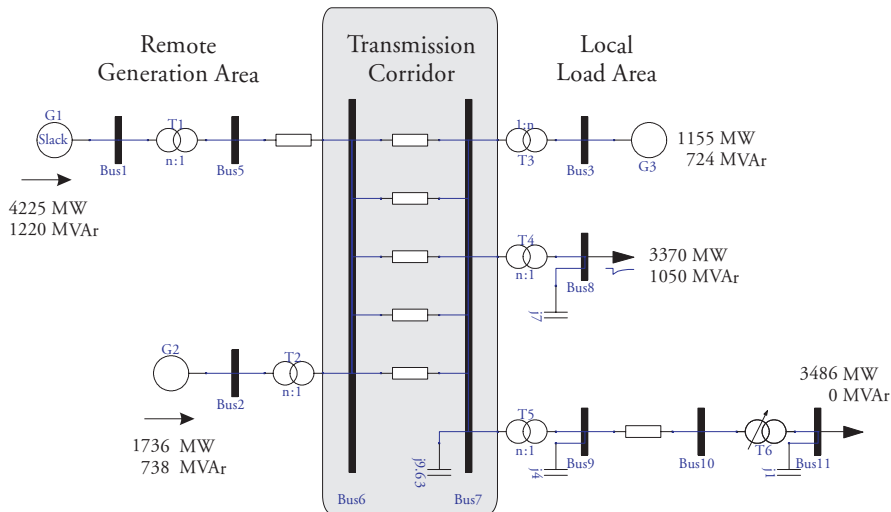


Figure 2.6: The BPA test system (CIGRE, 1995b).

unstable equilibrium, the system will approach the stable equilibrium. Since the equilibrium point (b) is unstable, it has no region of attraction. Operating points on the lower half of a p - v -curve can still be stable with other load characteristics than constant power. For example, all operating points are stable when the steady-state load characteristic is constant impedance.

Case Study - BPA Test System

Figure 2.6 shows a one-line diagram of the BPA⁴ test system (CIGRE, 1995b) that will be used to illustrate some of the mechanisms of voltage instability by time simulation. This small system shares some of its characteristics with the Nordic system studied in Paper E. Both systems have most of their generation in a remote area that is connected to a main load area through five transmission lines. Most of the load is supplied by generators G1 and G2 in the remote generation area and is transported to the load area through the transmission lines. Generator G3 in the local area supplies a small amount of active power, but another important role is to regulate the voltage at Bus 7, to maximize the transfer capability of the lines of the transmission corridor.

⁴Bonneville Power Administration (<http://www.bpa.gov>)

Generator G1 is modelled as an infinite bus and generators G2 and G3 using 6th-order dq-models with IEEE ST1A excitation systems and integral-type overexcitation limiters. The load at bus 8 is modelled with instantaneous constant impedance characteristics but recovers to constant power load with a time constant of 1 s. The load at bus 11 is modelled as a constant impedance and is connected through the tap changing transformer T6. The transformer T6 is controlled by an inverse-time relay according to model *Detailed* in Paper C that adds load recovery dynamics to the load at bus 11. The full simulation model in ObjectStab format can be downloaded from Larsson (2000b).

Figure 2.7 shows simulation results of a fault and the subsequent disconnection of one of the five parallel lines at simulation time 10 s. The course of events is fairly typical for voltage instability incidents triggered by a fault in the transmission system.

1. At time 10.07 s, the fault is cleared and the line is disconnected.
2. At approximately time 13 s, the short-term dynamics which include the generator electromechanical and the fast load recovery dynamics at bus 8 have settled. The voltages at buses 8 and 11 settle at 0.89 and 0.9 p.u., respectively, and the field currents of both G2 and G3 are below their overexcitation limits. Since the voltage at bus 11 is below the OLTC deadband, its internal timer is started.
3. At time 22.5 s, the OLTC makes its first operation and slightly increases the voltage of bus 11, however it is still below the tap changer deadband. The OLTC operation further depresses the voltage of Bus 10 and increases the reactive power demand from generator G3, which now exceeds its overexcitation limit and its internal timer is started.
4. At time 32.5 s, the overexcitation limiter limits the field voltage of the generator G3 to its internal setting at 2.9 p.u., and voltage support of the load area end of the transmission corridor is lost.
5. Between times 37-97 s, the tap changer of T6 operates and aims to restore the voltage of bus 11. However, the tap changer also increases the apparent admittance of the load at bus 11 and thereby puts additional strain on the transmission system. Since G3 is now unable to supply the necessary reactive power to regulate the voltage at bus 7, the voltage decreases further and consequently the reactive losses in the lines of

the transmission corridor increase. The increased reactive power demand must now be supplied from the remote generators G1 and G2, and G2 reaches its limit at approximately time 87 s. The limiter is activated ten seconds later.

6. After time 97 s, with both generators G2 and G3 at their field limitations, the voltages of both bus 6 and bus 7 decrease and the transfer capability of the lines in the transmission corridor is further decreased. The tap changer of T6 makes two more operations and is now at its maximum setting. Hereafter, the load recovery dynamics of the load at bus 8 drive the final stage of the collapse until the simulation terminates at time 160 s.

We observe, in agreement with for example Taylor (1994) and Kundur (1994) who have made similar studies of the BPA test system, that the voltage collapse is due to a complex interaction of the following factors:

- The apparent impedance and consequently the voltage drop and losses across the lines of the transmission corridor increase when the line has been disconnected.
- The load recovery dynamics of the load at bus 8 and the combined transformer and constant impedance load at bus 11 are unfavourable, since they aim to restore the load demand even at the reduced voltage.
- After the overexcitation limiters have been activated, the generators are unable to supply enough reactive power to compensate for the increased losses in the lines of the transmission corridor, and consequently they can no longer regulate their respective terminal voltages.

Other mechanisms that can cause or play a significant role in voltage collapse phenomena include; line protection, the response of governor and automatic generation controls following generation outage, the control limits of FACTS devices and rapid load increase (Kundur, 1994). As illustrated above, voltage collapses are often cascades of events, with many contributing factors, that leads to the final breakup of the system. Arnborg (1997, and references therein) describe the course of events in several actual voltage collapses.

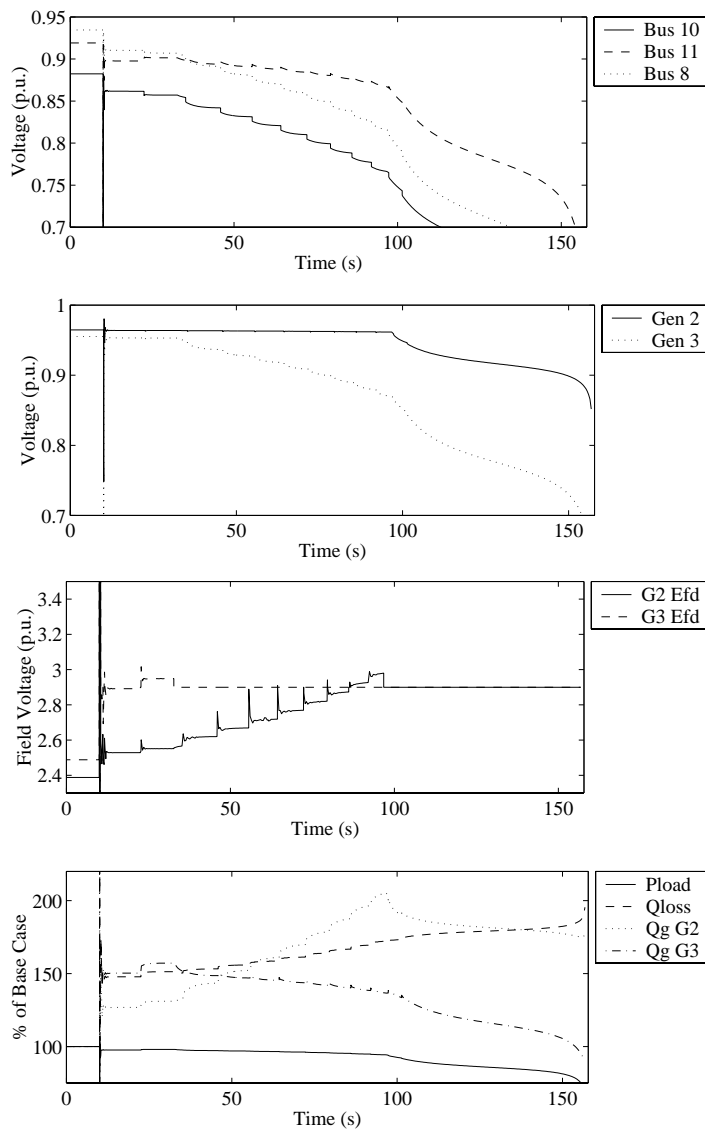


Figure 2.7: Simulation results illustrating voltage collapse in the BPA test system. Pload denotes the sum of the active load as buses 8 and 11, and Qloss denotes the reactive losses in the lines of the transmission corridor.

Countermeasures Against Voltage Collapse

Many countermeasures against voltage collapse have been proposed (CIGRE, 2000). Some examples are undervoltage load shedding, switching of capacitor banks, activation of fast-starting generation, rescheduling of active and reactive power generation, and locking or backstepping of tap changers. The effect of some of these countermeasures can be understood from the p - v -curves shown in Figure 2.8.

Assume again that the combined network and load is modelled by the model (2.15)–(2.16). Thus, the purely active load has instantaneous constant impedance characteristics but recovers to constant power with a time constant. Referring to the left figure in Figure 2.8, assume that the load has the internal setpoint set at $p_0 = 0.55$, that is, its steady-state load characteristic is given by the line (a). There is then no intersection of the steady-state load characteristic and the p - v -curve. Such a situation can present itself following a rapid load increase or, perhaps more likely, due to the tripping of transmission lines. Based on the observations on pages 41–44, we can conclude that voltage collapse will occur due to loss of equilibrium. Load shedding can be modelled by decreasing the load setpoint p_0 . The load characteristic (a') corresponds to $p_0 = 0.45$ and has two intersections with the p - v -curve, each corresponding to an equilibrium point. Again, based on the observations on pages 41–44, we can conclude that one of those is stable. Thus, load shedding appears to be a way of stabilizing the system in case of voltage instability.

Figure 2.9 illustrates the effect of load shedding in the BPA test system using undervoltage load shedding relays as proposed by Vu et al. (1995). At time 93.5 s, the voltage at bus 8 decreases below the load shedding threshold at 0.82 p.u., and 1.5 s later the relay sheds 5 % of the load at bus 8. The OLTC of transformer T6 then makes two more operations to restore the voltage at bus 11 and all voltages settle to stable values. The load reduction corresponds to about 3 % of the combined pre-disturbance load at buses 8 and 11.

Referring to the middle figure in Figure 2.8, the connection of a capacitor bank at the load end can improve the apparent power factor of the load and create equilibrium points on a new, more favourable, p - v -curve. Assume again that the load has steady-state constant power characteristics given by the line (b). Then there are no equilibrium points without a capacitor bank, and voltage collapse will occur due to loss of equilibrium. Switching in a capacitor bank will create two new equilibrium points given by the intersections of the new

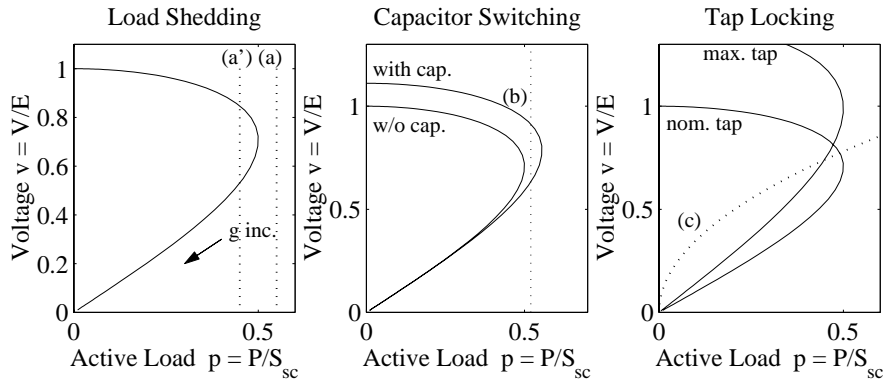


Figure 2.8: Illustration of various countermeasures against voltage collapse. The solid lines are pv -curves with constant $\tan(\phi)$ and the dotted lines correspond to steady-state load characteristics.

pv -curve and the steady-state load characteristics. It can be concluded in the same way as for load shedding that one of these equilibrium points is stable.

Referring to the right figure in Figure 2.8, as tap changers increase their ratio, the pv -curve is scaled along the v -axis. Suppose now that the load has constant impedance steady-state characteristics as indicated by the figure. The load thus lacks the recovery dynamics assumed earlier in this section. Based on results presented for example by Pal (1995), we can thus conclude that any intersection of the (constant impedance) steady-state load characteristic and the pv -curve would indicate the existence of a stable equilibrium point. Suppose that the operating point is in the stable equilibrium given by the intersection of the nominal tap pv -curve and the load characteristic. If the voltage here is lower than the voltage defined by the control system deadband, the tap ratio will increase towards the maximum tap unless the tap is locked. Under normal operation this would correspond to increased load side voltage—standard relay controllers for tap changers make that assumption—but due to the high load in the case considered, the voltage actually decreases further as the tap ratio is increased. By locking the tap changer, the destabilizing control loop is broken and the controlled voltage can settle at a low but stable voltage. The sign change in the effect of tap changer control is known as the reverse action phenomena and is described in for example Ohtsuki et al. (1991). The effect of tap changer controls is a major factor in the development of voltage collapse, especially where

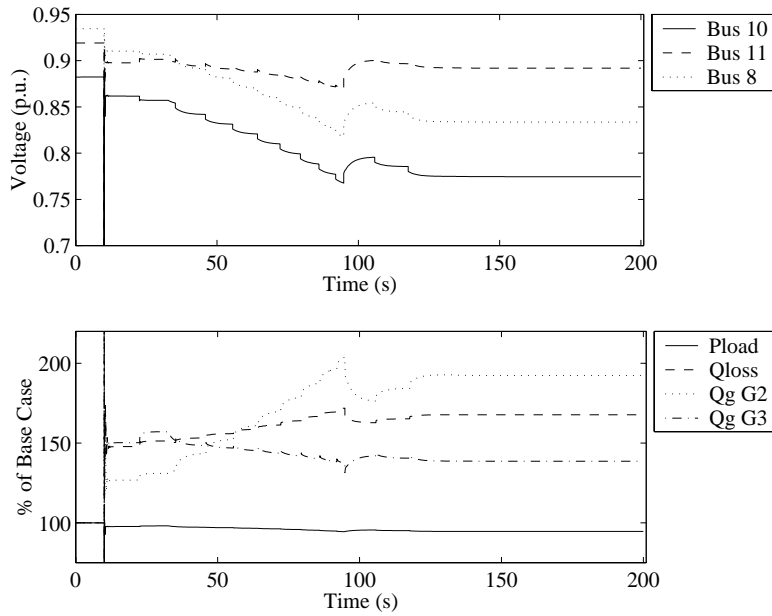


Figure 2.9: Simulation results illustrating successful stabilization of the voltages in the BPA test system by undervoltage load shedding of 5 % of the load at bus 8 at simulation time 95 s.

there are cascaded tap changers and when their effect is combined with the effect of generator current limiters. The effect of tap locking is highly dependent on the steady-state load characteristics. For tap locking to be an effective control, the load must have a high degree of steady-state voltage dependence. If the load has instantaneous constant power characteristics and is connected directly to the transformer, tap locking has no effect at all (Pal, 1995).

Figure 2.10 illustrates the effect of tap locking in the BPA test system. At time 82.5 s, the voltage at the primary side of transformer T6 decreases below the tap locking threshold at 0.82 p.u. and the tap is immediately locked. The voltages then settle at stable values. Since the voltage at bus 11 is lower than the pre-disturbance voltage, it draws less power than at the pre-disturbance operating point. Although the voltage at Bus 11 may be unacceptably low, the collapse has been arrested and the time frame within which other emergency controls can be taken has been extended. The load reduction corresponds to about 5 % of the combined pre-disturbance load at buses 8 and 11.

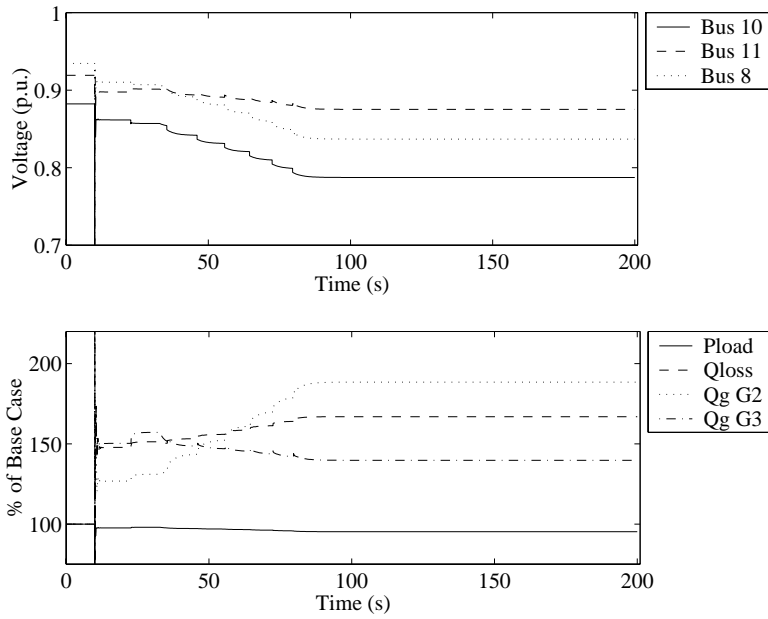


Figure 2.10: Simulation results illustrating successful stabilization of the voltages in the BPA test system by locking of the tap changer of T6 at simulation time 81 s.

Note that the discussion above considers only the *existence* of stable operating points and consequently whether or not it is at all possible to stabilize the system using the considered countermeasures. Also, quite strong assumptions on the steady-state load characteristics are made, such as that they are constant power and constant impedance. To guarantee attraction to the stable equilibria created by the countermeasures, also transient load characteristics and the issues of regions of attraction must be considered. In turn, this implies that proper timing of emergency control is also necessary. The discussion of these issues is however out of scope of this introductory chapter. Detailed studies of load shedding, accounting for transient load characteristics in aggregate load models are given for example in Xu and Mansour (1994), Arnborg et al. (1998), Pal (1995), Balanathan et al. (1998b). Similar studies on capacitor switching are given in for example Vu and Liu (1992), Pal (1995) and on tap locking in Vu and Liu (1992), Popović et al. (1996a). A general conclusion that can be

made regarding the use of these countermeasures is that exact and well-timed control actions are necessary, and that their effect is highly dependent on the current operating point and the load characteristics. The scheme described later in Papers D–E employs voltage predictions based on aggregated dynamic load models to account for these dynamic effects.

The current limiters of generators G2 and G3 played a central role in the voltage collapse in the BPA test system studied in the previous section. Starting emergency generation at the load end will support the load end with reactive as well as active power, reduce the load of the limited generators and support the voltage at the load end. Even if the limited generators are not taken out of their limits, the support may be enough to arrest a voltage collapse. When generators situated at the load end that are equipped with armature current limiters reaches their armature limit, it may be beneficial to reduce their active power production and thereby increase their capacity of supplying reactive power (Johansson, 1999). Another approach is to include "soft" generator current constraints, allowing temporary overloading of a generator to utilize the thermal capacity of the generator windings (Johansson and Daalder, 1997). Soft current constraints may not be enough to arrest a collapse by themselves, but may slow the speed of the collapse and thereby provide time to take other emergency control actions.

2.4 Distribution System Voltage Control

Distribution system voltage control is sometimes referred to as volt/var control (VVC), which Grainger and Civanlar (1985) specify as follows: The objective is to minimize the peak power and energy losses while keeping the voltage within specified limits for a variety of nominal load patterns. This objective is formulated as an optimization problem that is solved off-line, based on nominal load patterns. The optimization variables are the locations, sizes and control deadbands of capacitors and tap changer voltage regulators.

The primary means of on-line voltage control in Swedish distribution systems are tap changers, but in many places also capacitor banks are used. Tap changers are normally automatically controlled by a relay controller that measures and regulates the secondary side voltage of the transformer. Such relays are described in for example Papers A, B and C and the references cited therein. The control of transformers operating in parallel in the same substation must be coordinated to minimize circulating reactive power flows (Lakervi and Holmes, 1989). Capacitor banks may be controlled automatically, by a voltage- or time-

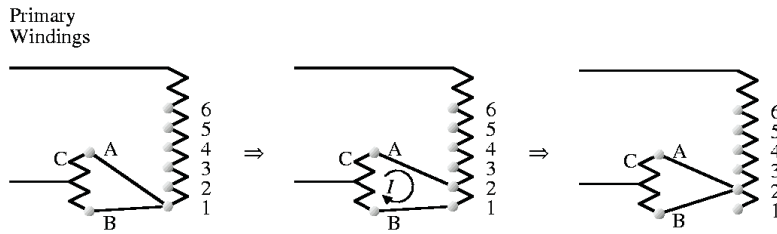


Figure 2.11: The three stages of a tap operation.

relay, or by manual switching orders given by operators.

According to the Swedish standard (SS 421 18 11, 1989), the voltage RMS value must stay within

$$V_N - 10 \% < V < V_N + 6 \% \quad (2.19)$$

for LV⁵ networks, where V_N is the nominal voltage. There is no similar standard for the MV voltages, but since there is often no direct voltage control at the LV level, the MV voltages must be regulated to keep the LV voltages within acceptable limits requiring a narrower band at the MV level. The limits used in Papers A–B are

$$-3.5 \% < V_{dev} < 3.5 \% \quad (2.20)$$

during normal service conditions for MV networks, where V_{dev} is the voltage deviation from set-point.

Tap Changing Transformers

Most distribution transformers are equipped with a tap changer for regulation of the secondary side voltage. A tap changer is capable of changing the number of active turns on one winding of each phase, and thereby adjust the transformer ratio. The fundamental principle of the tap changer design can be understood from Figure 2.11. Since the tap changer must operate without interrupting the load current, two separate switching arms are used (A, B). The arms are connected to a bridging reactor (C) whose middle point is connected to the primary winding.

⁵With MV and LV as defined in Figure 1.1.

In the left figure, illustrating operation at tap step 1, both arms are positioned at connector 1. To make a tap operation to the tap step 2, arm A is first moved to the connector 2 (middle figure) by means of a spring mechanism operated by an electric motor. The voltage between connectors 1 and 2 now creates a circulating current through the bridging reactor and the two switching arms. The purpose of the bridging reactor is to reduce this circulating current. Then, arm B moves to connector 2 and the tap operation is completed (right figure). The turns between connectors 1 and 2 are now bypassed, changing the number of active turns of the primary winding and therefore the transformer ratio. Since the current now flows in opposite directions in the two halves of the bridging reactor, it introduces a negligible reactance. Possible tap ratio change is typically $\pm 10 - 15\%$ in steps of $0.6-2.5\%$. The mechanical delay time (T_m) is usually in the range 2-5 s (including operation of the spring mechanism). The actual tap operation needs 0.1-0.2 s to be completed.

Most tap changer mechanisms are filled with oil for the purpose of insulation. When the switching arms are moved, arcing occurs between the arms and the connectors. According to a report reviewing the failure modes of transformers (Spence and Hall, 1995), the most common reason for tap changer failure and maintenance is degradation of the insulation oil and wear on the connectors and switching arms. According to Häring (1995) a typical maintenance interval is every 100000 operations or 6-7 years, whichever occurs first. The maintenance typically involves replacing the connectors and the insulation oil. Papers A–B are mainly aimed at minimizing the number of operations made by tap changers to prolong the maintenance intervals.

2.5 Transmission System Voltage Control

In practical operation of transmission systems the voltage needs to be continuously monitored and controlled to compensate for the daily changes in load, generation and network structure. In fact, the control of voltage is a major issue in power system operation. Kundur (1994) identifies the main objectives of voltage control as:

- Voltage at the terminals of all equipment in the system should be kept within acceptable limits, to avoid malfunction (of) and damage to the equipment.
- Keep voltages close to the values for which stabilizing controls are de-

signed, to enhance system stability and allow maximal utilization of the transmission system.

- Minimize reactive power flows, to reduce active as well as reactive power losses.

Whereas distribution systems as a rule are operated in radial configuration as illustrated in Figure 1.1 on page 6, transmission systems are meshed as illustrated in Figure 1.3 on page 12. The meshed structure makes the voltage control problem more complicated. Consequently, more sophisticated control schemes than those used in distribution systems are necessary. The control of voltage is often divided into the normal, preventive and emergency state control. A brief overview of the strategies used in the different operating states follows in the next section.

Normal State Control

The control of voltage in a large power system such as the Nordel system, shown in Figure 1.3 on page 12, is a very complex issue with several different and possibly contradictory objectives. The control problem is therefore decomposed, both in time and geographical authority.

Primary Control

Primary voltage controllers are used in all power systems to keep the terminal voltages of the generators close to reference values given by the operator or generated by a secondary controller. An *automatic voltage regulator* (AVR) acts on the exciter of a synchronous machine, which supplies the field voltage and consequently the current in the field winding of the machine and can thereby regulate its terminal voltage. The response time of the primary controller is short, typically fractions of a second for generators with modern excitation systems.

Furthermore, many generators use a so-called power system stabilizer (PSS) to modulate the terminal voltage of the machine based on a local frequency measurement to contribute to damping of electromechanical oscillations. Although the power system stabilizer in most cases is integrated in the AVR, it only introduces fast oscillations around the mean value given by the AVR as long as the generator remains synchronized with the rest of the network. Several textbooks provide details about the characteristics of AVRs, for example Kundur (1994).

Most generators are also equipped with protection systems limiting the field voltage or even tripping (Taylor, 1994) the generator in order to avoid thermal damage to the field winding in case the field current exceeds the rated values for a prolonged period of time. Such limiters are called *overexcitation* or *field current limiters* (Kundur, 1994, Van Cutsem and Vournas, 1998). In some countries, for example Sweden, it is also common to use a similar limitation of the armature current to avoid thermal damage to the armature windings. These limiters are typically integrated in the primary voltage controller and generate a signal that overrides, or is added, to the signal given by the AVR. Thereby, the armature and field currents are kept close to or below their respective limits.

Also tap changers and their associated controllers present in the transmission system can be said to belong to the primary control layer. In some countries it is common to have the generator step-up transformers equipped with tap changers (Taylor, 2000a), however these are seldom under automatic control. They can however be used to balance reactive production between generation units if there are separate step-up transformers. Transformers between the transmission and subtransmission system may be controlled by control systems similar to those used in distribution systems, by manual operation, or by a secondary control layer.

Secondary Control

Secondary voltage control acts on a time-scale of seconds to a minute and within regions of the network. The aim of secondary voltage control is to keep an appropriate voltage profile in a region of the system and to minimize circulating reactive power flows and maximize reactive reserves. Secondary voltage control is in operation in some European systems, for example in France (Vu et al., 1996) and Italy (Corsi, 2000). Simulation studies have also been conducted on the Spanish (Sancha et al., 1996), Belgian (Janssens, 1993) and Chinese (Sun et al., 1999) systems.

Normally, the network is divided in a number of geographic regions. One or a few so-called pilot nodes, which are assumed to be representative of the voltage situation in the region, are selected for voltage regulation by the secondary controller. The main actuators are the setpoint voltages of the primary controllers of the generators within a region, although the French implementation also uses static compensation devices such as capacitor banks and reactors. The setpoint values are calculated by an optimization procedure using a lin-

earized static network model to make each generator in the region contribute to the control of the pilot node voltage(s). This optimization takes the individual generators' control authority and equipment limits into account. Furthermore, each region is assumed to be independent.

Tertiary Control

Tertiary voltage control acts system-wide on a time scale of about ten to thirty minutes. The traditional method of tertiary control is so-called reactive power optimal power flow (OPF) (Carpentier, 1962, Dommel and Tinney, 1968). The desired operating conditions are specified in the form of a cost function, which is minimized using nonlinear optimization techniques. Usually, the main goal is to minimize losses and to keep voltages close to rated values. A secondary goal may be to maximize and distribute reactive reserves. The main control variables are voltage setpoints for the generators, or pilot nodes if secondary control is used, and switching orders to compensation devices such as shunt capacitors and reactors. The power flow equations (Glover and Sarma, 1994) are specified as equality constraints in the optimization whereas operational limits such as transfer limits, limits on reactive reserves and voltages are specified as inequality constraints. Where there is a secondary voltage control scheme, the tertiary control may also aim to minimize reactive flows between regions to validate the assumption that the regions are independent. Some implementations also include so-called N-1 security constraints. The optimization then minimizes the cost function with respect to the base case but also checks that the constraints are fulfilled even with fault or outage of any single component (Harsan et al., 1997). OPF is a general method that does not require specific knowledge about the system and can find the optimal operating point based on information available from a SCADA system and a snapshot from a state estimator.

Contrary to the optimization used in the French implementation of the secondary control layer, the nonlinear power flow equations are used in OPF and the optimization cannot be guaranteed to converge. OPF is therefore generally not relied upon to control the system in closed loop, but more as a decision-support tool to the operators and as a planning tool. Since the optimization often makes continuous approximations of discrete controls, it may not find the optimal setting of those. Furthermore, OPF tends to recommend small variations in many control variables and the optimization cannot produce a switching sequence that can be used to reach the optimum control settings.

The secondary control can be seen as a tool to close the loop between OPF and the power system, since the secondary control layer can automatically handle intermediate switching states.

As an alternative to the traditional OPF, a number of so-called hybrid tools have been presented (Liu and Tomsovic, 1986, Cheng et al., 1988, Godart and Puttgen, 1991, Ramos et al., 1995). The hybrid methods typically use a less rigorous mathematical representation of the system, e.g. a linearized equation system, and heuristic rules to generate switching sequences on the basis of the mathematical representation. The switching sequence is then simulated by the hybrid tool before it is presented to the operator. However, a drawback of the heuristic methods is that their design requires some knowledge about the specific system for which the tool is supposed to operate. With a well-adjusted rule base, these tools have been shown to yield near-optimal results compared to traditional OPF tools, but can present results that are significantly easier to use for the operators (Gomez et al., 1996).

Preventive and Emergency State Voltage Control

The operation of power systems can be divided into the states normal, alert or emergency (Kundur, 1994). The system normally operates in the normal state, but enters the alert state if the system cannot be expected to be robust to the contingencies that have been considered in the design of the system. Such situations may occur for example due to unexpected load increase or outage of some component, such that a single contingency may force the system into the emergency state. The system enters the emergency state if a severe enough contingency occurs, so that the system will experience instability or exceed operational limits unless emergency control actions are taken. However, the system is still synchronized in the emergency state. Kundur (1994) also considers the extremis state in which the network has been broken up in smaller islands, and the restorative state where the loads and generators are being reconnected following collapse of the system. However, the extremis and the restorative states are not considered in this thesis, and therefore not further described.

In the normal state, voltages are regulated using the available compensation devices described in Section 2.2 with the aims of minimizing losses and keeping an appropriate voltage profile. Generator active production is generally scheduled using market mechanisms where such are available. Preventive control is sometimes integrated in the secondary and tertiary levels of the nor-

mal state control, and may then include more drastic actions such as rotating disconnection of low-priority loads and rescheduling of generation or HVDC imports/exports. Both the normal state and preventive control are normally based on static system models and their operation is not time-critical.

Emergency control has a time frame of seconds to minutes and requires well-timed control actions. Many different schemes based on for example undervoltage load shedding, capacitor switching, emergency tap changer control and fast active power generation rescheduling have been presented and some utilities have such protection systems in operation. An overview of such installations and the research on protection systems against voltage collapse is given in Section 1.2.

Chapter 3

Solving Problems by Search

This chapter outlines some of the fundamentals of the search methods employed to find the optimal emergency control in Papers D–E. Readers interested in a more detailed account are recommended the doctorate theses by Plaat (1996), Breuker (1998) and Junghanns (1999) as starting points.

Search was one of the first decision methods successfully used in artificial intelligence research, and then especially in computer game playing. The first computerized search technique to play chess was described by Shannon (1950). Although many refinements and additions have been made to the original ideas, these ideas are still used in state-of-the-art chess programs. Other combinatorial games such as Backgammon, Othello and Checkers have also been used as testbeds in the development of new and improved search methods. Junghanns (1999) reports that the best Othello, Checkers and Scrabble programs based on search methods now play superior to the best human players. Also, the chess computer Deep Blue became in 1997 the first chess computer to defeat the current world champion in match play under tournament conditions (Hsu, 1999). In addition to their natural appeal, such combinatorial games are well-suited for the purpose of studying and developing search methods because of their well-defined nature; the set of rules is clear and there is no chance involved. This makes the search problem easy to formulate and enables different research groups to compare their results on a common platform.

Methods developed using these testbeds have found applications also in many other fields. Some examples are: shortest path and travelling salesman

problems, diagnosis, automated discovery, VLSI¹ layout, and assembly sequencing (Stewart et al., 1994, Russell and Norvig, 1995). The research on search has to some extent also driven the development of parallel supercomputers. Hamilton and Garber (1997) give the following more practical potential applications of the chess-playing Deep Blue supercomputer: molecular dynamics, pharmaceutical modelling, crack propagation, data mining and financial risk assessment.

Some early applications of search in power systems research are: coordination of protection systems (Lai, 1988), data validation (Sahba, 1988), dynamic stability evaluation (Chang and Hui, 1988), unit commitment (van den Bosch and Honderd, 1985), feeder reconfiguration (Morelato and Monticelli, 1989, Wu et al., 1991) and power system planning (Pessi et al., 1990). The first application in emergency state voltage control was to the author's knowledge Larsson (1999).

3.1 Short Introduction to Search

The basic assumption when using search methods is that all decision variables can be represented in a discrete state space (normally a graph), and that a solution can be given as a sequence of state transitions. Take for example the classic problem of route-finding (Russell and Norvig, 1995). The problem statement is as follows: A person is at present in Lund and wants to reach Halmstad using the shortest possible route as defined by the road network illustrated in Figure 3.1. Distances are indicated on the lines drawn between the towns.

In the search problem formulation, each town is represented by a state (or node) in a graph and the available state transitions by arcs in the graph. Such transitions are referred to as *actions*. In the literature on game tree search, the equivalent term *move* is most often used for the transitions. Each transition has an associated *cost*, which in the example is taken as the length of the road to the next town. The *initial state* is Lund, the *goal state* is Halmstad and the available actions are given by the road network in the region. A sequence of actions is called a *path*, and finding a solution to the problem is thus equivalent to finding a path that terminates in the goal state. Such paths are called *solution paths*. The *path cost* is the sum of the costs of each individual action in a path. From a quick inspection of the graph we see that there are several possible so-

¹Very Large Scale Integration—a term used to describe complex microchips.

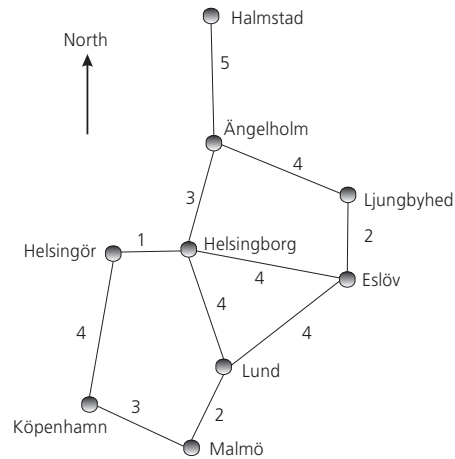


Figure 3.1: Route map for the search example.

lution paths, for example Lund–Eslöv–Ljungbyhed–Ängelholm–Halmstad (at an accumulated cost of 15) and the lowest cost (or *optimal*) solution Lund–Helsingborg–Ängelholm–Halmstad (at an accumulated cost of 12). Some additional terminology is useful in order to formulate solution methods for the search problem: A *successor function* generates a list of the states reachable by any single action in a node, for example, the list Eslöv–Helsingborg–Malmö when evaluated in Lund. An *evaluation function* returns the accumulated cost of making a sequence of actions, that is, the sum of the action costs along a path in the search space.

Furthermore, the cost of a path s originating in the initial node to the final node in s is denoted $g(s)$ and the minimum path cost from the final node in the path s to a goal node is denoted $h^*(s)$. It is also convenient to define the function $f^*(s) = g(s) + h^*(s)$ which then corresponds to the minimum cost of reaching a goal state via the path s .

Uninformed Search

Many different methods for exploration of a search state space have been proposed. Some examples are depth-first, random-walk and breadth-first. We will concentrate on the depth-first² method, which is an example of an uninformed

²Table D.1 on page 133 shows a pseudocode of the depth-first search method.

search method. Uninformed search methods explore the state space in a blind manner without knowledge of the environment—only the available actions in each node are known. This method always expands the first node given by the successor function until it reaches a dead-end node where no more transitions are available. Then it retraces its steps until it reaches a node with successors that were ignored at the first visit, and expands the first of those. The search continues in this way until a solution path is found or until all possible paths in the state space have been expanded. In this way, the state space is organized in a tree structure where the initial state corresponds to the root of the tree.

Since the uninformed search has no preference between different actions, the successor function may return nodes in an arbitrary order. Assume for the sake of presentation that the successor function returns the available actions in alphabetical order. A depth-first search would then expand the sequence Lund–Eslöv–Helsingborg–Helsingör–Köpenhamn–Malmö–Lund–Eslöv, in an infinite cycle. The sensitivity to cycling paths is an inherent property of depth-first search for problems where the state space is a graph, which in this case prevents the search from finding a solution. A simple, although partial, solution is to introduce a maximum *search depth* corresponding to the maximum length of any explored path and consequently to the number of actions necessary to reach the goal state.

Figure 3.2 shows the search tree generated by a depth-first method using different search depths. Search to depth 1 and 2 fail to find a solution, but the search is successful at depth 3 when it finds the goal state through the optimal solution path Lund–Helsingborg–Ängelholm–Halmstad, and the search is terminated. Many nodes not on the solution path have been expanded and still cyclic paths such as Lund–Helsingborg–Eslöv–Lund are explored. Also note that a search to depth 4, which one might expect find a better or at least the same solution, would find the suboptimal solution path Lund–Eslöv–Helsingborg–Ängelholm–Halmstad. Thus, depth-first search does guarantee *completeness* of the search, which means that a goal node is always found if there exists a solution path of shorter or equal length to the search depth. However, *optimality* of the search is not guaranteed unless the complete state space is explored.

Search Enhancements

From the uninformed search example, we see that there is much room for improvement of the basic depth-first search. It is sensitive to cyclic paths, it spends

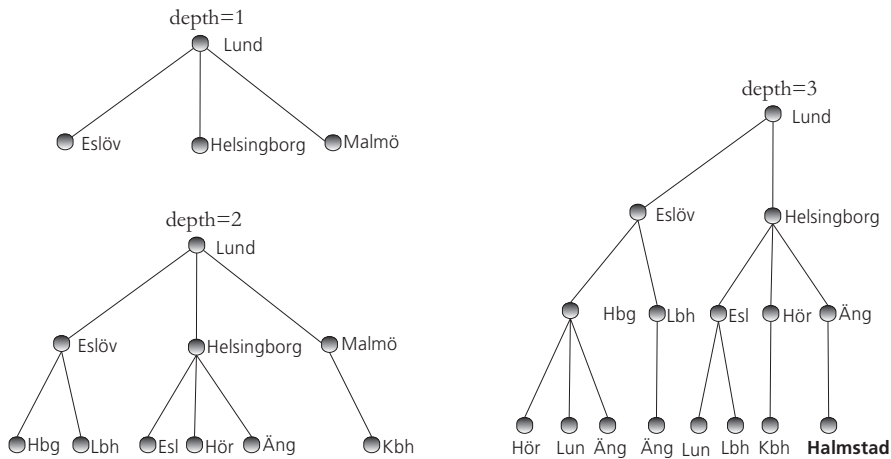


Figure 3.2: Illustration of depth-first search to depth 1,2 and 3 (excluding back-tracking moves).

much time in fruitless parts of the search tree and it cannot guarantee optimality of a solution path unless the complete state space is searched.

These drawbacks make the basic depth-first method inadequate for most practical problems, since the search effort would be huge when all possible paths have to be explored. However, many enhancements to the basic algorithm have been suggested. The purpose of such enhancements is to make the search effort tractable by reducing the number of paths that has to be searched before a solution path is found. This introduction covers only those enhancements used in Paper E. A more complete survey of such enhancements is given in Junghanns (1999).

Transposition Table

Because the search space is actually a graph and not a tree as assumed by the basic depth-first method, many nodes or subtrees are searched more than once during a search. For example, the node Eslöv is visited twice in the search to depth 3 in Figure 3.2. The second time the node Eslöv is visited (on the path Lund–Helsingborg–Eslöv), the subtree below this node has already been searched to a greater depth than the depth remaining here. Since the previous search did not find a solution, the subtree can be safely discarded without sacri-

ficing completeness of the search. The removal of branches in the search tree is referred to as *pruning*.

Transposition tables are often used to store such directing knowledge about subtrees already evaluated. By storing knowledge about evaluated states or subtrees in a table along with some additional information about the status of the search³, a transposition table may reduce the search tree considerably without sacrificing completeness of the search, since redundant searches are eliminated. Generally, the potential reduction depends on the application. A detailed study on the implementation of transposition tables and their average effect on the size of the search tree in chess can be found in Breuker (1998), who reports about a 40 % reduction of the search tree. Plaat (1996) reports the corresponding figure 28 %. As a beneficial side-effect, transposition tables also prevent the occurrence of cycles in the search.

Transposition tables can reduce the search tree for all search problems where the state space is a graph, even if no application-specific knowledge is used. Their implementation, most often as hash tables, are however often application-specific since different applications use hash keys of different lengths.

Move Ordering

In the uninformed example, nodes were expanded in alphabetical order. The purpose of move ordering is to organize the search such that the search space is explored in an order where the goal node is most quickly reached.

Consider for example how such domain-specific knowledge can help reduce search complexity by move ordering: Assume in our example that it is known that the goal node (Halmstad) is north of the initial state (Lund). If moves leading north are expanded first, the search will explore the nodes Lund–Helsingborg–Ängelholm–Halmstad, thus visiting only the four nodes in the optimal solution path.

Using more formal definitions, the strategy described above minimizes an estimate $h(s)$ of the remaining distance $h^*(s)$ to the goal node from the last node in the path s . Typically, the exact distance $h^*(s)$ is hard to compute, but approximations can often be found using domain-specific knowledge. The estimator function $h(s)$ is often referred to as a *search heuristic*. In the example,

³At the minimum, the best solution path s^* and the corresponding solution cost $h^*(s^*)$ found in the subtree below must be stored along with the depth to which the subtree has been explored.

nodes with lesser estimate of the remaining distance are expanded first. Such strategies, which aim to minimize the remaining distance to the goal $h(s)$, are called *Greedy* strategies. Another widely used strategy is to expand nodes in the order minimizing $f(s) = g(s) + h(s)$, aiming to account for the cost of the next segment in the candidate path as well as the goal distance. Such move ordering is used for example by the A*-method (Russell and Norvig, 1995).

The construction of search heuristics requires sound domain knowledge. A poorly designed search heuristic can often do more harm than good since it systematically leads the search off track. A desired property of search heuristics is that they are *admissible*, meaning that they never overestimate the effort of reaching a goal node, that is, $h(s) \leq h^*(s)$.

The heuristic devised here illustrates one of the pitfalls in designing such functions—it only works when travelling north. The straight-line distance between two towns is a more robust and also admissible heuristic, which works when travelling between any two towns.

Pruning based on Lower Bounds

If all action costs are non-negative, the accumulated action cost $g(s)$ always increases as the search progresses deeper into the tree. Therefore, for the path s , $LB(s) = g(s)$ can be used as a lower bound on the cost of any solution path via node s . If we have an admissible search heuristic $h(s)$, the stronger criteria $LB(s) = g(s) + h(s)$ can be used as a lower bound. Consequently, once a solution path s^* with $g(s^*) = b$ has been found, all subtrees originating from the last node in the path s where $LB(s) \geq b$ can be pruned without risk of ignoring better solutions than the one already found⁴.

Lower bound pruning can have a dramatic effect on search complexity, especially when used in conjunction with good move ordering criteria so that good solution nodes are found early in the search.

Iterative Broadening

A depth-first search can venture deep into the search tree and quickly find long solution paths. An obvious drawback is however that a huge amount of time may be spent in less than fruitful regions of the search space if there are only a few goal nodes and/or the move ordering is ineffective. On the other hand,

⁴Since $h^*(s^*) = 0$ and thereby $h(s^*) \leq 0$ for all solution paths s^* .

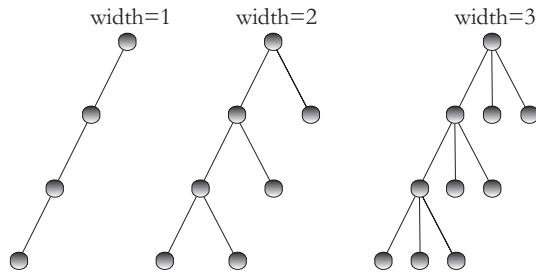


Figure 3.3: Illustration of iterative broadening search with width 1, 2 and 3.

a breadth-first search expands the root node, then all of its successors and *then* the successors of the successors and so on. The obvious drawback of this approach is that a huge amount of time may be spent before the search ventures deep enough to find a solution. Therefore, breadth-first searches usually excel over depth-first searches when there are a few goal nodes distributed at shallow depth, and depth-first approaches excel when there are many goal nodes distributed at large depth. Attempting to overcome the drawbacks of both approaches, an iterative broadening search (Ginsberg and Harvey, 1992) carries out a number of successive depth-first searches as illustrated in Figure 3.3. Only the best move according to the move ordering criteria is considered in the first iteration. In the second iteration also the second best move is considered and so on. The basic idea is to quickly find one reasonably good solution by venturing deep into the tree and then use remaining time available to improve this solution. Since the size of the search tree depends exponentially on the breadth, the effort spent on the search is usually dominated by the last iteration. Transposition tables can be used efficiently in conjunction with iterative broadening if they are modified to store the breadth as well as the depth to which subtrees are searched. In fact, the information collected in these intermediate searches and saved in the transposition table can often make more lower bound cut-offs possible, and an iterative broadening search to a certain depth and width may therefore be computationally cheaper than a single search.

3.2 Combinatorial Optimization using Search

The idea of using search methods to solve combinatorial optimization problems as in Papers D–E is not new. Well-known methods such as hill-climbing, tabu-

search, and branch-and-bound methods are all variations on this theme (Russell and Norvig, 1995). Hill-climbing is a special case of best-first search where the search tree is not retained during the search. Tabu-search is a type of best-first search where a special table, similar to a transposition table, is used to store states that must not be revisited. Branch-and-bound search uses a mechanism similar to lower bound cut-off to prune subtrees that cannot contain solutions better than one already found. Optimization by genetic algorithms can be seen as a random-walk search method, which uses a random mechanism to overcome local minima. A fitness criterion in terms of a cost function is used to facilitate successor generation and thereby concentrate the search on promising parts of the search space. The approach taken in this thesis uses a more traditional search formulation in order to benefit from the many search enhancements developed and analyzed in the research on game tree and single-agent search (Junghanns, 1999, Schaeffer and Plaat, 2000).

A combinatorial optimization problem

$$\text{minimize } J(\mathbf{x}) \quad (3.1)$$

$$\text{subject to } \mathbf{x} \in \mathcal{S}(\mathbf{x}_0) \quad (3.2)$$

$$\mathbf{x} \text{ integer} \quad (3.3)$$

$$\mathbf{G}(\mathbf{x}) \leq \mathbf{0} \quad (3.4)$$

can be solved by search as follows: the search state space is given by the integer constraint and the limits on the optimization variables given in $\mathcal{S}(\mathbf{x}_0)$, and $\mathbf{G}(\mathbf{x})$ defines a goal test. The optimization problem is equivalent to searching the state space for the node that has the minimum value of the cost function among all nodes that pass the goal test. The vector of optimization variables is denoted \mathbf{x} and \mathbf{x}_0 is the initial state. In case the problem contains a mix of continuous and discrete optimization variables, each evaluation of the cost function involves the solution of a reduced (continuous) optimization problem where the discrete optimization variables are fixed.

An important advantage over conventional optimization methods when applied to the voltage control application studied in this thesis, is that the search method can provide not only the optimal control state \mathbf{x}^* but also a switching sequence to reach \mathbf{x}^* from the initial state.

Part II

Included Papers

Paper A

Coordinated Control of Cascaded Tap Changers in a Radial Distribution Network

Mats Larsson Daniel Karlsson

*Stockholm Power Tech, International Symposium on Electric Power
Engineering, IEEE (1995)*

Abstract: *This paper deals with normal state control of cascaded tap changers in a radial distribution network. Field measurements have shown that a number of unnecessary tap operations are made due to lack of OLTC coordination. A tuning rule for the existing local control scheme is suggested as well as a new multivariable control scheme based on on-line tap optimization. The tuning rule has been verified in simulations and field measurements. In simulations, the performance of the multivariable control scheme is compared to that of the existing controllers. It is shown that coordinated control of tap changers can significantly reduce the number of OLTC operations. The reduction is especially pronounced for lower level OLTCs.*

A.1 Introduction

The purpose of distribution network voltage control is to compensate for distribution load variations and disturbances in the feeding transmission network. A number of on-load tap changers (OLTC) are available to regulate distribution network voltages. OLTC operations cause transients and wear on the OLTCs themselves. Therefore, it is desirable to minimize the number of tap operations.

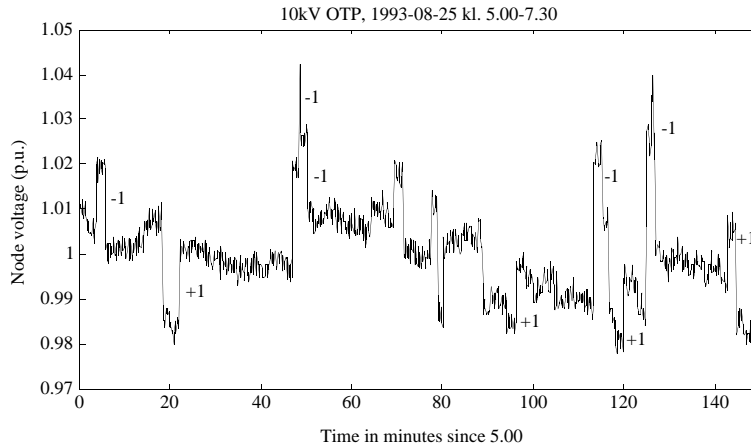


Figure A.1: Field measurement of voltage in the 10 kV substation at Östra Tommarp during load pickup. The tap operations made at ÖTP are marked with +/-1.

Presently, OLTC control is based entirely on local measurements with no coordination between different voltage levels or branches of the network. Since there are many cascaded tap changers, this gives rise to unwanted effects. For example, tap operations in different levels or branches of the networks might counteract one another. Figure A.1 shows a field measurement of the voltage in a 10 kV substation which has three cascaded OLTCs in the network above. The short spikes are due to counteracting tap operations.

A desired property of the OLTC control systems is *selectivity*, i.e., only the correct OLTCs should act to a given disturbance. For a voltage disturbance in the feeding network, this is always the top level OLTC. Efficient coordinated control has to be centralized and needs communication channels between the substations. In the future these will be present and make coordinated control possible.

In this paper a tuning rule for the conventional OLTC control systems is suggested as well as a new control scheme based on on-line tap optimization. It is shown that with coordinated control of cascaded OLTCs, fewer tap operations are needed to compensate for the daily load variations. Only normal state operation is considered.

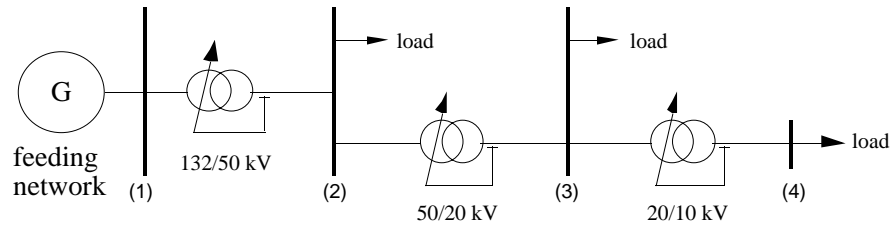


Figure A.2: The network branch used in the simulations.

| Load data | | | Line data | | |
|-----------|----------------------|----------------------|-----------|------------|------------|
| | P_{peak} (p.u.) | Q_{peak} (p.u.) | | R (p.u.) | X (p.u.) |
| 50kV (2) | 0.2865 | 0.1283 | (1) - (2) | 0.0304 | 0.1276 |
| 20kV (3) | 0.0641 | 0.0321 | (2) - (3) | 0.2643 | 0.6963 |
| 10kV (4) | 0.0171 | 0.0090 | (3) - (4) | 0.4002 | 0.5851 |

| transformer data | R (p.u.) | X (p.u.) | tap step (%) | available steps | max MVA |
|------------------|------------|------------|--------------|-----------------|---------|
| (1) - (2) | 0.0028 | 0.2229 | 1.67 | [-9,9] | 70 |
| (2) - (3) | 0.0859 | 0.8539 | 1.67 | [-9,9] | 16 |
| (3) - (4) | 0.0666 | 5.6246 | 1.67 | [-9,9] | 4 |

$S_{base} = 233.84$ MVA, $U_{base} = [130, 50, 20, 10]$ kV
 Peak loads correspond to about 100 % loading of transformers

Table A.1: Network data used in simulations.

A.2 Power System Model

To evaluate the control schemes, a number of simulations have been done with Simulink on a SUN SparcStation 10. The simple network branch in Figure A.2 with three cascaded tap changers has been simulated. The model used represents the branch Tomelilla, Järrestad and Östra Tommarp in a rural distribution area in the southeast of Sweden.

A.2.1 Network Model

Throughout the simulations a single-line equivalent of the power system has been used. Transformers are modelled by an ideal transformer in series with a short-circuit impedance and the distribution lines as simple series impedances. The network data is tabulated in Table A.1. Tap operations are modelled by changes in the transformer ratio. A constant frequency model of the network with the feeding network as a Thevenin source is used.

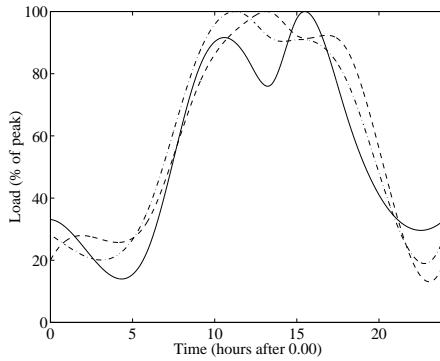


Figure A.3: The load curves used for the 50 kV (solid line), 20 kV (dashed) and 10 kV (dash-dotted) loads.

A.2.2 Load Model

For the aggregated load at each voltage level, the load model suggested in Karlsson and Hill (1994) is used. It is a load model featuring exponential load recovery and nonlinear load-voltage dependency. It is accurate on a time scale of seconds through minutes.

In the simulations the following parameter values have been used for all loads: $\alpha_s = 1.37$, $\alpha_t = 1.92$, $\beta_s = 1.27$, $\beta_t = 1.92$, $T_p = 173$ s and $T_q = 83.5$ s. To model the daily load variations, P_0 and Q_0 are varied according to the load curves in Figure A.3 and the multipliers for the different load patterns.

A.3 Conventional OLTC Control Systems

In the conventional control scheme, each OLTC has its own independent control system. In the simulations only OLTCs with constant-time characteristics have been considered. The conventional control is a simple integrator control with a time delay and a deadband. The size of the deadband sets the tolerance for long-term (longer than the time delay) voltage deviations and the time delay is primarily intended for noise-rejection. An extensive study of the OLTC control systems used in the Swedish distribution systems can be found in Altsjö (1993).

The control system can be modelled by the state graph of Figure A.4. The system remains in state *wait* while the deviation from the secondary voltage

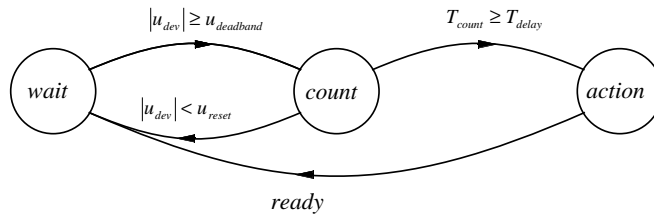


Figure A.4: State graph illustrating function of local OLTC control systems.

setpoint (u_{dev}) is less than the function voltage ($u_{deadband}$). If the limit is exceeded, there is a transition to state *count*. When entering *count* a timer is started and is kept running until either it reaches the delay time, firing a transition to the state *action*, or the voltage deviation is less than the reset voltage (u_{reset}), firing a transition to the state *wait* and reset of the timer. In the state *action* a control pulse to operate the tap changer is given. When the operation is done, the control system gets a *ready* signal from the tap changer and returns to state *wait*.

The aim of this paper is to show that the number of tap operations can be reduced without increasing the voltage deviations. Therefore, the deadbands have been fixed at the present settings (1.5 %) in the simulations and field measurements.

A.3.1 Response to Voltage Disturbance in Feeding Network

It is a common observation in Sydkraft's distribution networks that the delay times of cascaded tap changers are tuned to the same value. Figures A.5–A.6 show excerpts from simulations with different sets of time delays. There are three voltage steps at the 132 kV-level (solid line) due to the connection of three capacitor banks at bus 1 at simulation time 330, 345 and 360 min. In Figure A.5, the same delay time is used for all the OLTCs. After the second and third step voltage steps, more than one of the OLTCs compensate for the voltage deviation at the same time. Since the voltage disturbance already has been compensated for at the highest level, the lower level tap changers have to make reverse tap changes. In Figure A.6, the OLTCs are tuned according to the rule derived, with longer delay time for lower level OLTCs. Four tap operations are avoided with the new tuning.

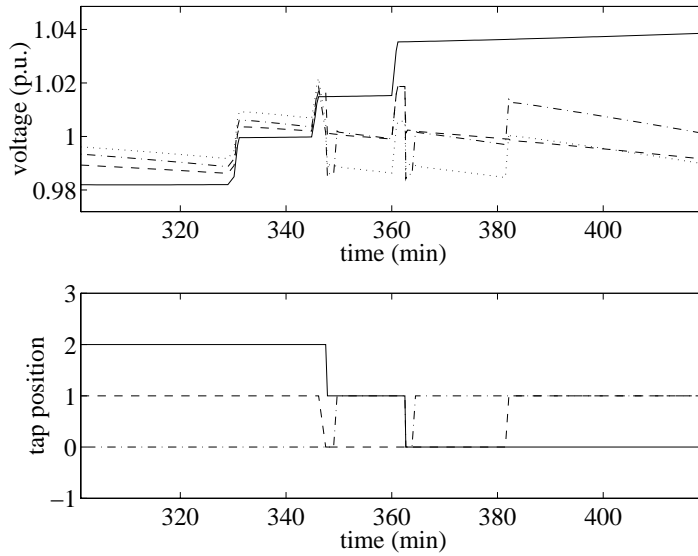


Figure A.5: Simulation, connection of capacitor banks. Conventional control with delay times 110 s. Top, node voltages-132 kV (solid line), 50 kV (dashed), 20 kV (dotted) and 10 kV (dash-dotted). Bottom, 132/50 kV (solid), 50/20 kV (dashed) and 20/10 kV (dash-dotted).

A.3.2 Suggested Tuning Rule

In the simulations in Section A.3.1, unnecessary tap operations are avoided by adjusting the time delays. Based on these simulations the following tuning rule for cascaded OLTCs in radial networks, giving gradually longer delay times for lower level units, is therefore proposed:

Set the delay time (T_1) of the top level OLTC adequately long to filter out fast transients. For a worst case voltage disturbance at the top level, compute the number of tap operations needed (N_1) for the top level OLTC to compensate for the disturbance. For lower level OLTCs, make $T_{k+1} > N_k T_k$. Check that the delay time of the lowest level OLTC provides fast enough customer voltage restoration.

The basic idea is that for step disturbances, no OLTC should act until all higher level OLTCs have compensated for the disturbance. This holds for both

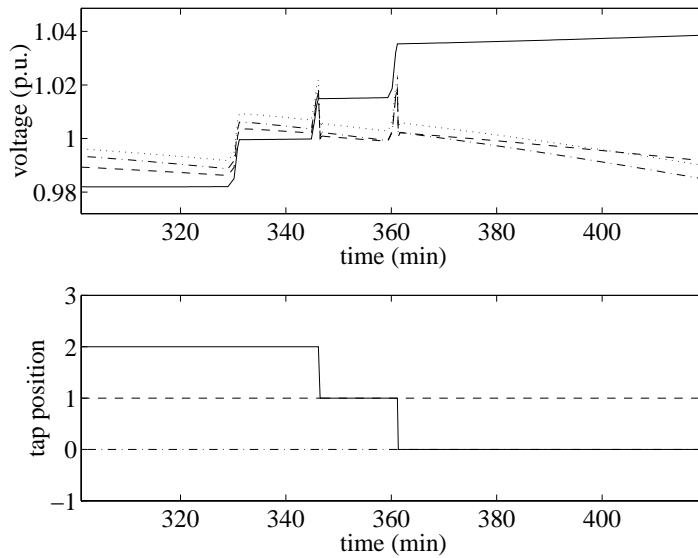


Figure A.6: Simulation, connection of capacitor banks. Conventional control with delay times [30, 70, 160] s. Compared to Figure A.5, four tap operations are avoided with the new tuning.

load and feeding network disturbances. This type of tuning was initially suggested, but not confirmed, in Karlsson (1992).

A.3.3 Simulation of Daily Operation

The purpose of the simulation is to verify the tuning rule under different load patterns. Nine cases with permutations of low (33 %), normal (66 %) and high (100 %) active and reactive load have been studied. For the case of high active and reactive loading, all transformers is loaded to rated load.

Figure A.7 shows a barchart of the number of required tap operations for the different load patterns for the conventional control with the old tuning. The labelling of the bars is made as first active then reactive power with L,N,H for the low, normal and high load level. Thus, the load pattern NH means normal active load and high reactive load. The corresponding barchart for the new tuning is shown in Figure A.8.

We can conclude that for all of the load cases, the new tuning reduces the number of tap operations required. With the old tuning the average (over the

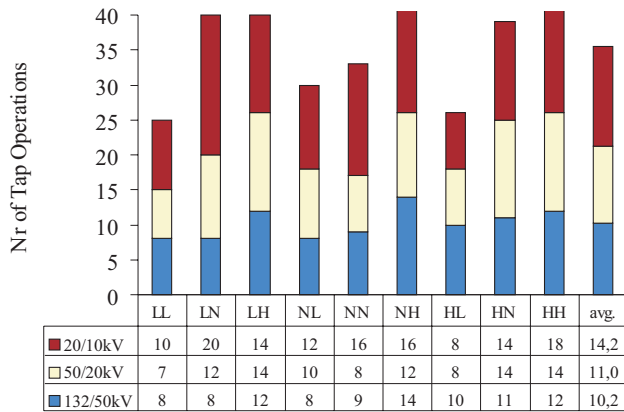


Figure A.7: Simulation. Number of tap operations during daily operation for the nine load patterns. Conventional control with delay times [110,110,110] s.

load patterns) number of operations is 35.4 and with the new 28.5, corresponding to a 19 % reduction. The reduction is especially pronounced at the lowest voltage level. This is important since these units are the most numerous because of the structure of the network.

A.3.4 Field Measurements

The tap changer operations in the branch Tomelilla, Järrestad and Östra Tommarp have been recorded for about two weeks to verify the impact of the OLTC delay times on the number of tap operations. The recordings have been performed for maximum delay time on each control unit (120 s) and for 30 s (132/50 kV), 60 s (50/20 kV) and 120 s (20/10 kV) corresponding to the proposed tuning rule in Section A.3.2. From the recordings it can be concluded that the total number of tap operations has been reduced, from 69 operations/day to 49 (Figure A.9). This corresponds to a 28 % reduction. It is clear that the largest reduction is achieved at the lowest voltage level.

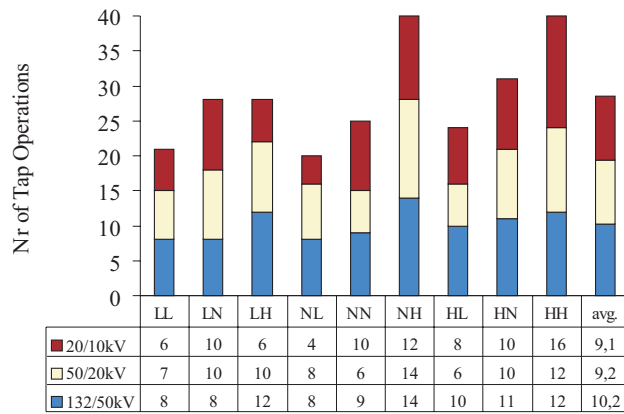


Figure A.8: Simulation. Number of tap operations during daily operation for the nine load patterns. Conventional control with delay times [30, 70, 150] s. Notice the substantial reduction of the number of tap operations made by the 20/10 kV OLTC compared to Figure A.7.

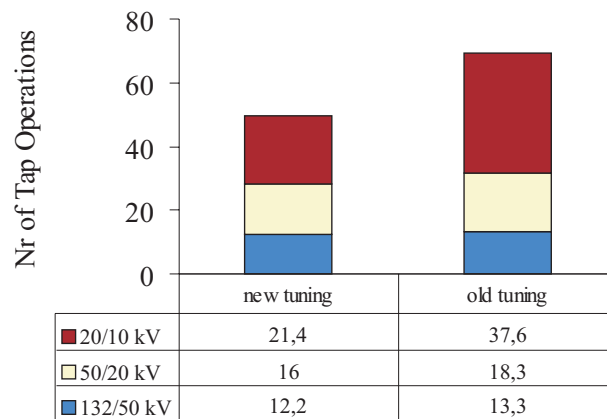


Figure A.9: Chart showing the daily average number of tap operations during a two week field measurement with the new and old tuning.

A.4 Multivariable Control

The coordinated voltage control problem is formulated as a multivariable control problem based on on-line constraint optimization. Operational limits, such as line capacity limits or tap limits, are specified as inequality constraints. The optimization is dependent on network data.

In this paper the optimization is done *statically*, i.e., only the latest measurements and control signals are considered in the objective function, as opposed to *dynamically* where control signals are calculated for times up to a prediction horizon based on both present and old measurements. Using a dynamic approach would improve performance further at the cost of a more complex and computationally demanding optimization.

A.4.1 Control Problem Formulation

The coordinated voltage control problem is formulated as the constrained optimization problem

$$\begin{aligned} & \text{minimize} && f(x) \\ & \text{subject to} && g(x) = 0 \\ & && h(x) \leq 0 \end{aligned} \quad (\text{A.1})$$

where

$$\begin{aligned} x & & - & \text{vector of tap positions} \\ f(x) & & - & \text{objective function} \\ g(x) = 0 & & - & \text{power balance equations} \\ h(x) \leq 0 & & - & \text{network operational constraints} \end{aligned}$$

This is a formulation similar to that used for the Optimal Power Flow problem (OPF). The difference lies in the objective function used. The objective function minimized in the OPF case is based on network losses, but for the OLTC control problem considered here an objective function based on voltage deviations from setpoints and control effort has been used

$$f(x) = \sum_i c_i (u_{devi})^2 + \sum_j d_j (\Delta n_j)^2 \quad (\text{A.2})$$

where

- u_{devi} - voltage deviation at bus i
- Δn_j - change of tap ratio of tap changer j
- c_i - multiplier for voltage deviation at bus i
- d_j - multiplier for operation of tap changer j

Thus, penalties are given for voltage deviations and tap operations in the objective function. The tuning parameters are c_i and d_j , by which the desired trade-off between voltage deviations and tap operations can be achieved. Tap changer operations are inherently discrete events, whereas most optimization algorithms need continuous variables. Since tap changer steps are quite small (0.5-2 %), linear approximation can be used in the optimization. This has been stated for example in Liu et al. (1992). The optimization problem is solved periodically with a sampling time of one minute, and the solution is rounded off to integer values.

A.4.2 Simulation of Daily Operation

In the simulations, the optimization problem was solved with Matlab's constraint optimization package by a Quasi-Newton method with finite-difference approximation of derivatives. Several more efficient methods have been suggested for the OPF case. Most of them are suitable for the problem formulated in (A.1). A sampling time of one minute for the control system was used.

In the simulations, the controller has been tuned empirically with the parameter values $c = (1 \ 2 \ 3)$ and $d = (1 \ \frac{1}{2} \ \frac{1}{3})$, to give about the same voltage fluctuations as the conventional control scheme. Figure A.10 shows the number of tap operations registered for the nine load patterns. An average of 19.4 operations has been registered.

A.5 Results

Figure A.11 shows the average number of tap operations registered in the simulation of the three control schemes. Generally, higher load means more tap operations. From the simulations, we can conclude that the reactive loading has a greater impact than the active load.

We also see that retuning the existing controllers gives a reduction of about 20 %, from 35.4 operations with the old tuning to 28.6 for the retuned sys-

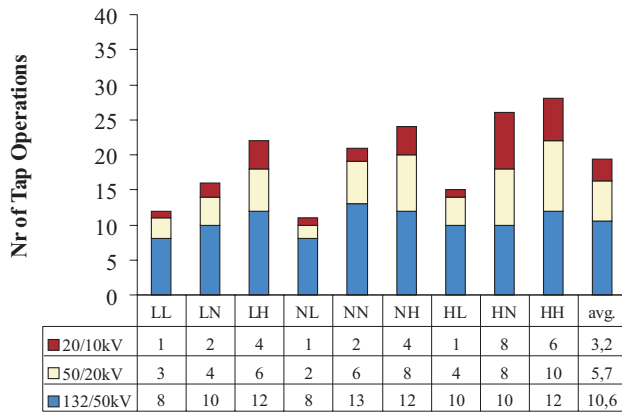


Figure A.10: Simulation. Number of tap operations during the daily operation for the 9 load patterns. Optimal control. Notice the substantial reduction of the number of tap operations made by the 20/10 kV OLTC compared to Figures A.7–A.8.

tem. For the multivariable control, an average of 19,4 operations is needed which corresponds to a reduction of 45 % compared to the existing controllers with the old tuning or 32 % compared to the retuned systems. The reduction achieved by retuning the conventional control systems has been verified in the field measurements that showed a 28 % reduction. For both the retuned conventional control and the multivariable control, the reduction is especially pronounced at the lowest voltage level.

Figure A.12 shows the profile of the 10 kV voltage for the three control schemes. We see that for the multivariable and retuned conventional control, fewer spikes are present compared to the old tuning. The multivariable control lacks integral action and therefore gives a small bias when the load is changing rapidly.

A.6 Discussion

In this paper, we have chosen to consider only a single branch of the network. An actual distribution system is successively branching into a large number of nodes at the lower voltage levels, but due to the radial topology of the networks,

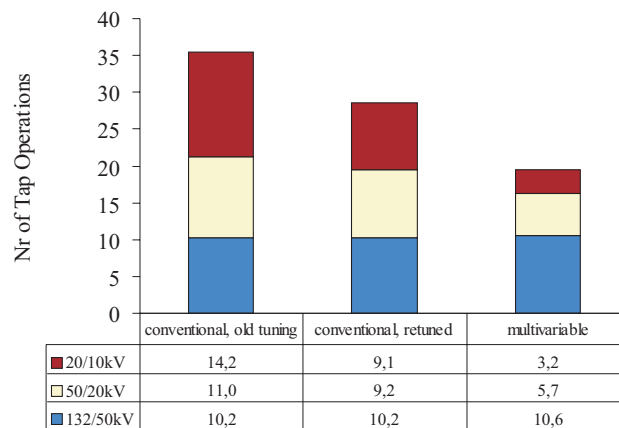


Figure A.11: Comparison of the average number of tap operations for the three control schemes.

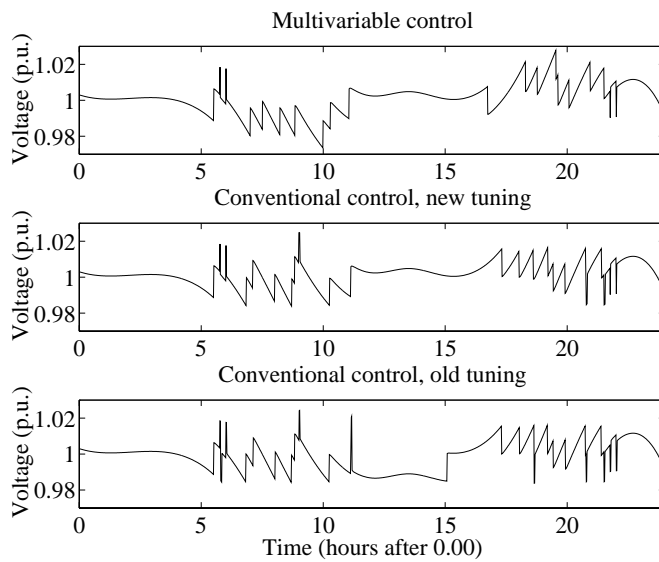


Figure A.12: Simulation. 10 kV voltage profile for the different control schemes. The standard deviation of the voltage time-series is approximately the same for all schemes.

giving weak coupling between different branches, the results should apply to the entire network as well. The reductions achieved are especially pronounced at the lower voltage level, where the number of units is large.

The properties of the two control schemes can be summarized as follows:

Conventional Control

- local control system, no need for communication
- preserves the existing controllers
- some selectivity can be achieved
- robust, no model needed
- difficult to tune
- slow customer side voltage restoration

Multivariable Control

- good selectivity properties
- easy to tune using the multipliers in (A.2)
- flexible
- fast customer side voltage restoration
- needs accurate network model
- needs measurement of load powers
- centralized, dependent of communications
- computationally demanding

By retuning the OLTCs, we incorporate knowledge of the radial topology of the network in a coordinated but still local control scheme. This provides some selectivity. Of the disadvantages of the optimizing control, the need for precise network data seems to be the most serious. On-line estimation of network

impedances or reformulation of the optimization to include integral action, can be used to eliminate this problem.

Apart from needing fewer tap operations than the conventional control scheme, the flexibility of the multivariable control is an interesting property. New actuators, e.g., SVCs or controllable loads, and control objectives can easily be integrated.

Also, the conventional tap changer control systems are not suitable for meshed networks where transformers are connected in parallel because of the circulating reactive currents and voltage control that might arise (Lakervi and Holmes, 1989). By adding a term proportional to system losses in (A.2), the multivariable control scheme can be used for meshed networks as well.

It is important to realize that performance alone is not the only requirement of a control scheme. It should also be reasonably simple to implement. Given that the multivariable control needs precise network data, implementation of the controller might be too awkward. The multivariable control might therefore be more of use as a reference for other controllers than for implementation. Another approach to the control problem is to try to mimic the multivariable control with a centralized rule-based controller, which could make use of heuristics concerning load trends and voltage deviations as base for its inferences. This type of controller can be implemented without exact knowledge of network data. Field tests of the multivariable control scheme and a rule-based controller is planned in the Tomelilla area during 1995–96.

A.7 Conclusions

The aim of this work was to reduce the number of unnecessary tap operations made due to lack of coordination between OLTCs in radial distribution networks. A tuning rule for the conventional OLTC control systems which gives selectivity of cascaded OLTCs in normal state operation has been presented. The rule assigns long time delay to lower level OLTCs. The tuning rule has been verified in simulations and field measurements, and has been shown to reduce the number of tap operations by a good 20 %, compared to the tuning presently used. A more sophisticated multivariable control scheme based on on-line tap optimization is presented. In simulations, the multivariable control scheme has been shown to reduce the number of operations some further 30 %. The control schemes have been tuned to yield voltage deviations of the same average magnitudes in the simulations as well as the field measurements.

A.8 Acknowledgments

The authors would like to thank our helpful colleagues, especially Curt Lindqvist, Head of System Operation at Sydkraft, who initiated the project, Prof. Gustaf Olsson who supervised the work at IEA and Hans Gjöderum of Österlen Energi, for his help during the field tests at Tomelilla. The work in this paper has been funded jointly by Sydkraft AB and Elforsk AB through the Elektra programme.

Paper B

Coordination of Cascaded Tap Changers using a Fuzzy-Rule Based Controller

Mats Larsson

Fuzzy Sets and Systems, 102 (1), 113–123, Elsevier Science (1999)

Abstract: *This paper deals with the issue of coordination of cascaded tap changers in radial distribution feeders. Poor coordination causes unnecessary operations of the tap changers and consequently unnecessary wear as well as poor voltage quality. A new fuzzy-rule based controller that coordinates tap operations at different voltage levels is proposed and compared to the existing controllers and an optimal controller. Whereas the existing controllers rely only on local measurements, the fuzzy-rule based and optimal controllers are centralized and therefore require communication between substations. Results from simulations based on load patterns recorded during different seasons in a rural distribution system indicate that the proposed fuzzy-rule based controller reduces the daily number of tap operations by some 36 % compared to the existing controllers in the selected test system. The corresponding reduction by an optimal controller is about 45 %. The optimal controller is however significantly more complex to implement, because of its dependency on an exact network model. A prototype of the fuzzy-rule based controller has been installed and successfully tested in a distribution feeder in the south of Sweden. The prototype was also used to validate the simulation results presented in the paper.*

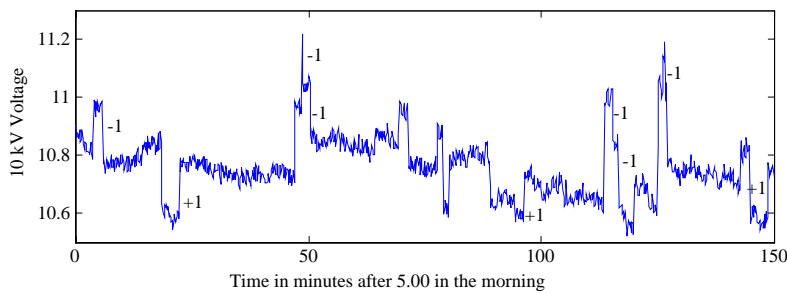


Figure B.1: Field measurement of the voltage in the 10 kV sub-station at Östra Tommarp during load pickup. The tap operations made at ÖTP are marked with +/-1.

B.1 Introduction

The Swedish distribution feeders are typically radial and have tap changers (OLTCs) cascaded in up to three levels. Therefore, interaction among OLTCs at different voltage levels is possible. OLTC control is presently based on local criteria with no coordination of OLTCs at different voltage levels.

Figure B.1 shows a voltage measurement recorded in a preliminary study at a 10 kV sub-station, which is fed through three cascaded transformers with OLTCs, with the conventional voltage control in operation. 24 voltage steps can be observed during the 150 minute recording. Nine of the steps are due to operations of the local OLTC (marked ± 1) and the rest are due to tap operations and capacitor bank switchings higher up in the network. Most of the tap operations made locally counteract the effect of tap changers higher up in the network.

Poor coordination of cascaded tap changers can be dangerous from a voltage stability point of view. A sudden voltage drop in the feeding network may result in considerable voltage overshoot at the load level (Karlsson, 1992). Since loads are voltage sensitive, the overshoot will temporarily increase the loading of the feeding transmission system. This type of disturbance is likely to arise during voltage instability incidents as a result of tripped lines or generation units in the transmission system. During such incidents, the transmission system is already operating close to its transfer limits and increased loading is highly undesirable.

With coordinated control of tap changers it should be possible to reduce

the number of, or eliminate counteracting tap operations. Consequently, the total number of operations and the number of voltage spikes due to OLTC interaction would decrease. Wear on the tap changer mechanism is the most common reason for transformer maintenance and therefore a reduction of the number of tap operations is highly desirable.

Referring to the role of OLTCs in voltage instability incidents, the new rule-based controller proposed in this paper prevents voltage overshoot due to OLTC interaction following voltage drops in the feeding system. With coordinated control, it would also be possible to use alternative control strategies during voltage instability incidents, although this possibility is not explored in this paper.

In the paper, a new centralized control scheme based on fuzzy reasoning is described. The performance of this new control scheme is compared to the existing controllers and an optimal controller which has been described in detail in Larsson and Karlsson (1995). A prototype of the new controller has been installed in a distribution system in Sweden and extensive simulation and field measurement results obtained using this prototype are presented.

B.2 The Österlen Test System

A branch of the distribution system at Österlen, a rural area in the southeast of Sweden, was chosen for the pilot installation. Figure B.2 shows a schematic of the test system. The relevant parameter values are given in Table B.4.

At Tomelilla (*TLA*), there is a 100/100/40 MVA, 130/50/20 kV tap changing transformer. The 50 kV side of the TLA transformer is connected through overhead lines to three 50/20 kV substations, one of which is Järrestad (*JSD*). The tap changer in TLA is placed on the 130 kV winding and controls the 20 kV voltage in steps of 1.67 %. There is also a capacitor bank present at the 130 kV bus. At Järrestad (*JSD*), there is a 16 MVA tap changing transformer which controls the 20 kV voltage in steps of 2.5%. JSD supplies the Östra Tommarp (*ÖTP*) and five other 20/10 kV transformers mainly through overhead lines. The ÖTP sub-station with its 4 MVA tap changing transformer supplies 42 10/0.4 kV transformers mainly through overhead lines. These transformers are only equipped with off-load tap changers, and they are therefore not included in the simulation model. The OLTC in ÖTP have steps of 1.67 %. The loads are represented as exponential recovery loads according to Karlsson and Hill (1994).

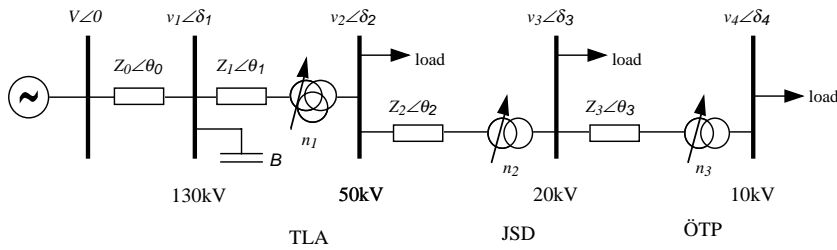


Figure B.2: Schematic of the test system at Österlen.

B.3 Conventional OLTC Controllers

The conventional OLTC controller consists of a time delay and a deadband with hysteresis. The size of the deadband, tuned by the parameters u_{function} and u_{reset} , sets the tolerance for long-term voltage deviations and the time delay, tuned by T_d , is intended for noise rejection. Detailed descriptions of OLTC control systems can be found in Altsjö (1993), Čalović (1984), Sauer and Pai (1994). Possible tap ratio change is typically $\pm 10 - 15\%$ in steps of 0.6-2.5%. The typical setting of delay time is in the range 30-120 s, whilst the dead zone is usually chosen slightly smaller than two tap steps. The mechanical delay time is usually in the range 1-5 s. A tuning rule that ensures proper coordination of cascaded OLTCs using the conventional controllers was presented in Larsson and Karlsson (1995).

B.4 Optimal Controller

In the optimal control scheme (Larsson and Karlsson, 1995) the voltage control problem is formulated as a multivariable control problem which is solved by on-line constraint optimisation. This ensures an optimal trade-off between voltage deviations and OLTC operations using a quadratic loss function. It is a pure feed-forward controller that measures load and feeding voltage variations and compensates for these by adjusting the tap ratios. Therefore, it needs a perfect network model if it is to avoid stationary control errors. This motivates the development of the simpler and more robust rule based controller.

B.5 Fuzzy-Rule Based Controller

Fuzzy control has been most successfully used for control problems where the control objectives are difficult to quantify or where one has some heuristic knowledge that can improve control. The basic idea is that an observation of each physical process variable can be translated to a fuzzy variable, giving it a linguistic interpretation. This process is usually called *fuzzification*. A fuzzy variable has a value between 0 and 1 describing to what extent the observation has the property described by the fuzzy variable.

The fuzzy variables can be manipulated with the fuzzy set operators (\wedge (intersection), \vee (union), \neg (complement) etc.) so that combinations of fuzzy variables can be formed and used to determine the controller output. The mathematics involved in these manipulations are described in Jantzen (1991). They are written as a set of rules on the form:

$$\underbrace{\text{some action}}_{\text{fuzzy controller output}} = \underbrace{\text{some property}}_{\text{fuzzy variable}} \overbrace{(\text{some variable})}^{\text{physical variable}} \quad (\text{B.1})$$

The right hand side of (B.1) may contain several fuzzy variables related by the fuzzy set operations. Together, these rules define the *rule-base* of the controller and should express the heuristic knowledge one has of the desired controller. The process of evaluation of the rules is called *inference*.

The output of the inference is a fuzzy variable for each control signal. These fuzzy variables have to be translated to physical controller outputs. This translation is called *defuzzification*.

The entire process is a simple mapping from measurements to controller outputs. Therefore, the rule base and membership functions can be seen as an intuitive way of defining nonlinearities for use in feedback control.

B.5.1 Control Problem Formulation

By inspection of results from simulations with the conventional and optimal controller, the following heuristic rules that express some desired properties of the controller were derived:

1. If the (local) voltage is high, order a downward tap operation.
2. If the (local) voltage is low, order an upward tap operation.

3. Cancel an upward tap operation if any tap changer higher up in the network is about to order an upward operation.
4. Cancel a downward tap operation if any tap changer higher up in the network is about to order a downward operation.
5. If voltage deviation is very large, order an operation regardless of rules 3–4.

The next step is to determine which process variables are relevant and define membership functions corresponding to the properties they may possess. Rules 1, 2 and 5 clearly rely on a voltage measurement that can have the properties *veryLow*, *low*, *high* and *veryHigh*. The corresponding membership functions are shown in Figure B.3. Since the tap changer in JSD has a larger step size than the other two, it has its own set of membership functions for low and high voltage. No new memberships have to be introduced for rules 3–4, since these rules can be realized using the controller output fuzzy variables *UP* and *DOWN* by forward chaining. Using the fuzzy variables and heuristic rules, the rule base can be formulated as follows

$$UP_{TLA} = low(v_{TLA}) \vee veryLow(v_{TLA}) \quad (B.2)$$

$$DOWN_{TLA} = high(v_{TLA}) \vee veryHigh(v_{TLA}) \quad (B.3)$$

$$UP_{JSD} = (low(v_{JSD}) \wedge \neg UP_{TLA}) \vee veryLow(v_{JSD}) \quad (B.4)$$

$$DOWN_{JSD} = (high(v_{JSD}) \wedge \neg DOWN_{TLA}) \vee veryHigh(v_{JSD}) \quad (B.5)$$

$$UP_{OTP} = (low(v_{OTP}) \wedge \neg (UP_{TLA} \vee UP_{JSD}) \vee veryLow(v_{OTP})) \quad (B.6)$$

$$DOWN_{OTP} = (high(v_{OTP}) \wedge \neg (DOWN_{TLA} \vee DOWN_{JSD})) \vee veryHigh(v_{OTP}) \quad (B.7)$$

The fuzzy sets *UP* and *DOWN* are generated using fuzzified voltage measurements as input for each tap changer. The controller outputs are then determined by defuzzification of the fuzzy sets *UP* and *DOWN*. The defuzzification is done by subtracting the memberships of *UP* and *DOWN*, giving a number in the interval $[-1, 1]$ describing to what degree a tap operation should be done and in what direction. The resulting surfaces are called *control surfaces*. The

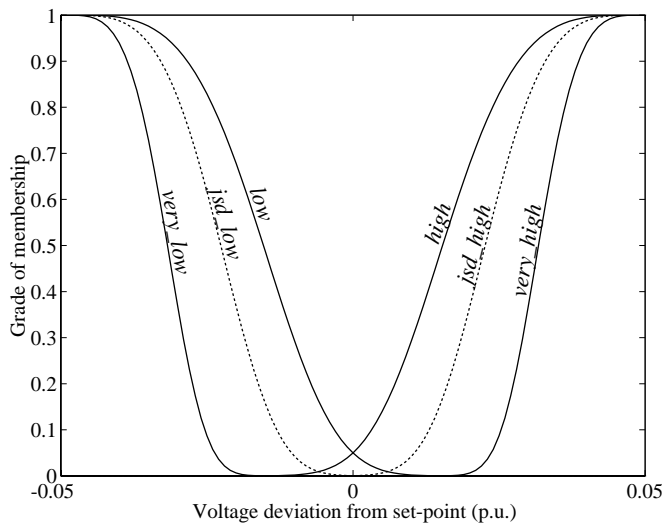


Figure B.3: Membership functions for voltage deviations.

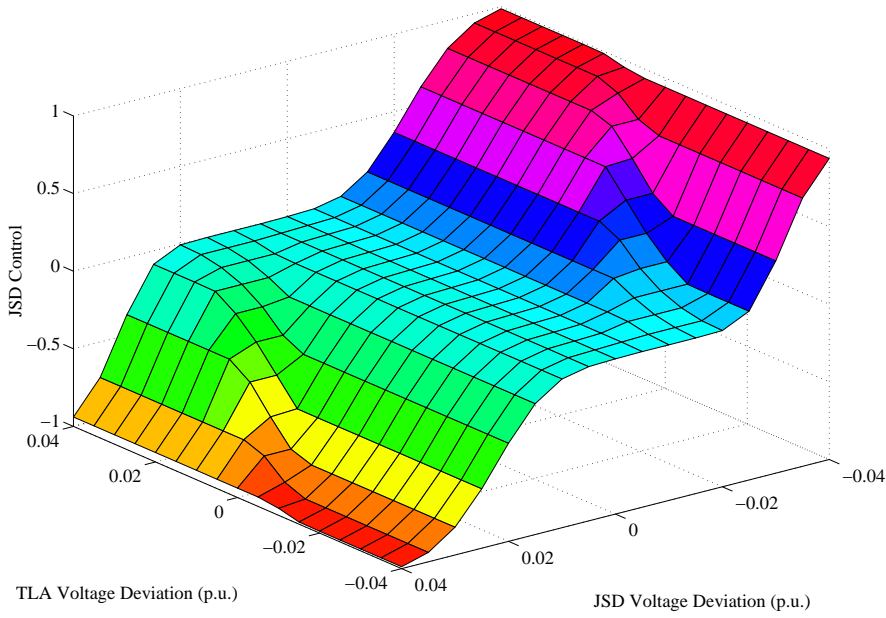


Figure B.4: Control surface for the OLTC in JSD.

control surface for the OLTC in JSD is shown in Figure B.4. The control surfaces for the TLA and ÖTP OLTCs are similar.

Because of the OLTC's discrete nature, the control surfaces have to be discretized. In the design, the degree +0.5 is considered enough for an upwards operation and -0.5 enough for a downward operation.

B.5.2 Tuning

The controller is tuned by adjusting the membership functions. The membership functions and the defuzzification threshold was chosen such that the voltage tolerance given by the first two heuristic rules is roughly the same as for the conventional controllers (1.5 % in TLA and ÖTP and 2.25 % in JSD yields membership to the degree of 0.5). By adjusting the membership functions for *very_high* and *very_low* the maximum allowable voltage deviations are set to about 3%. When the heuristic rules 3–4 are active due to large voltage deviations, they specify modifications to the first two rules that cancel operations ordered by rules 1–2, but not those ordered by rule 5.

B.6 Prototype

To validate the simulation results and to demonstrate the implementation of the coordinated control schemes, a prototype controller was developed and installed in the test system at Österlen. It is a distributed control system, with a local control loop in each sub-station. A supervisory controller in the TLA sub-station coordinates the local control loops, with the necessary communication between the sub-stations provided by radio links. Each local control loop can operate autonomously using a conventional (local) control system whenever contact with the supervisory controller is lost. The supervisory controller operates with a sampling time of one minute.

B.7 Simulation and Field Test Results

To be able to compare the control schemes using realistic load patterns, the prototype was used to record the load variations at TLA, JSD and ÖTP and the feeding 130 kV voltage at TLA during three two-week measurement periods:

Summer July 10-16 and July 21-27, 1996.

Autumn October 16-22 and 24-30, 1996.

Winter January 13-26, 1996.

The local control scheme was in use during the summer, winter and first week of the autumn measurement. The fuzzy-rule based controller was in use during the second week of the autumn measurement. To assess the performance of the fuzzy-rule based control scheme, simulation results for four different schemes are presented:

- conventional control scheme with normal tuning, that is, all OLTCs have delay times of 120 s (*CCN*)
- conventional control scheme with revised tuning, that is, the top level OLTC has a delay time 30 s, the middle one has 70 s and the lower one has 150 s. (*CCR*)
- fuzzy-rule based control scheme (*FRB*)
- optimal control scheme (*OPT*)

Figures B.5–B.7 show simulations of a single days operation, using the different control schemes. For this particular load pattern, the optimal and fuzzy-rule based controllers perform more or less identically and both eliminate the OLTC interaction present with the local controllers. The new control schemes sometimes allow voltage deviations outside the deadbands of the conventional controllers in order to avoid OLTC interaction, and therefore several operations are avoided. The variation with respect to the control scheme is the most important factor to consider. The total number of tap operations per day averaged over the three periods organized by control scheme is tabulated in Table B.1.

Again, Table B.2 summarizes the total number of tap operations per day averaged over the three periods, but here organized by OLTC level. Since the control of the top level OLTC is similar for all control schemes, the variation in the number of operations made by this OLTC is small. The most distinctive difference is that the *OPT* tend to use more operations at the top level, in order to save operations at the middle and bottom levels. The major savings are made at the middle and bottom level for both the *FRB* and *OPT*.

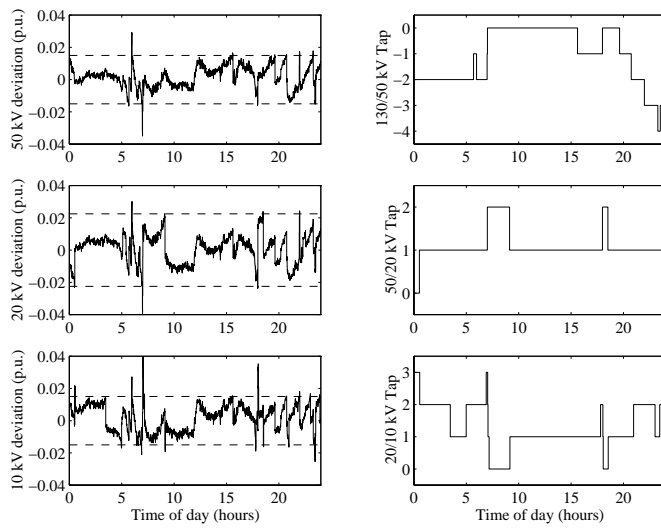


Figure B.5: Simulation of daily operation. Load pattern recorded October 22, 1996. Conventional control with the normal tuning.

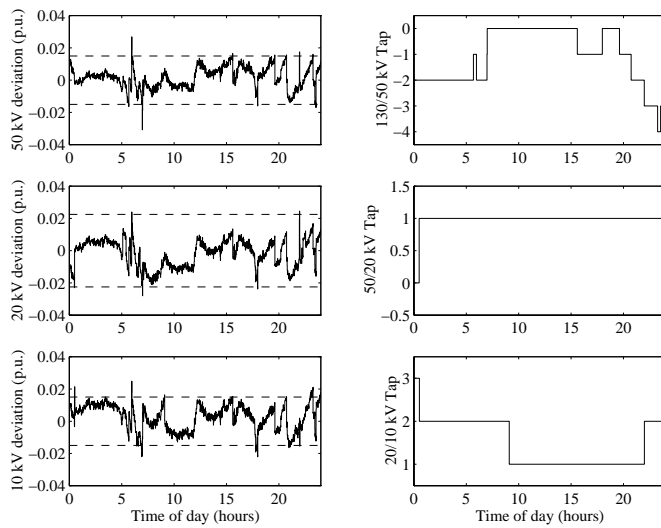


Figure B.6: Simulation of daily operation. Load pattern recorded October 22, 1996. Rule-based control. The dashed lines show the deadbands of the conventional control scheme.

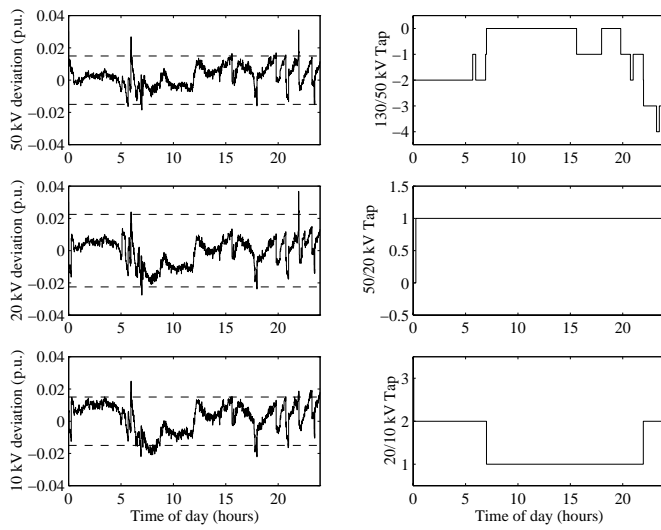


Figure B.7: Simulation of daily operation. Load pattern recorded October 22, 1996. Optimal control. The dashed lines show the deadbands of the conventional control scheme.

| | CCN | CCR | FRB | OPT |
|----------------------|-----|-------|-------|-------|
| Number of operations | 27 | 24 | 15 | 13 |
| Compared to CCN | | -3 | -12 | -14 |
| Relative to CCN (%) | | -10 % | -43 % | -51 % |
| Compared to CCR | | | -9 | -11 |
| Relative to CCR (%) | | | -36 % | -45 % |
| Compared to FRB | | | | -2.1 |
| Relative to FRB (%) | | | | -14 % |

Table B.1: The number of tap operation organized by control scheme.

| | CCN | CCR | FRB | OPT |
|-----------------|-----|-------|-------|-------|
| 130/50 kV | 8.7 | 8.7 | 8.4 | 9.8 |
| Relative to CCN | | 0 % | -3 % | +13 % |
| 50/20 kV | 4.4 | 3.8 | 1.8 | 1.1 |
| Relative to CCN | | -12 % | -60 % | -74 % |
| 20/10 kV | 14 | 12 | 5.3 | 2.4 |
| Relative to CCN | | -16 % | -62 % | -83 % |

Table B.2: The number of tap operation organized by OLTC level.

B.7.1 Validation

The simulation results were validated during the autumn measurement period. The CCN was in operation during the first week and the FRB during the second. Figure B.8 shows a comparison of the average number of tap operations with the different control schemes during the validation measurement. To the left, simulation results for the two weeks can be compared for the different control schemes. The conclusion that can be drawn, is that the overall number of operations tends to be slightly larger during the first week than during the second. The two rightmost bars show the number operations observed in the measurements, with the CCN during the first week and the FRB during the second week. This measurement supports the simulation results, since the observed reduction by the FRB compared to the CCN is about 60 %, while the simulations indicate a 59 % reduction. Figure B.9 shows the voltage standard deviations, which are roughly the same in the measurements and simulations.

B.7.2 Simulation of a Complete Distribution System

The development and prototype installation of the new controllers has been done using a three tap changer test system. An actual distribution system is successively branching into a large number of nodes at the lower voltage levels. Thanks to the radial topology of the networks, giving weak coupling between different branches, the controllers can be expected work for the entire network as well.

To demonstrate this, a simulation of a fictitious but realistic rural system whose structure is shown in Figure B.10 was done. Network impedances and load curves for the different voltage levels have been slightly varied around the

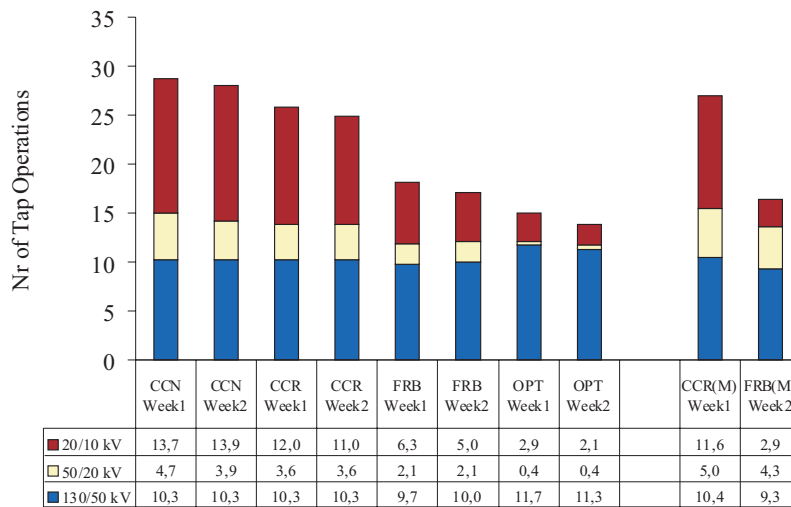


Figure B.8: Average number of tap operations during the autumn validation measurement. CCR(M) and FRB(M) denotes measurement results with the CCR and FRB respectively.

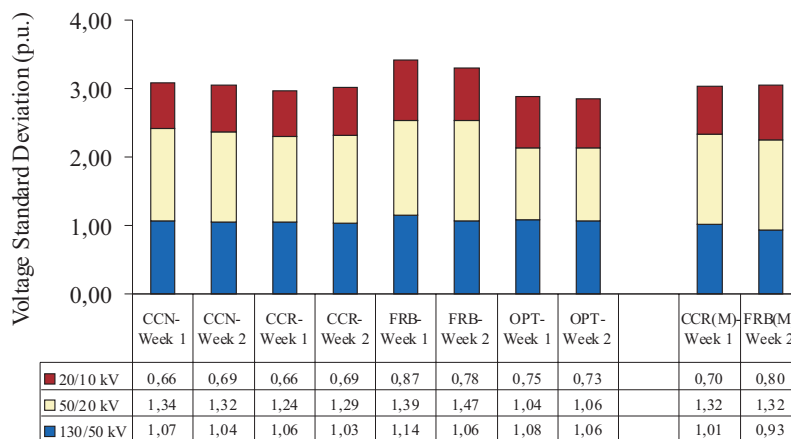


Figure B.9: Voltage standard deviations during the autumn validation measurement. CCR(M) and FRB(M) denotes measurement results with the CCR and FRB respectively.

| | CCN | CCR | FRB |
|-----------------|------|-------|-------|
| 130/50 kV | 8.0 | 8.0 | 8.0 |
| Relative to CCN | | 0 % | 0 % |
| 50/20 kV | 11.7 | 9.3 | 3.0 |
| Relative to CCN | 0.0 | -20 % | -74 % |
| 20/10 kV | 12.6 | 7.2 | 3.5 |
| Relative to CCN | | -43 % | -72 % |
| Total | 32.3 | 24.5 | 14.5 |
| Relative to CCN | | -24 % | -55 % |

Table B.3: The number of tap operations in the complete distribution system organized by OLTC level.

values for the smaller test system (Table B.4). The results from the simulation are summarized in the table below, with the number of tap operations averaged for each voltage level in Table B.3.

The results from these simulations are similar to those for the smaller test system. Note however that these results are based on a single days operation, and are therefore not as reliable as those presented for the smaller test system. The lower level taps, for which the largest savings are done, are the most numerous in a full distribution system. Also, when the coordinated control is implemented in a whole distribution network, some of the 50 kV and 20 kV buses need not necessarily be accurately voltage controlled since they have no loads directly connected. This additional freedom has not been exploited in the simulations, but can possibly reduce the number of tap operations made further.

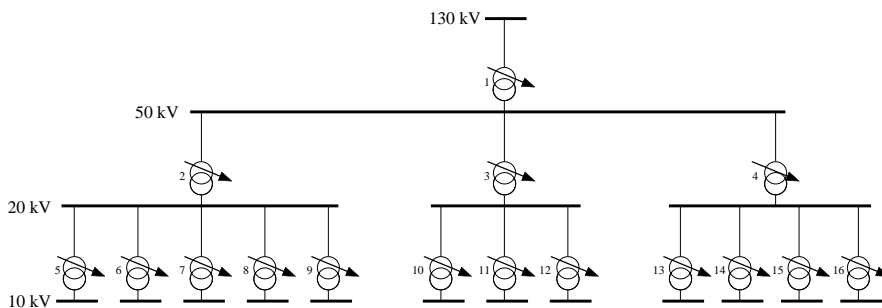


Figure B.10: Structure of the full distribution system simulated.

B.8 Conclusions

The fuzzy-rule based controller has been shown to reduce the number of OLTC operations in the test system by some 36 %, compared to properly tuned existing controllers. The corresponding reduction for the optimal controller is 45 %. However, the optimal controller requires an exact network model whereas the fuzzy-rule based does not. Therefore, the fuzzy-rule based controller was chosen for the prototype installation, and the optimal controller is merely used as a benchmark in the simulations.

The simulation results have been obtained using a representative choice of load patterns ranging over 14 summer, 14 autumn and 14 winter days. An important aim has also been to demonstrate the feasibility of centralized tap changer control. A prototype of the fuzzy-rule based controller was designed and installed in the distribution system at Österlen in southern Sweden. The prototype was also used to validate the simulation results presented.

B.9 Acknowledgements

The author is indebted to Prof. Gustaf Olsson at Lund Institute of Technology and Dr. Daniel Karlsson at Sydkraft AB for their constant support and valuable suggestions throughout the project, and the local personnel at Österlen for allowing me to play around with their distribution system. This piece of work has been funded jointly by Elforsk AB and Sydkraft AB.

| <i>Load Data</i> | | | | | | | |
|------------------|------------|-------|-----------|-----------|-------|--|--|
| α_s | α_t | T_p | β_s | β_t | T_q | | |
| 1.28 | 1.92 | 173 | 1.32 | 2.92 | 83.5 | | |

| <i>OLTC Data</i> | | | | | | |
|------------------|----------------|-----------------|-----------------------------|--------------------------|----------------------|--|
| <i>TLA</i> | | | | | | |
| <i>min tap</i> | <i>max tap</i> | <i>tap step</i> | <i>u_{function}</i> | <i>u_{reset}</i> | <i>T_d</i> | |
| 1 | 19 | 1.67% | 1.50% | 1.35% | 120 s | |

| <i>JSD</i> | | | | | | |
|----------------|----------------|-----------------|-----------------------------|--------------------------|----------------------|--|
| <i>min tap</i> | <i>max tap</i> | <i>tap step</i> | <i>u_{function}</i> | <i>u_{reset}</i> | <i>T_d</i> | |
| 1 | 9 | 2.50% | 2.25% | 2.00% | 120 s | |

| <i>ÖTP</i> | | | | | | |
|----------------|----------------|-----------------|-----------------------------|--------------------------|----------------------|--|
| <i>min tap</i> | <i>max tap</i> | <i>tap step</i> | <i>u_{function}</i> | <i>u_{reset}</i> | <i>T_d</i> | |
| 1 | 17 | 1.67% | 1.50% | 1.35% | 120 s | |

| <i>Network Data</i> | | | | | | | |
|-----------------------------|------------------------------------|-----------------------------|------------------------------------|-----------------------------|------------------------------------|-----------------------------|------------------------------------|
| <i>Z₀ (p.u.)</i> | <i>θ_0 (rad)</i> | <i>Z₁ (p.u.)</i> | <i>θ_1 (rad)</i> | <i>Z₂ (p.u.)</i> | <i>θ_2 (rad)</i> | <i>Z₃ (p.u.)</i> | <i>θ_3 (rad)</i> |
| 0.0561 | 1.3369 | 0.0953 | 1.5584 | 0.6796 | 1.3486 | 2.663 | 1.4958 |

| <i>p.u. Conversion Data</i> | | |
|--|---------------------------------------|---------------------------------------|
| <i>V_{base} (130 kV level)</i> | <i>V_{base} (50 kV level)</i> | <i>V_{base} (20 kV level)</i> |
| 132 kV | 55 kV | 22 kV |
| <i>V_{base} (10 kV level)</i> | <i>S_{base}</i> | |
| 10.7 kV | 100 MVA | |

Table B.4: Parameter values for the Österlen test system.

Paper C

Limit Cycles in Power Supply Systems due to OLTC Deadbands and Load-Voltage Dynamics

Mats Larsson Dragana H. Popović David J. Hill

Electric Power Systems Research 47 (3), 181–188, Elsevier Science (1998)

Abstract: *In this paper, the phenomenon of limit cycles due to load-tap changer interaction is investigated. The role of the OLTC deadband in creating a limit cycle phenomenon is addressed. The impact of tap dynamics modelling on system/voltage behaviour is carefully considered. Analytical insights into observed behaviour of power systems with different tap models are given using eigenvalue analysis, the describing function method and time simulation. The conditions for occurrence of limit cycles and the identification of key parameters influencing their characteristics are other important aspects of this investigation.*

C.1 Introduction

Studies of serious contingencies and associated voltage instability problems during the past decade have revealed different mechanisms underlying those events. Voltage misbehaviour has been shown as not necessarily just monotonic, influencing researchers to investigate various potential sources of the system oscillatory behaviour. This paper further explores the oscillatory behaviour of power supply systems with emphasis on illustrating interactions between on-load tap changer (OLTC) and load dynamics.

OLTCs have been shown to play an important role in long-term voltage collapse (Walve, 1986), since they aim to keep load voltages and therefore the load power constant even though transmission system voltages may be reduced. Considerable effort has been given to voltage behaviour research indicating that the dynamics of voltage collapse are closely linked to dynamic interaction between the OLTCs and loads. It led to significant progress in the area of dynamic load modelling. However, dynamic modelling of OLTCs was given little attention during the last decade. An early detailed description of a typical OLTC control system was given in Čalović (1984). The proposed OLTC model was a complex nonlinear dynamic model that encompassed some inherent time delays. Recent work presented in Sauer and Pai (1994) explored further the tap changer modelling issue. Depending on the OLTC characteristic (type of time delay), various discrete state dynamic models and corresponding continuous approximations were derived. However, most of the power system dynamic studies so far have used quite simplified OLTC representations. The main focus of these studies which mainly relate to voltage stability questions has been on understanding of the complex dynamic nature of voltage collapse to which OLTC dynamics significantly contributes. The role of OLTCs in combination with aggregate loads has received considerable attention (Abe et al., 1982, Liu and Vu, 1989, Medanić et al., 1987, Popović et al., 1996b, Vu and Liu, 1992). Voltage instability problems concerned with OLTC dynamics were analyzed in Abe et al. (1982), Liu and Vu (1989), Popović et al. (1996b), Vu and Liu (1992) using the continuous state OLTC model. Stability conditions providing proper coordination of multiple OLTCs were derived in Medanić et al. (1987), Yorino et al. (1997) using a discrete state tap model. Limit cycles and other oscillatory voltage instability problems created by interaction between cascaded tap changing transformers and/or by load-tap interaction were investigated in Hiskens and Hill (1993), Popović et al. (1996a), Vournas and Van Cutsem (1995).

C.2 Example System

A single load, single OLTC system such as shown in Figure C.1 is considered. The example system represents a distribution bus fed through a tap changing transformer and a transmission system equivalent. To increase transfer limits, the distribution system has been compensated by a capacitor bank. Although simple, the system contains all the principal components which affect voltage behaviour, especially after line fault or under heavy load conditions.

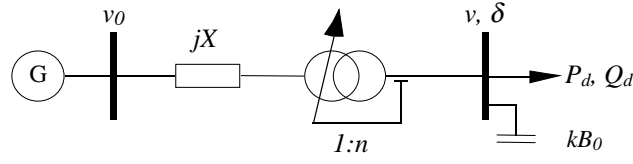


Figure C.1: Example power system studied.

C.2.1 Load and Network Models

Focusing on tap changer dynamics and therefore on a slower time scale (below ~ 0.1 Hz) than the one relevant to generator dynamics, the generator bus is modelled as an infinite bus. The load is modelled as an exponential recovery load according to Karlsson and Hill (1994)

$$\dot{x}_p = \frac{1}{T_p}(-x_p + P_s(v) - P_t(v)) \quad (\text{C.1})$$

$$P_d = x_p + P_t(v) \quad (\text{C.2})$$

where $P_s(v) = kP_0v^{\alpha_s}$ is the steady-state and $P_t(v) = kP_0v^{\alpha_t}$ the transient voltage dependency. P_d is the actual active load power and T_p is the active power recovery time constant. For the reactive load power, a similar model is used with corresponding characteristics $Q_s(v) = kQ_0v^{\beta_s}$, $Q_t(v) = kQ_0v^{\beta_t}$ and time constant T_q . The transformer is modelled as a pure reactance in series with an ideal transformer. The parameter k has been introduced as a scale factor on the load parameters P_0 , Q_0 and B_0 .

Combining the load dynamics with power balance equations at the load bus, the model can be written in the differential-algebraic (DA) form

$$\dot{x} = f(x, V) \quad (\text{C.3})$$

$$0 = g(x, V, n) \quad (\text{C.4})$$

where $x = [x_p \ x_q]^T$ is the load state vector, $V = [v \ \delta]^T$ is the load voltage vector and n is the transformer tap ratio. For the example system, functions f and g can be written as

$$f(x, V) = \begin{bmatrix} \frac{1}{T_p}(-x_p + kP_0(v^{\alpha_s} - v^{\alpha_t})) \\ \frac{1}{T_q}(-x_q + kQ_0(v^{\beta_s} - v^{\beta_t})) \end{bmatrix} \quad (\text{C.5})$$

$$g(x, V, n) = \left[\begin{array}{l} \frac{v \sin(\delta) v_0}{Xn} + x_p + kP_0 v^{\alpha_t} \\ \frac{v_0(v_0 - \cos(\delta)v_0 n)}{Xn^2} + x_q + kQ_0 v^{\beta_t} - kB_0 v^2 \end{array} \right] \quad (\text{C.6})$$

| Network Data | X | B_0 | Load Data | P_0 | Q_0 | $T_p=T_q$ | $\alpha_s=\beta_s$ | $\alpha_t=\beta_t$ |
|--------------|----------|------------|-----------|-------|--------------|-------------|--------------------|--------------------|
| | 0.5 | 0.5 | | 1.0 | 0.5 | 60 | 0 | 2 |
| OLTC Data | tap step | tap limits | $DB/2$ | T | T_{d0} | T_m | | |
| | 1% | $\pm 15\%$ | 0.9% | 30 | $25*(1/0.9)$ | $5*(1/0.9)$ | | |

Table C.1: Network, load and OLTC parameter values.

C.2.2 OLTC Models

The conventional OLTC control is a simple incremental control with a time delay and a deadband. The size of the deadband sets the tolerance for long-term voltage deviations and the time delay is primarily intended for noise rejection. Detailed descriptions of OLTC control systems can be found in Čalović (1984), Sauer and Pai (1994).

The typical non-sequential OLTC control system can be modelled by the state graph of Figure C.2. The system remains in the state *wait* while the voltage deviation ($|v - v_r|$) is less than the function voltage (u_{function}). When the limit is exceeded, a transition to the state *count* occurs. Upon entering *count*, a timer is started and is kept running until either it reaches the delay time T_d , causing a transition to the state *action*, or if the voltage deviation becomes less than the reset voltage (u_{reset}), firing a transition to the state *wait* and reset of the timer. When entering the state *action*, a control pulse to operate the tap changer is given. After the mechanical delay time (T_m), the tap operation is completed. The control system then receives *ready* signal from the tap changer and returns to state *wait*. The time delay is tuned by the time delay constant T_{d0} . The actual time delay can then be either fixed ($T_d = T_{d0}$) or inversely proportional to the voltage deviation ($T_d \sim T_{d0}/|v - v_r|$).

For agreement with Sauer and Pai (1994), function and reset voltages have been chosen to be identical ($u_{\text{function}} = u_{\text{reset}} = DB/2$). Possible tap ratio change is typically $\pm 10 - 15\%$ in steps of 0.6-2.5%. Typical setting of delay times (T_d) is in the range 30-120 s, whilst the deadband (DB) is usually chosen

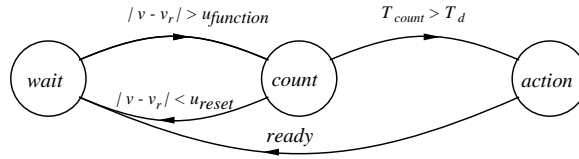


Figure C.2: State graph illustrating function of a non-sequential OLTC control system.

slightly smaller than two tap steps. The mechanical delay time (T_m) is usually in the range 1-5 s.

Several models with different types of time delay are given in Sauer and Pai (1994). Here, for the purpose of studying the limit cycling phenomenon, we will restrict our attention to the following three OLTC models:

ODE This is a model often used in voltage stability analysis. It approximately describes the dynamics of an OLTC with an inverse-time delay characteristic, but does not account for the deadband or discrete tap steps. The model can be written as

$$\frac{dn}{dt} = -\frac{1}{T}(v - v_r) \quad (\text{C.7})$$

where v is the regulated voltage, v_r is the voltage setpoint and T is the controller time delay.

DBODE Augmenting the *ODE* model with a deadband on the input we get

$$\frac{dn}{dt} = \begin{cases} -\frac{1}{T}(v - v_r - DB/2) & \text{if } v - v_r > DB/2 \\ -\frac{1}{T}(v - v_r + DB/2) & \text{if } v - v_r < -DB/2 \\ 0 & \text{if } |v - v_r| < DB/2 \end{cases} \quad (\text{C.8})$$

where DB is the size of the deadband.

Detailed is the control system described by Figure C.2 with $T_d = \frac{DB T_{d0}}{2|v - v_r|}$ and $T_m = \frac{DB T_{m0}}{2|v - v_r|}$.

It is shown in Sauer and Pai (1994) that if T in (C.7) is chosen such that $T \frac{DB/2}{\text{tap step}} = T_{d0} + T_{m0}$, the *ODE* model makes the best continuous state match to the *Detailed* model in the sense of time response.

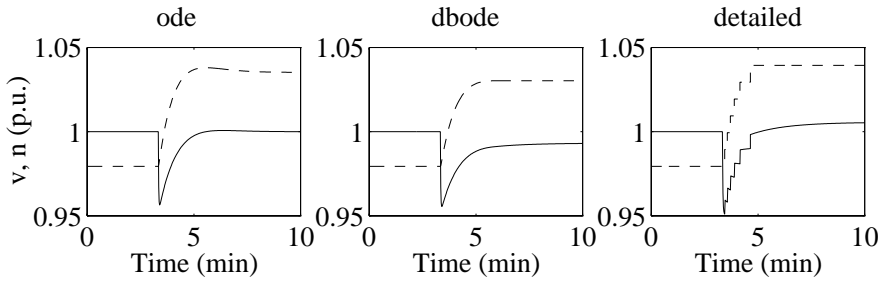


Figure C.3: Response to voltage disturbance for the three OLTC models - Load side voltage (solid line) and tap ratio (dashed line).

To illustrate potential differences in OLTC responses (Figure C.3), a 5 % disturbance in the feeding voltage, v_0 , is assumed in the moderately loaded ($k = 0.5$) power system of Figure C.1. System parameter values are given in Table C.1. With the *ODE* model, the tap ratio is adjusted until the voltage deviation becomes exactly zero. Since at that time, the load dynamics have not settled yet, there is a slight overshoot. With the *DBODE* model, the feedback path is broken as soon as the voltage deviation is within the deadband. Therefore, overshoot due to the load dynamics is avoided. With the *Detailed* model, the tap state is changed in fixed steps. Additional voltage restoration due to load dynamics following the last tap operation is also present with this model.

Despite the slight differences in responses in Figure C.3, the overall behaviour of the moderately loaded system is similar for all OLTC models. The sensitivity to the OLTC modelling is however more significant in a heavily loaded power system. As it will be shown in the following sections, the occurrence of voltage collapse or limit cycles is greatly affected by the OLTC model used in the analysis.

C.3 Small Signal Stability Analysis

The system equilibrium can be found by solving the equations $f(x, V) = g(x, V, n) = 0$ for the unknowns x , n and δ . Linearizing (C.3)-(C.4) around

the equilibrium point yields

$$\frac{d(\Delta x)}{dt} = \frac{\partial f}{\partial x} \Delta x + \frac{\partial f}{\partial V} \Delta V \quad (\text{C.9})$$

$$0 = \frac{\partial g}{\partial x} \Delta x + \frac{\partial g}{\partial V} \Delta V + \frac{\partial g}{\partial n} \Delta n \quad (\text{C.10})$$

Eliminating ΔV from (C.9) using (C.10), the linearized system model can be written in the standard state space form with Δn as an input and ΔV as an output. That is,

$$\frac{d(\Delta x)}{dt} = A \Delta x + B \Delta n \quad (\text{C.11})$$

$$\Delta V = C \Delta x + D \Delta n \quad (\text{C.12})$$

where $A = \frac{\partial f}{\partial x} - \frac{\partial f}{\partial V} \left(\frac{\partial g}{\partial V} \right)^{-1} \frac{\partial g}{\partial x}$, $B = -\frac{\partial f}{\partial V} \left(\frac{\partial g}{\partial V} \right)^{-1} \frac{\partial g}{\partial n}$, $C = -\left(\frac{\partial g}{\partial V} \right)^{-1} \frac{\partial g}{\partial x}$ and $D = -\left(\frac{\partial g}{\partial V} \right)^{-1} \frac{\partial g}{\partial n}$. The state space form has the more convenient transfer function equivalent

$$G_n(s) = C(sI - A)^{-1}B + D \quad (\text{C.13})$$

By combining the *ODE* OLTC model with the linearized system model, small signal stability analysis is made using the parameter values given in Table C.1. Figure C.4 shows a contour map of the real part of the dominant mode eigenvalue as a function of the OLTC time delay (T) and the load scale factor (k). The stability bound is thus given by the 0-contour. Two observations that can be made regarding the system small-disturbance stability are as follows: first, for $T = 30$ s, the system is stable if $k < 1.082$, and second, for $k < 0.986$, the system is stable for all positive T . In the next sections, these stability results will be verified by simulation.

C.4 Mechanisms in the Limit Cycle Phenomenon

To illustrate the contributing mechanisms to the limit cycle phenomenon, a simulation is made using the *Detailed* OLTC model. The reactive load has been made overcompensated by setting $B_0 = 0.6$ p.u. The other parameter values are as given in Table C.1 and the load factor is set to $k = 1$.

Referring to the simulation results in Figure C.5, the course of events is as follows. Initially, the voltage deviation is positive and growing. When the

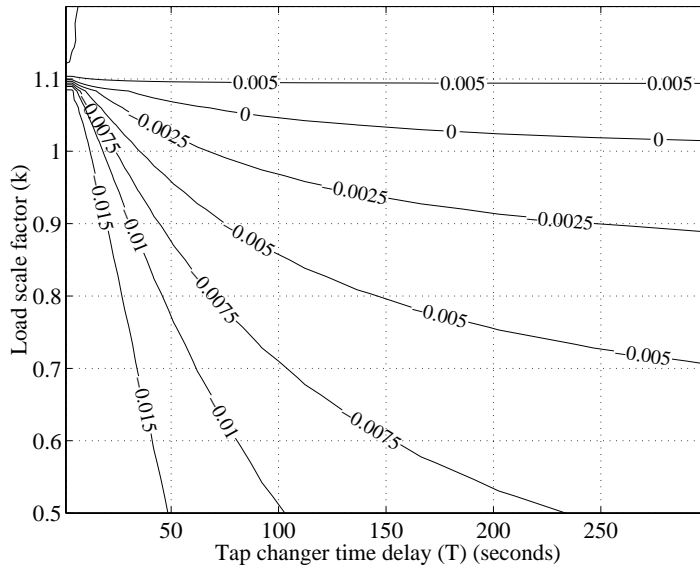


Figure C.4: Stability contours as a function of load factor (k) and OLTC time delay (T).

deadband is exceeded, the timer is started. As soon as the timer expires, a tap operation is made and the new operating point is determined by the change in tap ratio, the change in reactive output from the capacitor bank and the instantaneous load relief according to $P_t(V)$. As the load recovers to the value dictated by $P_s(V)$, the load-side voltage decreases further, and consequently also the output of the capacitor bank decreases. If the capacitor bank and load recovery is sufficiently strong, as is the case here, the voltage continues to decrease until a reverse tap operation is executed.

Voltage then starts to increase due to the change in tap ratio, capacitor bank output and load response. The influence of the load dynamics is now opposite compared to the downward tap operation and voltage now increases until a new downward tap operation is necessary. The resulting cyclic behaviour is called *limit cycle*. From this simulation it is evident that a limit cycle results from an interaction between OLTC deadbands, OLTC and load dynamics accompanied by the load/capacitor voltage sensitivity.

Note however that the instability observed in this example originates from the unstable load dynamics (including capacitor bank) and the interaction be-

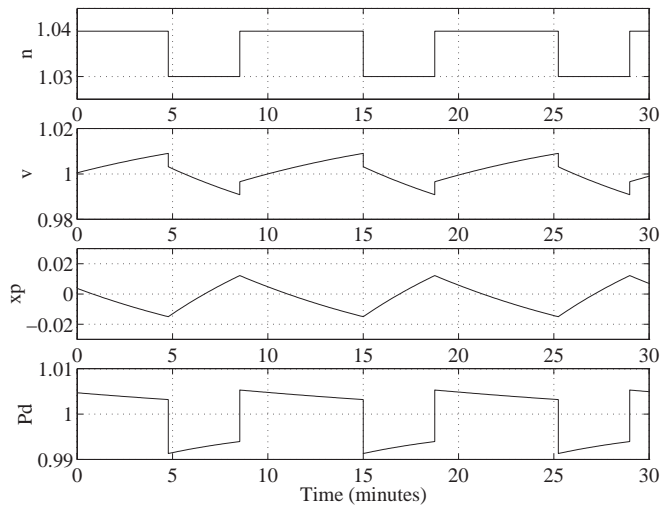


Figure C.5: Illustration of limit cycle.

tween load and tap changer. This indicates that it is not possible to avoid limit cycle behaviour simply by retuning the OLTC deadbands or time delays. This issue will be further discussed in Section C.5 where an analytical insight is given using the describing function method and time simulation.

C.5 Describing Function Analysis

The describing function method can be used to predict existence, period time and amplitude of limit cycles in linear systems under nonlinear feedback such as shown in Figure C.6b. A thorough presentation of the describing function method and describing functions of some standard nonlinearities are given in Hsu and Meyer (1968).

The method is based on the assumption that since all limit cycles are periodic, they are approximately sinusoidal. This assumption is reasonable if the transfer function $G(s)$ in Figure C.6b has low pass characteristics, i.e., filters out higher order harmonics. The linearized model $G_n(s)$ given by (C.13) does not have this property (since the matrix D in (C.12) is nonzero). However when lumped with the ODE part of the *DBODE* model denoted by $G_c(s)$ in Figure C.6a, it achieves this.

The describing function of the deadband in the *DBODE* model is (Hsu and Meyer, 1968)

$$N(A) = \begin{cases} 1 - \frac{2}{\pi}(\sin^{-1}(\frac{DB}{2A}) + \frac{DB}{2A}\sqrt{1 - (\frac{DB}{2A})^2}) & \text{if } A > DB/2 \\ 0 & \text{if } A < DB/2 \end{cases} \quad (\text{C.14})$$

where A is the amplitude of a sinusoidal input. A necessary condition for existence of a limit cycle is (Hsu and Meyer, 1968)

$$G(j\omega) = -\frac{1}{N(A)} \quad (\text{C.15})$$

This equation is not easily solved analytically in terms of load and OLTC model parameters, but can be solved graphically or numerically. A limit cycle exists for each intersection of the curves $G(j\omega)$ and $-1/N(A)$ in a Nichols diagram. From the point of intersection, the amplitude and frequency of the limit cycle are approximately determined.

In Figure C.7 the two curves are shown for different values of k in the interval $[0.8, 1.1]$ and $T = 30$ s. The following three cases can distinguished:

1. $k < 0.986$, the open loop system $G(s)$ has only stable poles, the closed loop system is stable, the phase changes from -90° at low frequencies to -90° at high frequencies, no intersection can occur (dotted lines);
2. $0.987 < k < 1.082$, the open loop system has one unstable pole, the closed loop system is stable, the phase changes from -270° at low frequencies to -90° at high frequencies, one intersection (thin solid lines);
3. $k > 1.083$, the open loop system has one unstable pole, the phase changes from -270° at low frequencies to -90° at high frequencies, the closed loop system experiences instability, no intersection (dash-dotted lines).

In case 2, the intersection indicates that a limit cycle exists. The amplitude of the limit cycle is determined by the curve $-1/N(A)$ which depends only on the deadband size and the frequency is determined from the curve $G(j\omega)$ that is independent of the deadband size. The describing function always maps on a line between $(0\text{dB}, -180^\circ)$ and $(\infty, -180^\circ)$ regardless of the deadband size. It

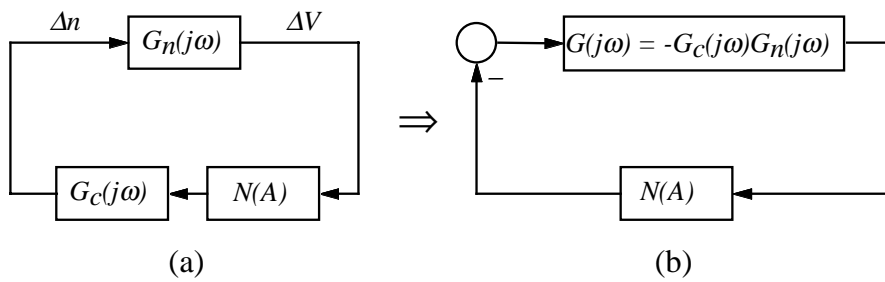


Figure C.6: Schematic of the feedback loop used in the describing function analysis.

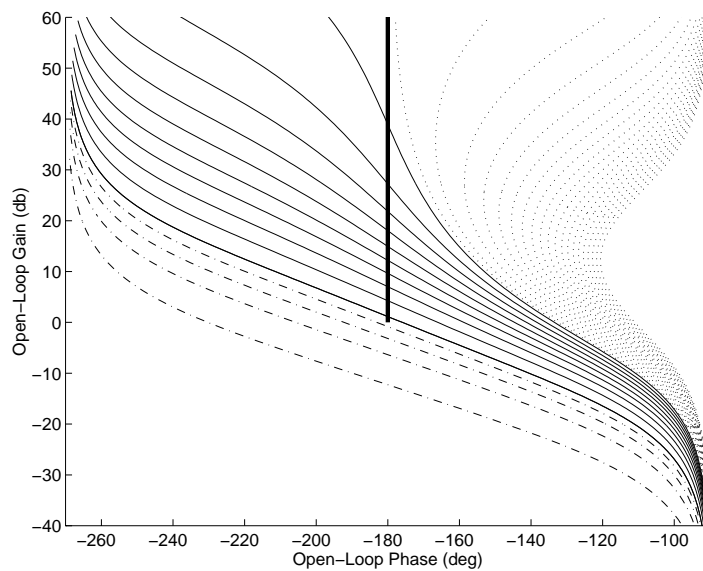


Figure C.7: Nichols diagram of $G(j\omega)$ for different values of k in the interval $[0.8, 1.1]$ ($T = 30$ s). The thick line is $-1/N(A)$.

implies that a change in the deadband size does not affect the existence of a limit cycle. The change in time constants, such as time delay or load recovery time constants, affects $G_c(j\omega)$ as a gain factor and therefore shifts the curve $G(j\omega)$ up or down in the Nichols plot. Consequently, the amplitude can be changed but not the frequency. Shifting the curve below the point $(0\text{dB}, -180^\circ)$ could remove a limit cycle, but would also cause instability of the closed loop system. Note however that load scaling (k) and the voltage sensitivity parameters of the load have a significant influence, and can affect existence, frequency and amplitude of limit cycles, since they directly affect the shape and position of the curve $G(j\omega)$.

Simulation is used to verify the predictions of the existence and stability of limit cycles. Figure C.8 (top) illustrates the stable system behaviour for the lower bound on k ($k = 0.986$) along with the describing function analysis result which correctly predicts that the system is free from limit cycles. Increasing the value of k yields limit cycles of various amplitudes. A_{lim} and T_{lim} given in the figure denote the amplitude and period time of limit cycle as predicted by the describing function method. As can be seen from Figure C.8, the limit cycle amplitude is predicted accurately for all values of k , but the frequency is not for small k . For $k = 1.09$, no limit cycle is present, but the closed loop system is unstable as predicted by the small-disturbance and describing function analysis. Note that for the describing function method to provide an accurate prediction of the limit cycle frequency, the two curves $G(j\omega)$ and $-1/N(A)$ should intersect at an angle as close as possible to 90° . Referring to Figure C.8, it is clear that for the smaller values of k , the angle of intersection deviates increasingly from the ideal 90° . The logarithmic scale of the y-axis partly conceals this deviation in Figure C.8.

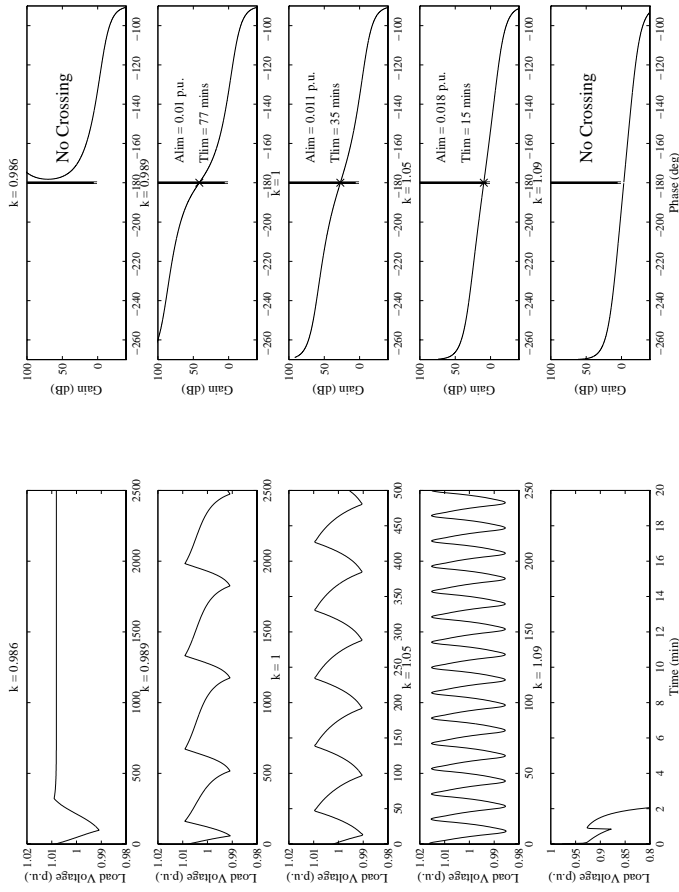


Figure C.8: Simulations and describing function analysis with different k , ($T = 30$ s, $DBODE$ model).

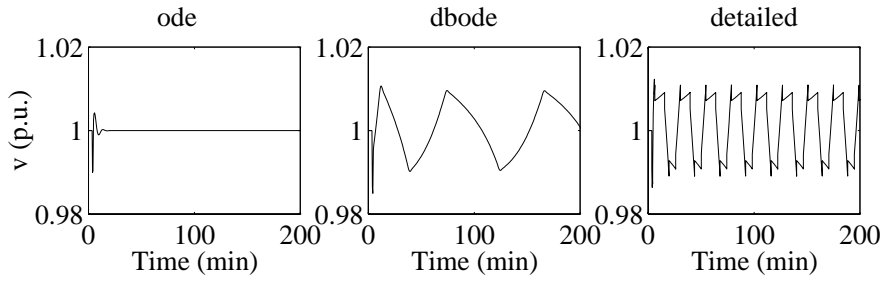


Figure C.9: Simulations of feeding voltage disturbance for different OLTC models. $k = 1$, $T = 30$ s.

C.6 Comparison of OLTC Models

In this section the sensitivity of system behaviour to OLTC modelling is investigated for a highly loaded power system. Figure C.9 presents simulation results obtained with $k = 1$ and $T = 30$ s. As seen in the figure, the system exhibits stable behaviour with the *ODE* model. This is in agreement with small-disturbance stability analysis. For the models that contain the deadband though, there are limit cycles with an amplitude of 0.01 p.u. and different frequencies, depending on the OLTC model used.

The small-disturbance analysis in Section C.3 also indicates, that the system with the *ODE* model is unstable if the load dynamics are sufficiently fast compared to the OLTC time delay. This is illustrated in Figure C.10 (top left) for $k = 1$, $T = 120$ s and $T_p = T_q = 10$ s. The system remains unstable with the *DBODE* model too, but the extra lag introduced by the deadband causes the oscillations to grow more rapidly and voltage collapse occurs one period earlier for that model than for the *ODE* model. However with the *Detailed* model the system exhibits a limit cycle preventing the occurrence of oscillatory voltage instability.

From the simulations in this section, we see that the modelling of the OLTC has a significant effect on the behaviour of the system model.

C.7 Discussion

The describing function analysis results in terms of conditions for limit cycle existence, presented in Section C.5, are valid only for the *DBODE* OLTC model.

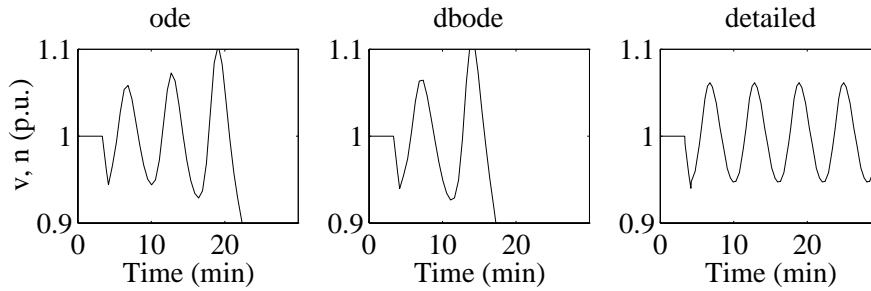


Figure C.10: Simulations of feeding voltage disturbance for different OLTC models. $k = 1$, $T = 120$ s, $T_p = 10$ s, $T_q = 10$ s.

Nevertheless, the analysis has clearly shown that the limit cycle phenomena are related to the load dynamics, deadbands and the interaction between load and tap changer. It has also been shown that the limit cycles are present in the mathematical model of the power system and that they do not occur due to numerical problems in the simulation. A similar analysis for the *Detailed* OLTC model is possible but would require derivation of the describing functions corresponding to the nonlinearities present in that model. Note that, since those nonlinearities have memory, the describing functions will be frequency dependent as well as amplitude dependent.

Because of the well-known limitations of the describing function method (Hsu and Meyer, 1968), only a single load single OLTC system has been considered here. However, the simulation of a power system model with cascaded OLTCs has been shown to exhibit a similar or even greater tendency to self-oscillate (Hiskens and Hill, 1993, Popović et al., 1996a).

A somewhat surprising conclusion made in the paper is that the limit cycles cannot necessarily be avoided by adjusting the OLTC deadband or time delay. The explanation is that when the voltage deviation is within the deadband, the system effectively operates in open loop. As soon as the deadband is exceeded, the control loop is closed again and the instability is arrested. Referring to Figure C.7, a necessary condition for the limit cycle to appear is that the open loop system is unstable (due to capacitor bank and load dynamics interaction). If that is the case, an increase of the deadband size will increase the amplitude of a limit cycle but will not remove it. Similarly, the different time delays in the OLTC control system have no influence on the existence of limit cycles,

only on the amplitude and period time. The only parameters that can affect the existence of limit cycles are the load and network parameters. Note that for the sake of getting more insights into the role of deadbands and load-tap interaction in creating the cyclic behaviour, the tap limits were turned off in our study. That potential source of limit cycles is illustrated in Vournas and Van Cutsem (1995).

Despite the lack of clear evidence for the deadband and load-tap interaction related limit cycles occurring in power systems, the analysis presented in the paper offers an analytical study which clearly illustrates the potential for this sort of phenomena arising in nonlinear highly stressed power systems.

C.8 Conclusions

In this paper the phenomenon of limit cycle behaviour due to tap changer deadbands and load-tap interaction has been investigated. The effect of tap dynamics modelling on system behaviour is illustrated. It has been shown that the results from small disturbance analysis based on a continuous OLTC model can be unreliable, especially in a heavily loaded power system. Under heavy load conditions, the system with a detailed OLTC model exhibits a limit cycle that will arrest oscillatory voltage instability predicted by small-disturbance analysis.

The key parameters in creating/avoiding this kind of limit cycles are identified as the system load level, degree of reactive compensation and the load-voltage dependency. In certain loading conditions, adjusting OLTC control system parameters such as time delays or deadband size is shown not to have any effect on the existence of the limit cycles.

C.9 Acknowledgements

This work was sponsored by a grant from Sydkraft AB, Sweden, Elforsk AB, Sweden, and by an Australian Electricity Supply Industry Research Board project grant "Voltage Collapse Analysis and Control".

Paper D

Emergency Voltage Control using Search and Predictive Control

Mats Larsson David J. Hill Gustaf Olsson

Accepted by *International Journal of Power & Energy Systems*

Abstract: *This paper presents a method of optimal coordination of load shedding, capacitor switching and tap changer operation using a dynamic system model in order to preserve long-term voltage stability. The method is based on model predictive control and tree search. A model of the controlled system, including the network and load dynamics, is used to predict the future system behaviour based on the current state and applied control actions. The optimal control state according to these predictions is then obtained using a search method similar to those used in chess computers. A detailed and three simplified predictors are presented along with a tuning procedure that aims to ensure that a minimum amount of emergency controls is scheduled by the controller.*

D.1 Introduction

Electric power systems are designed, through careful planning and preventive control schemes, to survive most foreseeable disturbances (Kundur, 1994). Not all possible disturbances, however, can be foreseen at the planning stage and these may result in instability that will eventually lead to collapse or islanding of the system. The objective of an emergency control system is to detect such

situations and carry out control actions necessary to prevent collapse of the system.

The emergency controls considered here are: capacitor bank switching, tap changer operation and load shedding. The principles of using these as efficient emergency controls have been established in Vu and Liu (1992), Xu and Mansour (1994), Popović et al. (1996b), Arnborg et al. (1998). Descriptions of some protection systems against voltage collapse that presently are in use can be found in CIGRE (1998). Most of these are rule-based and use only a single local or a few key measurements, with ad hoc coordination between controls of different types or in different locations.

The highly nonlinear nature of the problem calls for more sophisticated methods based on a dynamic system model in order to account for the current operating point and network state. In particular, proper coordination of all controls would minimize the amount of load shed. Furthermore, it is now understood that load dynamics play an important role in voltage instability incidents, and consequently contain information useful for the determination of emergency controls. Most controls are inherently discrete to their nature, for example, capacitor banks and tap changers must be switched in fixed steps and while most utilities lack direct load control schemes, load shedding must still be carried out by disconnecting whole feeders.

Coordinated voltage control in the normal state based on static models has received considerable attention in the research on secondary voltage control (Janssens, 1993, Corsi, 2000, Ilic et al., 1995, Vu et al., 1996), whose primary function is to determine voltage setpoints of generators in a coordinated way. However, this work does not consider control dissimilarity, system and load dynamics, or operation in the emergency state. Methods for coordination of secondary voltage control and load shedding using static system models have been described in Popović et al. (1997). Coordination of dissimilar controls in the emergency state based on a dynamic system model has so far received little attention. In Overbye and Klump (1998), emergency control actions are determined through analysis of the sensitivities of an energy function stability measure to controls. A method based on differential dynamic programming and a security measure as the distance to the closest bifurcation has been derived in Popović et al. (1998), Wu et al. (1999b). None of the above mentioned references take account of the discrete nature of controls or the inherent dynamics of the loads.

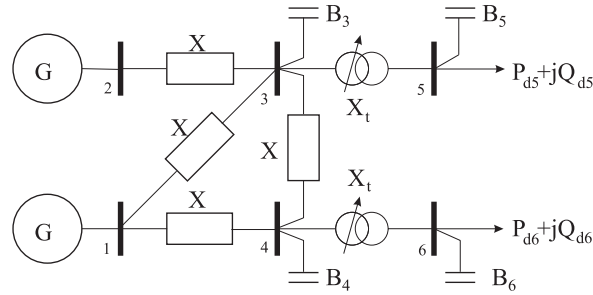


Figure D.1: Example power system studied.

Some preliminary results leading on to those in this paper, were presented in Larsson (1999), where tree search and predictive methods were first employed in order to account for the discrete nature of controls and the load dynamics. The present paper demonstrates the application of model predictive control (MPC) to emergency state voltage control. General model predictive control is well established for process control (Garcia et al., 1989, Morari and Lee, 1999) but the application to power systems control is believed to be new. A model of the controlled system, including the network and load dynamics, is used to predict the future system behaviour based on the current state and the applied control actions. The optimal control actions can then be obtained from the solution of a combinatorial optimization problem by a search method. Various predictors are employed, ranging from a detailed predictor based on simulation of the system to more computationally tractable linearized versions.

D.2 Modelling

D.2.1 Example System

Consider the simple power system in Figure D.1. There are two loads, four capacitor banks and two on-load tap changing transformers considered as actuators. These can be operated in the discrete fixed steps given in Table D.5.

D.2.2 Component Modelling

The generator at bus 1 is modelled as an infinite bus with fixed voltage and voltage angle while the generator at bus 2 is modelled using the standard sixth

order dq-model (Machowski et al., 1997) with a first order excitation system, an overexcitation limiter and a first order governor. The loads are modelled using the aggregate exponential recovery model (Karlsson and Hill, 1994)

$$T_p \dot{x}_p + x_p = P_s(V) - P_t(V) \quad (\text{D.1})$$

$$P_d = k_l(x_p + P_t(V)) \quad (\text{D.2})$$

where x_p is a continuous dynamic state that can be interpreted as a measure of the energy deficit in the load and $P_s(V) = P_0 V^{\alpha_s}$ and $P_t(V) = P_0 V^{\alpha_t}$ are the steady-state and transient voltage dependencies respectively. P_d is the actual active load power and T_p is the active power recovery time constant. For the reactive load power, a similar model is used with corresponding characteristics $Q_d, x_q, Q_s(V) = Q_0 V^{\beta_s}, Q_t(V) = Q_0 V^{\beta_t}$ and time constant T_q . The scale factor k_l models load shedding and is applied to the reactive as well as to the active power load model. The transformers are modelled as pure reactances in series with an ideal turns ratio change.

For the purpose of control determination, generators and their associated control systems are modelled more simply, using their quasi-steady state approximations given in Van Cutsem and Vournas (1998), i.e, the derivative terms in the mechanical and flux equations are neglected. Figure D.2 illustrates the correspondence between the detailed and simplified component models. The main difference is the absence of the fast electromechanical oscillations in the simulation with the simplified model. However, it does capture the essential long-term behaviour of the system. As has also been observed in Van Cutsem and Vournas (1998) the simplified model is slightly conservative in predicting the voltage collapse due to the static approximation of the generator and overexcitation limiter.

D.2.3 System Modelling

A power system network model is conveniently expressed in the hybrid differential-algebraic form (Van Cutsem and Vournas, 1998)

$$\dot{x} = f_{dae}(x, w, z(k)) \quad (\text{D.3})$$

$$0 = g_{dae}(x, w, z(k)) \quad (\text{D.4})$$

$$z(k+1) = h_{dae}(x, w, z(k)) \quad (\text{D.5})$$

The dynamic state variables x are variables that appear as derivatives in differential equations and cannot change instantaneously. On the other hand, the

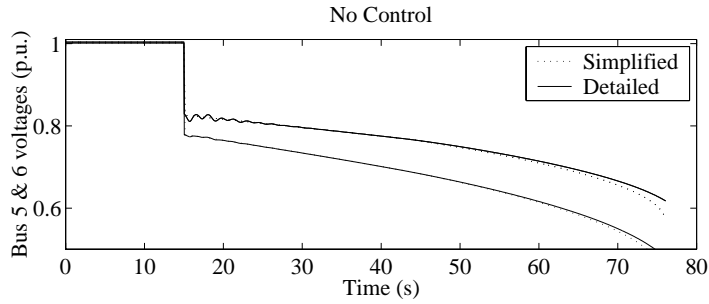


Figure D.2: Voltage response without emergency control.

algebraic state variables w do not appear as derivatives, and can thus change instantaneously due to changes in x or $z(k)$. The discrete state variables $z(k)$ have discrete-time dynamics and can change only at fixed time instants given by a selected sample time. The dynamic state variables relate to generator flux, control and load dynamics; algebraic state variables relate to network voltages and currents; and the discrete states $z(k)$ typically arise from discrete control logic such as relay controls.

The full system model can be obtained on the hybrid DA form, for instance using the modelling and simulation tool Dymola and the power system component library ObjectStab (Larsson, 2000a), for the component models given previously in this section. Furthermore, assuming that the Jacobian of (D.4) is nonsingular, the continuous part (D.3)-(D.4) of the hybrid DA form can be reduced to the ordinary differential equation form

$$\dot{x} = f(t, x, u) \quad (\text{D.6})$$

$$y = g(t, x, u) \quad (\text{D.7})$$

This reduction eliminates the algebraic and discrete states. Some variables in w can be solved for symbolically and the remainder must be solved for by an iterative solver when the functions f and g are evaluated. Additionally, u and y are vectors of external control and output signals that may be arbitrarily chosen. The reduction is done using the current values of the discrete state variables; thus the ODE form does not account for discrete behaviour, but is more convenient for steps of the control design.

D.3 Control Problem Formulation

D.3.1 Model Predictive Control

The principle of Model Predictive Control (MPC) is illustrated in Figure D.3. A model predictive controller uses a system model to predict the future output trajectories (dotted lines) based on the current state and for several different candidate input sequences. A cost function is defined based on the deviation of each predicted trajectory from a desired trajectory (dashed line). The optimal control sequence, in the sense that it minimizes the defined cost function, is then obtained by solving an optimization problem on-line each time a new instance of the control sequence is to be determined. The optimal control is then applied to the system, until the next sample time. The interval between the current time t^* and the prediction horizon $t^* + t_p$ is referred to as the prediction interval, and is chosen based on the settling time of the slowest dynamics. Usually, the prediction interval is chosen as a multiple of the sample time.

In the standard formulation it is assumed that all control signals are continuous, i.e., can assume all values within some fixed range. In the case of a linear system this leads to an optimization problem that can be solved using quadratic programming whereas nonlinear programming is required with a nonlinear system.

D.3.2 Application to Emergency Voltage Control

Our application differs from the general nonlinear case in that the control variables are constrained to fixed discrete values which makes it necessary to resort to a combinatorial optimization method. In the standard formulation a sequence of control inputs, for the first n samples during the prediction horizon, is obtained from the optimization. The first control signal in this sequence is then applied to the plant, and the rest are discarded when the next optimization has been carried out. Here, when computing the new control signal, it is assumed that it will be in use during the entire prediction interval (that is, $n = 1$).

Accordingly, the problem of selecting the new control vector u^+ at the operating point $(x^*, u^-) = (x(t^*), u(t^*))$ can be formulated as the combinatorial optimization problem

$$\begin{aligned} & \text{minimize} && J(x^*, u) \\ & \text{subject to} && u \in \mathcal{S}(u^-) \end{aligned} \tag{D.8}$$

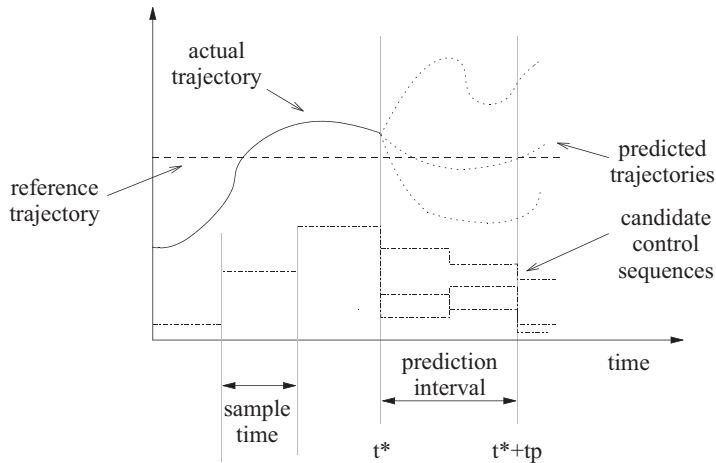


Figure D.3: Principle of Model Predictive Control.

where u is the optimization variable corresponding to the new control state to be used during the interval $[t^*, t^* + t_p]$ whereas u^- denotes the control state presently in use, in other words before the optimization starts at time t^* . $\mathcal{S}(u^-)$ is the set of available control states at time t^* and is normally a function of u^- . The scalar function $J(x^*, u)$ is referred to as a cost function and should evaluate the candidate control state u such that a smaller result indicates a more desirable state. Typically, the cost function should include a component based on the deviations of the chosen outputs from their reference trajectories and a component based on the control variations.

Constraints can be imposed on inputs as well as states and outputs as follows:

- Input constraints, for example actuator limits, are modelled using the set of available control states. Since the set may be a function of the present control state, actuator ramp limits can also be handled. More specific constraints can also be represented. For instance, a useful constraint is to set priorities for control actions.
- Output and state constraints could be modelled as hard constraints by letting the cost function assume an infinite value, thus ensuring that a control state leading to a constraint violation is never selected. However, it is generally not desirable to impose hard constraints on the outputs or

states since they may be impossible to strictly fulfil even with an optimal control sequence. The optimization problem would then be infeasible, and no control could be determined. Therefore, output and state constraints are modelled as soft constraints by adding terms to the cost function that represent the "cost" of violating a (soft) constraint (Mayne et al., 2000). If this cost is dominant over other terms in the cost function, the primary aim of the controller will be to minimize any constraint violation.

Control actions are divided into two classes:

- Normal control measures are those that will be routinely scheduled; capacitor and tap changer operations belong to this category.
- Emergency control measures are those that will be scheduled only when required for the satisfaction of a constraint. Such controls are activated only if the constraint cannot be satisfied using any combination of the normal control measures. Load shedding belongs to this category.

The cost function is defined in the form

$$J(u^+, x^*) = \int_{t^*}^{t^*+t_p} (\hat{y} - y_r)^T \mathbf{Q} (\hat{y} - y_r) + (u^+ - u^-)^T \mathbf{R} (u^+ - u^-) + P(t, x^*, u^+) dt \quad (\text{D.9})$$

where $\hat{y} = \hat{y}(t, x^*, u^+)$ is a prediction of the output trajectory using information up to time t^* if the new piecewise constant control u^+ is applied during the prediction interval. The control state presently in use is denoted u^- , the reference trajectory y_r , and the weighting matrices for output errors and control variations are denoted \mathbf{Q} and \mathbf{R} respectively. A special penalty term $P(t, u^+, x^*)$ is introduced whenever a constraint violation or a singularity-induced bifurcation is predicted to occur within the prediction horizon ($t \in [t^*, t^* + t_p]$). A suitable selection of \mathbf{Q} , \mathbf{R} and $P(t, u^+, x^*)$ ensures that none of the emergency controls are scheduled unless they are necessary to remove a constraint violation during the prediction interval. A tuning procedure is described in Appendix D.9.

D.3.3 Predictors

The cost function is calculated from predictions of the output trajectories. Different methods of obtaining (approximations of) these trajectories are presented below.

1. Nonlinear MPC (NLMPC)

The system (D.3)-(D.5) is a hybrid nonlinear system, and it is therefore generally impossible to find an analytical expression for the trajectories ($\hat{y}(t, u)$). The most straightforward method is to obtain them numerically. This requires simulation of the hybrid DAE model over the prediction interval for each evaluation of the cost function.

2. Euler State Prediction (ESP)

Long-term voltage behaviour is typically monotonic during voltage collapse scenarios. Based on this assumption, the output trajectories are approximated by straight lines between their respective values at the beginning and end of the prediction interval as follows: the instantaneous effect of applying the new control u^+ can be computed from

$$\hat{y}(t^*, u^+) = g(t^*, x^*, u^+) \quad (\text{D.10})$$

Assuming linear behaviour of the system state trajectories during the prediction interval, the change in the dynamic states is predicted using an Euler prediction

$$\Delta x(t^* + t_p, u^+) = t_p f(t^*, x^*, u^+) \quad (\text{D.11})$$

yielding the predicted outputs at the end of the prediction horizon

$$\hat{y}(t^* + t_p, u^+) \approx g(t^* + t_p, x^* + \Delta x(t^* + t_p, u^+), u^+) \quad (\text{D.12})$$

A straight-line approximation of the output trajectories during the interval $[t^*, t^* + t_p]$ to be inserted in (D.9) is then given by

$$\hat{y}(t, u) = \hat{y}(t^*, u^+) + \frac{t}{t_p} (\hat{y}(t^* + t_p, u^+) - \hat{y}(t^*, u^+)) \quad (\text{D.13})$$

After insertion of (D.13), the integral in (D.9) can be computed symbolically and thus does not require numerical computation, as with the nonlinear and linearized MPC.

3. MPC using off-equilibrium linearizations (LMPC)

Introducing the coordinate changes $\Delta x(t) = x(t) - x^*$, $\Delta u = u^+ - u^-$, $\Delta y(t) = y(t) - y^*$ and $\Delta \dot{x}(t) = \dot{x}(t) - \dot{x}^*$ and linearizing the system (D.6)-(D.7) at the point (x^*, u^-) yields

$$\Delta \dot{x}(t) = \frac{\partial f}{\partial x} \Delta x(t) + \frac{\partial f}{\partial u} \Delta u = \mathbf{A} \Delta x(t) + \mathbf{B} \Delta u \quad (\text{D.14})$$

$$\Delta y(t) = \frac{\partial g}{\partial x} \Delta x(t) + \frac{\partial g}{\partial u} \Delta u = \mathbf{C} \Delta x(t) + \mathbf{D} \Delta u \quad (\text{D.15})$$

By computing the step responses from every input to every output of the linearized model at the root of the tree, the output trajectories can be approximately computed using a linear combination of these step responses. The approximations are then inserted into (D.9) and the integral is computed numerically. The linearization and the corresponding step responses need to be computed only once, prior to the start of the optimization.

4. Euler State Prediction-Linear Output Approximation (ESPLO)

Each computation of the functions f and g involves an iterative solver. A further simplification is to predict the outputs at the beginning and end of the prediction interval using the linearized ODE model

$$\hat{y}(t^*, u) \approx y^* + \mathbf{D} \Delta u \quad (\text{D.16})$$

$$\Delta x(t^* + t_p, u) \approx t_p (\dot{x}^* + \mathbf{B} \Delta u) \quad (\text{D.17})$$

$$\hat{y}(t^* + t_p, u) \approx \mathbf{C} \Delta x(t^* + t_p, u) + \mathbf{D} \Delta u \quad (\text{D.18})$$

The approximation can then be computed by combining Equations (D.17), (D.18) and (D.13) and inserting into (D.9).

Comparison

The NLMPC predictor is the most accurate. It makes use of the full simulation model and thus accounts for hybrid as well as nonlinear behaviour of the system. The LMPC calculates its prediction based on a linearized model obtained using the current values of the discrete state variables and the control input before the optimization starts. If discrete events occur, for example due to activation of generator current limiters, this will be correctly accounted for by the NLMPC. The LMPC ignores such events until the system is relinearized at

the next sampling instant. Oscillatory behaviour will be detected and penalized with both the NLMPC and LMPC.

The ESP and ESPL0 employ another kind of simplification, where the output trajectories are assumed to follow straight lines between their current values and their predicted values at the prediction horizon. This neglects any oscillatory behaviour that may arise. This can be expected to give a good approximation of the trajectories in the case of monotonic behaviour, or if the period times of all oscillatory modes are significantly longer than the prediction interval. Otherwise, the controller will control the mean values of the outputs and not actively dampen the oscillatory mode. Oscillatory modes can be detected, and their damping and frequencies obtained through eigenvalue analysis of the matrix \mathbf{A} in (D.14). If discrete events occur due to the state evolution between sampling instants, they are ignored by both the ESP and ESPL0 until the next sampling instant. If discrete events occur due to the instantaneous effect of applying a new control state, this is correctly accounted for by the ESP but not by the ESPL0. Thus, the ESP provides a way of partially handling nonlinearities and discrete events in a computationally much cheaper way than the NLMPC.

With the NLMPC and ESP, which use the nonlinear system description, the optimization sometimes fails due to so-called singularity induced bifurcations. These arise when the Jacobian of (D.4) becomes singular and the transformation to the ODE form (D.6)-(D.7) can not be carried out. Since these bifurcations can be linked to a form of voltage collapse (Van Cutsem and Vournas, 1998), these control states are highly undesirable and are thus given large penalties. This penalty should be larger than the penalty applied in case of a constraint violation.

The linearized system description used by the LPMC and ESPL0 can only be expected to be accurate in a neighbourhood of the point of linearization. When a new control state is applied, the operating point moves instantaneously. Therefore, the accuracy of the linearized model will suffer if many controls are switched. Similarly, if the system is linearized at an off-equilibrium point, the accuracy of the linearized model may also deteriorate as the system trajectories move away from the point of linearization.

We will further investigate these approximations and their effect on the control response in Section D.5.

D.4 A Tree Search Method

Search methods are widely used in artificial intelligence research, especially in computer game playing (Stewart et al., 1994). In some simpler games, such as Checkers and Reversi, computer players based on search already play stronger than any human (Plaat, 1996). Strong chess programs can beat all but the very best humans, and in 1997, Deep Blue became the first chess computer to defeat a reigning human world chess champion in a regulation match (Campbell, 1999).

The combinatorial optimization problem (D.8) can be seen as a search problem, where the search state space is given by the control constraints. The set of available control states $\mathcal{S}(u)$ is explored searching for a best control state using the standard recursive depth-first algorithm (Russell and Norvig, 1995) shown in Table D.1. The algorithm relies on two auxiliary functions:

$\mathbf{s}(u)$ which generates all control states reachable from the current state u with a single switching of one control, that is, the subset of $\mathcal{S}(u)$ reachable from the state u by the switching of a single control.

$\mathbf{c}(u)$ which evaluates the state u , according to the cost criteria (D.9).

Figure D.4 shows the search tree for a simplified search problem where only the controls B_3 and B_4 in Figure D.1 are enabled; an additional constraint that each control may only change once in the tree has been imposed. The number shown below each node corresponds to the result reported by the function *search*. The search starts at the initial state (1) with $B_3 = 0.15$, $B_4 = 0.15$, corresponding to the root of the tree. From here four new states can be reached (2, 5, 8, 11) by changing either B_3 or B_4 one step up or down. From each of these four states another two can be reached by changing the other control. Here the optimum is found in nodes 3 and 9 for $B_3 = 0.3$, $B_4 = 0.3$. Note that the search tree (13 nodes) is larger than the state space ($3^2 = 9$ possible combinations) since it contains not only all possible control states but also all paths to them. The example search requires 13 evaluations of the cost-function.

For this trivial example, the search state space is limited by the control constraints because of the small number of controls. However, the tree grows exponentially with the number of controls and an exhaustive search of the tree is not feasible for practical cases. With a larger number of controls, the size of the tree is limited by applying a maximum search depth. This search depth conse-

```

[ $f_{out}$ ] = function search ( $f_{in}$ ,  $u_{in}$ ,  $m$ );
   $f$  = call c( $u_{in}$ )
  if  $m = 1$  /* the node is a leaf node */
     $best = f$ 
  else
     $best = \min(f, f_{in})$ 
    for  $u_i = \text{call } s(u_{in})$  do
       $f_{tree} = \text{call } \text{search}(f_{in}, u_i, m - 1)$ 
       $best = \min(f_{tree}, best)$ 
    end
  end
return  $f_{out} = best$ 

```

| | | |
|-----------|---|--|
| f_{in} | - | best value found prior to search of tree |
| u_{in} | - | initial (root) control state |
| m | - | search depth |
| f_{out} | - | best value found after search of tree |

Table D.1: Pseudocode for construction and traversal of the search tree.

quently corresponds to the maximum number of controls that may change in one search.

D.5 Simulation Results

To illustrate the performance of the emergency controllers, results from simulation of the system in Figure D.1 are presented in Figures D.5–D.6. The applied disturbances are changes of the four line impedances from $X=0.2$ to $X=1.0$ p.u. If no emergency actions are taken, voltage collapse will occur at simulation time 70 s as shown in Figure D.2. The simulations have been carried out with a 30 s sampling interval of the controller, i.e. the tree search optimization is carried out periodically every 30 s. By the use of voltage constraints, load shedding is authorized if the voltages at bus 5 or 6 are predicted to be lower than 0.9 p.u. at the prediction horizon. The search depth is 4, the prediction horizon 120 s and the weight matrices and penalty terms were chosen according to the tuning procedure in Appendix D.9, with the output vector y containing the voltages of buses 5 and 6.

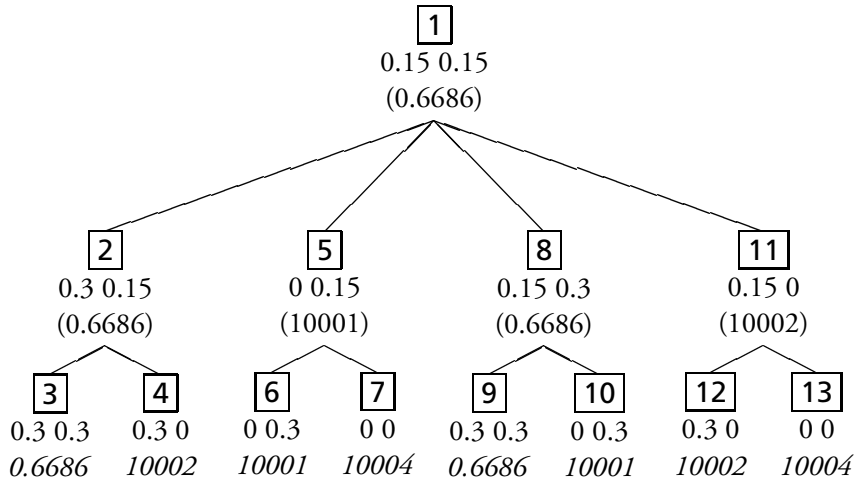


Figure D.4: Search example.

Figure D.5 shows the voltage response at buses 5 and 6 with all controls enabled. In this case, it is possible to stabilize the system without resorting to load shedding. All the predictors yield near-identical results. The NLMPC stabilizes and restores the voltages close to their pre-disturbance levels using 5 capacitor bank steps and 6 tap changer operations, whereas the three simplified methods use an extra capacitor switching for a total of 6. The control actions taken are listed in Table D.2. However, all predictors are capable of stabilizing the voltage.

Figure D.6 shows the voltage response to the same disturbance but with capacitor controls B_5 and B_6 disabled. The control actions taken are listed in Table D.3. The NLMPC stabilizes the voltages using 4 capacitor steps, 5 tap changer operations and 4 load shedding steps. The simplified predictors use an additional tap changer step at time 180 s respectively.

D.5.1 Summary

Table D.4 shows the average computation time of the different versions of the cost function using Matlab/Simulink and a standard 400 MHz Pentium II processor. A search for the example system with eight controls using a search depth of 4 typically results in a search tree with some 2000 nodes. This corresponds to a response time of 24 minutes using the NLMPC, which clearly makes it

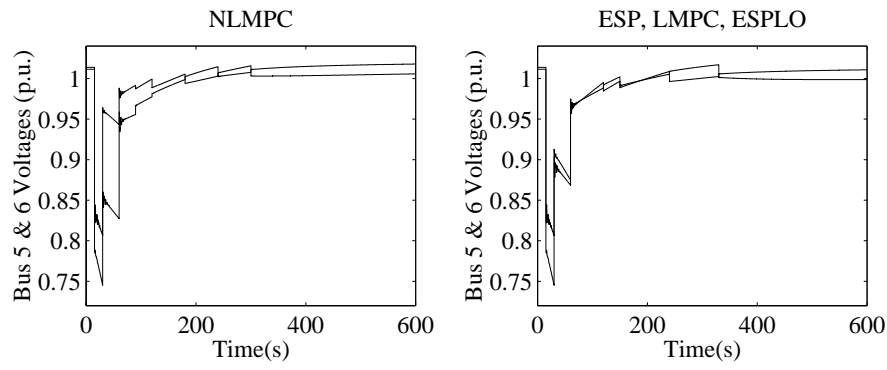


Figure D.5: Voltage response at buses 5 and 6 with all controls enabled. The three methods in the right hand figure yield identical results.

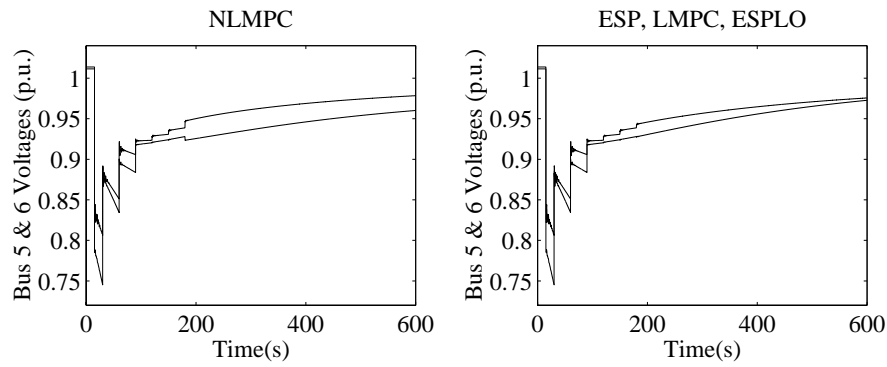


Figure D.6: Voltage response at buses 5 and 6 with B_5 and B_6 disabled. The three methods in the right hand figure yield identical results.

| Time (s) | Control |
|----------|---|
| 30 | $B_5 = 0.15, B_6 = 0.30$ |
| 60 | $B_4 = 0.15, B_5 = 0.30, n_{35} = 1.06$ |
| 120 | $n_{46} = 1.04$ |
| 150 | $n_{35} = 1.04, n_{46} = 1.02$ |
| 240 | $n_{46} = 1.00$ |
| 330 | $n_{35} = 1.02$ |

Table D.2: Control response with all controls enabled (LMPC, ESP, ESPLO).

| Time (s) | Control |
|----------|---|
| 30 | $B_3 = 0.15, B_4 = 0.15$ |
| 60 | $B_3 = 0.30, k_{l6} = 0.90$ |
| 90 | $n_{46} = 1.08, k_{l5} = 0.95, k_{l6} = 0.85$ |
| 120 | $n_{35} = 1.06, n_{46} = 1.10$ |
| 150 | $n_{35} = 1.08, n_{46} = 1.12$ |
| 180 | $n_{35} = 1.10, n_{46} = 1.14$ |

Table D.3: Control response with B_5 and B_6 disabled (LMPC, ESP, ESPLO).

| NLMPC | LMPC | ESP | ESPLO |
|--------|--------|-------|--------|
| 730 ms | 4.0 ms | 5.6ms | 1.6 ms |

Table D.4: Average computation time for the cost function.

unsuitable for on-line use. However, this method represents an 'exact' solution that can be used as a benchmark for the approximations. The various approximate methods use about 3-8 s for the same search, and produce results nearly identical to the NLMPC in the two simulated cases.

For this application, all the predictor yield satisfactory results, which makes the ESPLO the "best" choice since it is the computationally cheapest. If there are strong nonlinearities it may be necessary to use the ESP which to some extent account for these. The LMPC is a computationally cheap way of considering oscillatory dynamics, and finally the NLMPC can be used to fully account for hybrid behaviour. Note again, that only the hybrid behaviour between sampling instants is ignored with the simplified predictors. Before each optimization, the linearized model is updated using the present values of the discrete state variables. An attractive option is to normally use ESPLO which is the computationally cheapest, but periodically carry out an eigenvalue test of the matrix \mathbf{A} in (D.14) and switch to the LMPC whenever oscillatory modes are detected.

D.6 Further Work

The presentation here considers the emergency state operation. The same methodology can be used in an implementation that provides control coordination aimed at loss minimization in the normal state and for arresting voltage collapse

in the emergency state. The cost function would be based on system active power losses and two sets of voltage constraints would be used, for the normal and emergency states respectively. In principle the methodology described in this paper could be applied to any kind of stability problem in power systems, but we here restrict our attention to voltage stability.

We have used the simplest possible search scheme, concentrating on deriving simple and accurate predictors that can be rapidly computed. This makes the search problem tractable for the small system studied here. Unfortunately the number of nodes in the search tree grows exponentially with the number of controls as well as the search depth. This is a well-known problem that applies to all full-width search schemes. However, great progress has been reported from other applications in the use of search heuristics to order the expansion of nodes in the tree and cut off unpromising branches and thereby reduce the number of nodes searched. Similar techniques are the foundation of the success of modern chess computers (Campbell, 1999). Work is in progress to implement and demonstrate the method on a model of the Swedish power system with some 50 control handles, applying search heuristics to make the search problem tractable.

The predictors presented here are single-stage predictors, that is, they assume a constant control input during the entire prediction interval. Using multi-stage predictors, as in the standard MPC formulation in Section D.3.1, is likely to improve the control of systems with oscillatory dynamics. However, the number of optimization variables is multiplied by the number of stages in the predictor.

The controller is based on a system model, including the load dynamics. Whereas good models (and their parameters) are readily available for the generators and network components the load models are generally unknown. The aggregate load model employed here has been verified in several field tests and parameters for a wide range of operating conditions have been determined (Karls-son and Hill, 1994, Xu and Mansour, 1994, le Dous, 1999). These studies have found seasonal as well as daily variations in the parameter values. Therefore, the load parameters should ideally be estimated on-line. A method for on-line estimation of load parameters has been described in Balanathan et al. (1998b) but has yet to be tried out in practice. In the absence of reliable load parameter values obtained from on-line estimation, a conservative choice of parameters based on off-line field tests may be used.

D.7 Conclusions

The paper has demonstrated the application of model predictive control to emergency voltage control. The controller optimally coordinates capacitor switching, tap changer operation, and load shedding in different geographic locations, ensuring minimum usage of emergency controls such as load shedding. A search method is employed to minimize a cost function based on predictions of the system's future behaviour. Predictors of various accuracy and computational complexity are shown to be accurate enough for the emergency control problem.

D.8 Acknowledgements

The authors gratefully acknowledge the financial support from Sydkraft AB, Sweden, and the travel grant received from the Royal Swedish Academy of Engineering Sciences (IVA) through the Hans Werthén Foundation.

D.9 Appendix: Controller Tuning

This section outlines the considerations taken when selecting the penalty weight matrices in (D.9) for the example system. The procedure can easily be adapted to larger, more realistic systems.

The matrix $\mathbf{Q} = \text{diag}([q_1 \dots q_n])$ is chosen as the identity matrix of size n , where n is the number of controlled outputs. The control weight matrix is similarly defined as $\mathbf{R} = \text{diag}([r_1 \dots r_m])$, where m is the number of control inputs. Since \mathbf{Q} has been chosen arbitrarily, we have to select \mathbf{R} properly. The main idea is to select \mathbf{R} such that the cost of refraining from using a control (reflected in \mathbf{Q}) will equal the cost for performing a control change (reflected in \mathbf{R}). Thus, we compare the square of the output deviations and the square of the control changes.

Assume that one capacitor bank step (0.15 p.u.) may be switched if it reduces voltage deviations by 0.05 p.u., i.e.,

$$r_{\text{capacitor}} = \frac{0.05^2}{0.15^2} = \frac{1}{9} \quad (\text{D.19})$$

Similarly, one tap changer step (0.02 p.u.) may be switched to reduce voltage

deviations by 0.02 p.u.

$$r_{tap} = \frac{0.02^2}{0.02^2} = 1 \quad (D.20)$$

The weighting for load shedding should be tuned so that it is not scheduled in normal operation (without constraint violation). With voltage constraints at 0.9 p.u., $1-0.9=0.1$ p.u. is the maximum tolerable voltage deviation, i.e., the maximum penalty that can arise from output deviations is

$$n * 0.1^2 \quad (D.21)$$

where n is the number of controlled nodes. Since the minimum load shedding step is 0.05 p.u., choose

$$q_{shed} * 0.05^2 \gg n * 0.1^2 \quad (D.22)$$

In the example, the voltages at buses 5 and 6 are controlled, i.e., $n = 2 \Rightarrow q_{shed} \gg 8$, i.e., choose $q_{shed} = 100$.

The penalty for constraint violation $P_{constraint}$ should be large enough to ensure that the full range of all controls may be used to remove the violation. The penalty for violation should also increase with the magnitude of the violation, i.e., a violation of 0.02 p.u. should be penalized harder than one of 0.01 p.u. The cost of using the full control range is

$$(2 * 0.15^2 * 100 + 2 * 0.4^2 * 1 + 4 * 0.3^2 * 1/9) = 4.86 \quad (D.23)$$

Thus, the penalty can be chosen as

$$P_c(t, u^+, x^*) = 10 \left(1 + \sum_{k \in \mathcal{C}} (y_k - y_{c,k})^2 \right) \quad (D.24)$$

where $y_{c,k}$ is the limit dictated by the constraint imposed on output k , and \mathcal{C} the subset of outputs that violate a constraint. A singularity induced bifurcation is a more serious indicator of proximity to collapse than a constraint violation, and should therefore be assigned a larger penalty. Furthermore the penalty for collapse should be larger for bifurcations that appear closer to the present time than those further in the future. Since we can safely assume that the sum expression in (D.24) is less than 9, the penalty can be selected as

$$P_{SIB}(t, u^+, x^*) = 100 - \frac{(t_{SIB} - t^*)}{t_p} \quad (D.25)$$

for a singularity-induced bifurcation predicted at time t_{SIB} . The penalty term in (D.9) is then defined as

$$P(t, u^+, x^*) = P_{SIB}(u^+, x^*) + P_c(u^+, x^*) \quad (D.26)$$

| symbol | control | initial value | lower limit | upper limit | control step |
|-----------|---------|---------------|-------------|-------------|--------------|
| B_3 | cap. 3 | 0.00 | 0.00 | 0.30 | 0.15 |
| B_4 | cap. 4 | 0.00 | 0.00 | 0.30 | 0.15 |
| B_5 | cap. 5 | 0.00 | 0.00 | 0.30 | 0.15 |
| B_6 | cap. 6 | 0.00 | 0.00 | 0.30 | 0.15 |
| k_{t35} | tap 3-5 | 1.04 | 0.80 | 1.20 | 0.02 |
| k_{t46} | tap 4-6 | 1.06 | 0.80 | 1.20 | 0.02 |
| k_{l5} | load 5 | 1 | 0.85 | 1 | 0.05 |
| k_{l6} | load 6 | 1 | 0.85 | 1 | 0.05 |

Table D.5: Control variables (All data given in p.u.)

| Load | Generator (at bus 2) |
|--|--|
| $P_{05} = P_{06} = 0.6$ p.u. | $V_r = 1.05$ p.u. |
| $Q_{05} = Q_{06} = 0.3$ p.u. | $P_m = 0.3$ p.u. |
| $T_{p5} = T_{p6} = 60$ s | $H = 3.54$ MVA/MWs, $D = 0.0$ p.u. |
| $T_{q6} = T_{q6} = 60$ s | $r_a = 0.00327$ p.u. |
| $\alpha_{s5} = \alpha_{s6} = 0$ | $x_d = 1.76$ p.u., $x_q = 1.58$ p.u., |
| $\alpha_{t5} = \alpha_{t6} = 2$ | $x'_d = 0.42$ p.u., $x'_q = 0.30$ p.u. |
| $\beta_{s5} = \beta_{s6} = 0$ | $x''_d = 0.10$ p.u., $x''_q = 0.20$ p.u. |
| $\beta_{t5} = \beta_{t6} = 2$ | $T'_{d0} = 6.66$ s, $T'_{q0} = 0.44$ s |
| Network | $T''_{d0} = 0.02$ s, $T''_{q0} = 0.03$ s |
| $n_{max} = 1.2$ p.u. | Exciter & AVR (at bus 2) |
| $n_{min} = 0.8$ p.u. | $T_{exc} = 2.5$ s |
| $X_t = 0.1$ p.u. | $K_{avr} = 100$ |
| $T_t = 30$ s | $E_{fmax} = 3.5$ p.u. |
| $X = \begin{cases} 0.2, & time < 15 \text{ s} \\ 1.0, & time > 15 \text{ s} \end{cases}$ | $E_{fmin} = -3.5$ p.u. |
| $V_1 = 1.05 \angle 0$ p.u. | |

Table D.6: Network, Generator & Load Parameters

Addendum to Paper D

Mats Larsson

Abstract: *Much attention has been given to the design of so-called voltage instability indicators, whose purpose is to quantify the risk of voltage instability at a specific operating point. The proposals of the critical eigenvalue (Gao et al., 1992) or minimum singular value (Löf et al., 1992) of the static Jacobian matrix have been quite influential. These approaches are both based on a static system model. A straightforward way to extend this research to dynamic system models including the effect of load dynamics is to instead consider the eigenvalues of the dynamic Jacobian matrix. Emergency control methods based on this stability measure has been presented in Van Cutsem (1995), Makarov et al. (1998), Larsson (1999). However the investigation in this addendum, which has been adapted from Larsson (1999), finds some shortcomings that make the critical eigenvalue unsuitable for use as a stability measure in the tree search controller.*

Choice of Cost function

The approach taken here is based on modal analysis, and the idea is to move the rightmost eigenvalue as far as possible into the left half-plane. This corresponds to making the least stable (or most unstable) mode as stable as possible in a small disturbance sense. The cost function is chosen as

$$J(x^*, u) = \max(\text{real}(\text{eig}(\mathbf{A}))) \quad (\text{D.27})$$

where \mathbf{A} , as defined by (D.14) is the dynamic Jacobian matrix taken at (x^*, u) , thus a new linearization and eigenvalue computation is required for each evaluation of the cost function. When hard limits are activated, for example due

to tap limits or deadbands, a dynamic state and its corresponding eigenvalue is removed from the model. Note that this is a structural change in the model that introduces a discontinuity in the stability measure (D.27). Also note that the operating point where the linearization is taken is not always stationary. Both effects have a significant impact on the final result as will be demonstrated in the next section.

Simulation Results

The system in Figure D.1 is again studied, but the tap changers are now controlled by inverse-time relays according to the *DBODE* model in Paper C, and the emergency controls considered here are load shedding, capacitor switching and tap locking. Relevant parameter values can be found in Larsson (1999).

The same disturbance as applied in Section D.5 is studied. Figure D.7 shows the system response with the emergency controller using (D.27) as a cost function and the capacitors at buses 3 and 4 disabled. At 30 s, the controller begins by stepping up the capacitor controls at buses 5 and 6 and locks one of the tap changers. At time 60 s, the voltages have decayed further and the load shedding controls are enabled. The decision taken by the tree search controller is to step the capacitor at bus 5 up, the one at bus 6 down (!) and to shed 0.10 p.u. of load at bus 6. After the capacitor at bus 6 has been stepped down, the voltages of buses 5 and 6 decays rapidly and collapse follows shortly.

The surprising decision to step down the capacitor control at bus 6 can be explained as follows: The effect of a capacitor is twofold in the sense that it both increases the voltage at the bus where it is connected and at the same time decreases the stiffness of the system. Freely interpreted, the first effect moves the eigenvalues towards the left (more stable) and the second effect moves the eigenvalues towards the right (less stable) in the complex plane. The decision to switch out the capacitor is possibly due to that the second effect influences the dominant eigenvalue more than the first effect. As seen in the figure, the emergency controller fails to stabilize the system, which is rather surprising since the objective function aims to maximize small-disturbance stability. Another interesting observation is that the positive change in the dominant eigenvalue due the load dynamics seems to be larger, or at least on par with, the negative change achieved through the controls.

Figure D.7 shows the response using the predictive cost function ESP as described in Section D.3.3. In this simulation, the voltages are stabilized using

the capacitors at buses 5 and 6 and 0.10 p.u. load shedding at bus 6. The main work in stabilizing the voltages are made by the controls applied at 30 s and 60 s. During this time, the critical eigenvalue is made unstable. Thus, the critical eigenvalue does not appear to be a useful indicator in this case. In addition, the discontinuities introduced when the voltages enter the tap changer deadbands at about 320 s give rise to a large change in the critical eigenvalue—in fact it is on par with the change introduced by the line outage. Such discontinuities also make the critical eigenvalues less useful as the basis of computation of emergency control actions.

Conclusions

The critical eigenvalue of the dynamic Jacobian matrix is not a good stability indicator for the studied system and disturbance applied for the following reasons:

- The critical eigenvalue is calculated based on a linearization of the system at the current operating point. If there are unsettled dynamics, the operating point moves even if no change in control is made. The accuracy of the linearized model and consequently the quality of the stability measure provided by the critical eigenvalue decrease as the system trajectories move away from the linearization point.
- The change in the critical eigenvalue due to the load dynamics is on par with the change that can be achieved by applying controls.
- The discontinuities in the critical eigenvalue.

Note that the conclusions in this paper only apply to the use of the eigenvalues of the *dynamic* Jacobian matrix. Some similar conclusions on the usage of the minimum eigenvalue and singular value of the *static* Jacobian matrix have previously been presented by Cañizares et al. (1996). Also note that the results presented here do not invalidate the use of the critical eigenvalue in the general case. The discontinuities in the eigenvalue trajectories could possibly be avoided if the tap changer model is modified, for example by neglecting the tap changer deadband and limits. If the system is relinearized more often, the effect of unsettled dynamics at the linearization point is reduced. The purpose of this addendum is to illustrate these drawbacks and therefore a tap representation including the deadband and limits has been used.

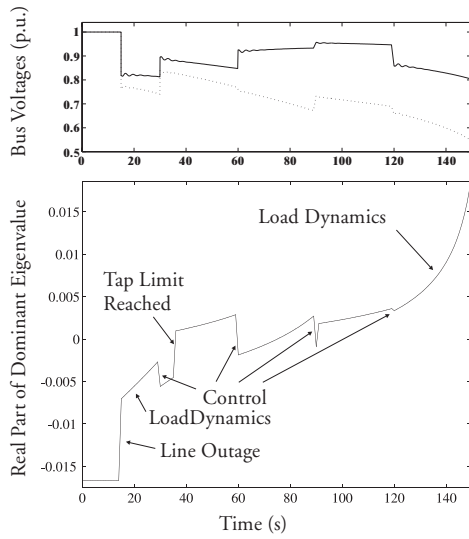


Figure D.7: Emergency control using dominant eigenvalue stability measure.

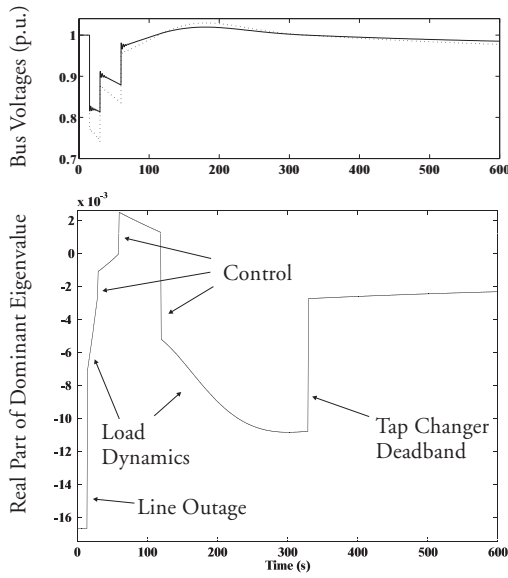


Figure D.8: Emergency control using model predictive stability measure (ESP). The comments in the figures refer to the mechanisms that affect the dominant eigenvalue trajectory.

Paper E

Coordinated System Protection Scheme against Voltage Collapse using Heuristic Search and Predictive Control

Mats Larsson Daniel Karlsson

submitted to *IEEE Transactions on Power Systems*

Abstract: *A coordinated system protection scheme (SPS) against voltage collapse based on model predictive control and tree search is presented. It optimally coordinates dissimilar and discrete controls such as generator, tap changer and load shedding controls in presence of soft and hard constraints on controls as well as voltages and currents in the network. The response with the coordinated SPS is compared to an SPS based on local measurements using simulation of the Nordic 32 test system. In terms of the amount of load shedding required to restore voltage stability, the simulations indicate that load shedding based on local criteria is near optimal in the system studied. However, when also generator controls are considered as emergency controls, the coordinated scheme reduces the amount of required load shedding by 35% compared to the local scheme.*

E.1 Introduction

Voltage instability mitigation has been discussed for some time now, and some protection systems against voltage collapse are installed and in operation (CI-GRE, 1998 2000). Most of these systems use rather simple criteria, such as low voltage, and quite rough actions, such as load shedding. Regarding the

rapidly growing capability in computer and communication technology, time has now come to introduce more smooth "emergency control systems", where system-wide voltage levels, reactive power flows, etc., are used in a wide-area emergency control system. Such a system, to be activated when the power system is in transition towards instability, must include different voltage levels and act on transformer tap changers, AVRs on generators as well as reactive power compensation devices available. To save a power system exposed to a disturbance, where the system survived the initial disturbance, but the system dynamics have been triggered and a transition towards instability has started, powerful and synchronized actions are required as the harm to the customers has to be minimized. In such a situation, i.e., a system exposed to a long-term voltage instability, there is some time, tens of seconds to some minutes, available to counteract the transition. Basic rules are to lower the voltage on the load level as much as possible to achieve a temporary load relief. The transmission, sub-transmission and distribution system voltages should, however, be kept as high as possible to reduce the losses and maximize the line and cable reactive power generation. Furthermore, most control variables have an inherently discrete nature; for example, capacitor banks and tap changers must be switched in fixed steps and while most utilities lack direct load control schemes, load shedding must still be carried out by disconnecting whole feeders.

The scheme presented uses a network model and wide-area measurements to account for the current power flow in the system, load models to account for load recovery dynamics and constraints are imposed to ensure that voltage and generator current limits are not violated.

E.2 Coordinated System Protection Scheme

The coordinated system protection scheme (CSPS) is based on the model predictive method described in Larsson et al. (2000). The principle is illustrated in Figure E.1. A system model, including the load dynamics, is used to predict the output trajectories (dotted lines) based on the current state and for several different candidate input sequences. A cost function is defined based on the deviation of each predicted trajectory from a desired trajectory (dashed line). The optimal control, in the sense that it minimizes the defined cost function, is then obtained by solving an optimization problem on-line, and applied to the system. The interval between the current time t^* and the prediction horizon $t^* + t_p$ is referred to as the prediction interval, and is chosen based on the set-

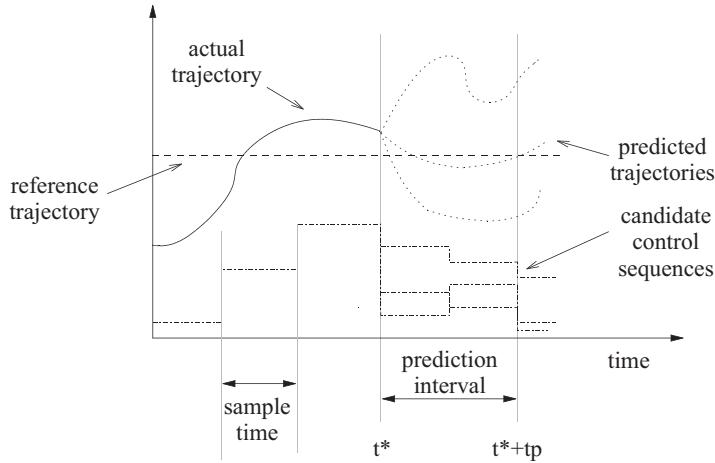


Figure E.1: Principle of Model Predictive Control.

ting time of the slowest dynamics. Usually, the prediction interval is chosen as a multiple of the sample time.

The problem of selecting controls at the instant t^* and operating point (x^*, u^-) is formulated as the combinatorial optimization problem

$$\begin{aligned} \min \quad & J(x^*, u^+) \\ \text{subject to} \quad & u^+ \in \mathcal{S}(u^-) \end{aligned} \quad (\text{E.1})$$

where u^+ is the optimization variable corresponding to the new control state to be determined whereas u^- denotes the control state presently in use, in other words before the optimization starts at time t^* . $\mathcal{S}(u^-)$ is the set of available control states. The scalar function $J(x^*, u^+)$ is referred to as a cost function and should evaluate the benefit of using the new control state u^+ such that a smaller result indicates a more desirable state. The cost function is defined as

$$J(u^+, x^*) = \int_{t^*}^{t^*+t_p} \tilde{y}^T \mathbf{Q} \tilde{y} + \tilde{u}^T \mathbf{R} \tilde{u} + P \, dt \quad (\text{E.2})$$

where $\tilde{y} = (\hat{y}(t, x^*, u^+) - y_r)$ is a prediction of the outputs deviations from their desired trajectories, provided the new control u^+ is applied during the prediction interval. The control state presently in use is denoted u^- , and thus

$\tilde{u} = (u^+ - u^-)$ is the applied change of controls. The reference trajectory is denoted y_r and the weighting matrices for output errors and control variations \mathbf{Q} and \mathbf{R} , respectively. The scalar penalty term $P = P(u^+, x^*)$ is introduced whenever a constraint violation or a singularity-induced bifurcation is predicted to occur during the prediction interval.

The power system network model is expressed as a set of linearized ordinary differential equations

$$\Delta \dot{x}(t) = \mathbf{A} \Delta x(t) + \mathbf{B} \Delta u \quad (\text{E.3})$$

$$\Delta y(t) = \mathbf{C} \Delta x(t) + \mathbf{D} \Delta u \quad (\text{E.4})$$

The linearized system representation is recomputed prior to each control signal computation, and is used to predict the output trajectories for different control states using the method described as Linearized Model Predictive Control (LMPC) in Larsson et al. (2000). Generators and their associated control systems are modelled using their quasi-steady state representation as given in Van Cutsem and Vournas (1998), i.e, the short-term dynamics are neglected in the linearized model used for control signal computation. However, these dynamics are retained in the simulations.

E.3 Heuristic Tree Search

When solving the combinatorial optimization problem (E.1) by tree search, the possible control states are organized in a tree structure. Using terminology from the literature on search, each control state is represented by a *node* or *position* in the tree and the transition from one node to another node is called a *move*. A move in this case corresponds to the switching of a single control. The maximum number of levels in the tree is called the *depth* of a search and corresponds to the number of controls that may be switched in a single search. The *width* of the search is the number of successors that are expanded in each node, that is, the number of moves that are explored in any intermediate position. Furthermore, the *Search space* of the optimization problem contains all unique control states reachable from the current state. However, in most practical cases it is not computationally feasible to explore all of the search space. The *Search tree* is the part of the search space actually explored by a search algorithm.

In Larsson et al. (2000), the combinatorial optimization problem (E.1) is solved using tree search using a standard *depth-first* search method as described

by Russell and Norvig (1995), which is an example of a so-called *uninformed* search method that explores all of the search-space. An *informed* search method makes use of search enhancements in order to reduce the size of the search tree and consequently the computational complexity. A survey of such enhancements are given, e.g., in Junghanns (1999). A short description of the enhancements used in this application are given in the following sections.

E.3.1 Transposition Table

It can be observed that some nodes are visited more than once during a search. For example, if there are two on-off controls and the initial state is *off-off* there are two ways of reaching the state *on-on*, by switching either one of the two controls first. By storing previously evaluated states in a table along with some additional information about the status of the search, a transposition table may reduce the search tree considerably without sacrificing completeness of the search. A detailed study of transposition tables and their effect on search complexity can be found in Breuker (1998).

E.3.2 Lower Bound

The cost function (E.2) can be decomposed in three components

$$f = f_y + f_u + f_P \quad (\text{E.5})$$

related to the output deviation, control and constraint violation costs respectively. All three components are implicitly determined by the control state in use. It is observed that the control cost cannot decrease as progress is made deeper into the search tree, that is, the control cost can be used as a *lower bound* on the cost function. Without sacrificing completeness of the search, the expansion of nodes can be stopped in every node where the control cost alone is greater than the total cost in any node encountered so far. However, lower bound cutoffs cannot be expected to reduce the search tree significantly when there are constraint violations, since the constraint violation term is designed to dominate the cost function when such violations are present.

E.3.3 Move Ordering

The purpose of move ordering is to make sure that the search space is explored in a good order, meaning an order where the number of lower bound cutoffs

is maximized. The following two measures have been used to order the moves: Firstly, the value of the cost function after the move and secondly, the change in the cost function divided by the cost of move. Thus, the first move considered in each node is the one with the best evaluation according to the first criteria, the second is the best one according to second criteria and the third is the second best according to the first criteria and so on.

E.3.4 Iterative Broadening

In an iterative broadening search (Ginsberg and Harvey, 1992), a number of successive searches are made. Ranked according to the move ordering criteria, only the best move in each intermediate node is considered in the first iteration. In the second iteration also the second best move is considered and so on. The basic idea is to quickly find one reasonably good solution by venturing deep into the tree and then use remaining time available to improve this solution. Since the size of the search tree depends exponentially on the breadth, the effort spent on the search is dominated by the last iteration. In fact, the information collected in these intermediate searches can often enable additional lower bound cutoffs, and an iterative broadening search to a certain depth and width may therefore be computationally cheaper than a single search.

Note, however, that the iterative broadening search sacrifices completeness of the search. Because in most cases only a fraction of the game tree search space is explored, the search is likely to miss the optimal solution unless good move ordering criteria are used. There is a potential risk that the iterative broadening search finds a local minimum or a plateau of the cost function (Russell and Norvig, 1995). No such behaviour has been detected in the work on this application, but can in such cases be circumvented by repeating the search using different initial control vectors.

E.4 SPS based on Local Measurements

The simulations have also been carried out with a rule-based SPS using only local voltage measurements. Load shedding is carried out using the scheme described in Vu et al. (1995) using an assumed "lowest normal voltage" of 1 p.u., i.e., 5 % of the bus load is shed at 0.9 p.u. with 3.5 s time delay, another 5 % is shed at 0.92 p.u. with 3 s delay and yet another 5 % is shed at 0.92 p.u. with 8 s delay. The tap changers are controlled by constant-time relays corresponding to

model D1 in Sauer and Pai (1994) with a delay time $Td0$ of 40 s. Tap changers are blocked if the primary side voltage stays below 0.93 p.u for 10 s or more. All loads and tap changers are equipped with these undervoltage and tap locking relays in the schemes LPSP1 and LSPS2.

E.5 The Nordic Test System

The model predictive method will be demonstrated using the Nordic 32 test system originally described in CIGRE (1995b), except for that generators connected to the same bus and parallel branches have been aggregated and generator saturation is neglected. Furthermore, the generator at bus N4011 is modelled as an infinite bus. The loads are modelled using the aggregate exponential recovery model (Karlsson and Hill, 1994)

$$T_p \dot{x}_p + x_p = P_s(V) - P_t(V) \quad (\text{E.6})$$

$$P_d = k_l(x_p + P_t(V)) \quad (\text{E.7})$$

where x_p is a continuous dynamic state that can be interpreted as a measure of the energy deficit in the load and $P_s(V) = P_0 V^{\alpha_s}$ and $P_t(V) = P_0 V^{\alpha_t}$ are the steady-state and transient voltage dependencies respectively. P_d is the actual active load power and T_p is the active power recovery time constant. A similar model is used for the reactive power load with corresponding characteristics $Q_d, x_q, Q_s(V) = Q_0 V^{\beta_s}, Q_t(V) = Q_0 V^{\beta_t}$ and time constant T_q . The scale factor k_l models load shedding and is applied to the reactive as well as to the active power load model. The parameter values $\alpha_s = \beta_s = 0.5, \alpha_t = \beta_t = 2, T_p = T_q = 60$ s have been used for all loads.

All generators are equipped with field current limiters, and the thermal power generators¹ also have armature current limiters. Both types of limiters are of integral-type and allow temporary overcurrents for the first 20 s. A detailed description of the limiters can be found in CIGRE (1995b). The armature current constraints are set at 1.05 p.u., whereas the field current constraints are set 15 % lower than in the report in order to compensate for neglecting saturation. The initial state is given by the load flow case called *lf28* in the CIGRE report. The following components are considered as controls:

- 11 Transformers with on-load tap changers (16 steps of 1.67 %)

¹at buses N1042, N1043, N4042, N4047, N4051, N4062, N4063

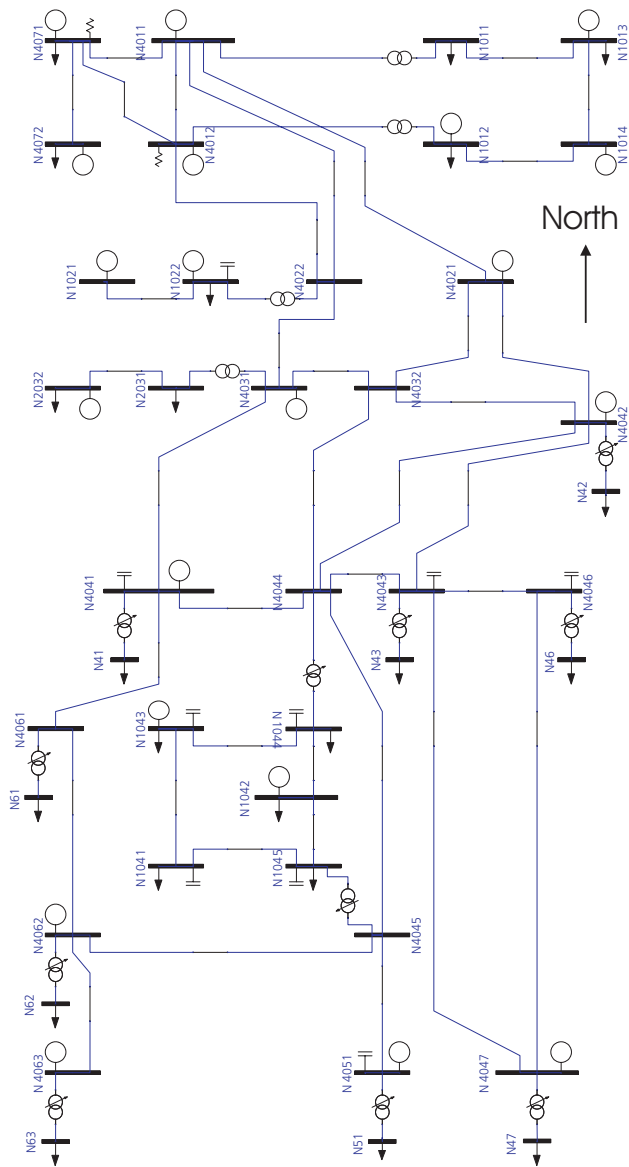


Figure E.2: The Nordic test system from CIGRE (1995b).

- 22 Load shedding points (3 steps of 5 % of nominal load)
- 19 Generator voltage setpoints (8 steps of 2 %)

Constraints are imposed on:

- Field currents of all generators, set to the same value as the internal generator field current limiter.
- Armature current of the thermal power generators, set to the same value as the internal generator field current limiter.
- All bus voltages should be kept above 0.92 p.u.

Voltages below tap changing transformers are considered controlled, and should be kept close to 1 p.u. unless transmission voltage constraints are violated. In cases where not all constraints can be satisfied, armature and field current constraints has priority over voltage constraints.

E.6 Scenarios and Simulation Results

The pre-disturbance state *lf28* has a higher load than would be allowed by normal reliability criteria. In fact, many single contingencies will lead to voltage collapse. Simulation of the scenarios listed in Table E.1 is used to evaluate the different schemes. The table also shows the system response without an SPS. In most cases, voltage collapse occurs unless emergency controls are initiated.

The simulations have been carried out with the local scheme in two versions; firstly, the LSPS1 where the generators control their respective terminal voltage and the LSPS2 where they use full line-drop compensation as described in Taylor (2000a), in order to make better use of their reactive capability. The coordinated scheme is used in two versions, the CSPS1 in which the generator controls have been disabled and the CSPS2 which has access to all controls. Thus, the results with CSPS1 should be compared to those with LSPS1, and the results with CSPS2 to those with LSPS2.

E.6.1 Case 1 - Tripping of Generator at Bus N4062

In the pre-contingency situation, the generator at bus N4062 supplies 530 MW active power and absorbs 8 Mvar reactive power. The tripping of the unit causes

| Case # | Tripped Component(s) | Without SPS |
|--------|--------------------------------|----------------------|
| 1 | Generator 4062 | Collapse at 150 s |
| 2 | Line 4045-4062 | Stable, no violation |
| 3 | Line 4032-4044 | Collapse at 340 s |
| 4 | Line 4031-4041 | Collapse at 45 s |
| 5 | Line 4011-4021, Generator 1012 | Collapse at 175 s |
| 6 | Line 1043-1044 | Collapse at 201 s |
| 7 | Generator 4041 | Stable, no violation |
| 8 | Line 4042-4044 | Collapse at 64 s |

Table E.1: Overview of the scenarios.

an active power deficiency in the south which is compensated mainly by the hydro generators in the north and consequently increases transfer through the central region. This leads to increased losses and low voltages in the south and central regions. In response, the remaining generators in the south almost instantaneously increase their reactive power output until after 20 s, the armature current limiters of generators 1043 and 4042 are activated. Voltage support is then lost in the areas close to these buses. Load recovery and tap changer dynamics will then further depress voltages in the south until system collapse occurs, unless emergency actions are taken. Tables E.4–E.5 list the emergency switching sequence ordered by the four schemes and Figure E.3 show the terminal voltage and armature current of the generator at bus N4042.

With both local schemes, the tap changing transformers in the southern region start acting to restore their controlled voltages after about 50 seconds. This depresses transmission voltages further and some tap changers are eventually blocked. Voltage decline then continues due to load dynamics and the first load shedding is ordered at about 100 s with the LSPS1. Once enough undervoltage relays have been activated, the voltage instability phase ceases and voltages slowly recover close to their pre-disturbance values. Since the terminal voltages of generators with reactive capability to spare are kept higher with the LSPS2, reactive capability is better utilized, and therefore load shedding action is initiated. Also, less load shedding is required before the voltages become stable.

While the voltage trajectories of the CSPS1 and CSPS2 look similar, the two schemes use different means of reaching a stable state. With the CSPS1, load shedding at buses N43 and N1044 combined with backstepping of transformer N4043 (which provides a temporary load relief at bus N43) relax the

| Case # | LSPS1 | LSPS2 |
|--------|--------------------------------------|--|
| 1 | Stable, 200+j69 MVA shed | Stable, 120+j36 MVA shed |
| 2 | Stable, no load shed | Stable, no load shed |
| 3 | Stable, 100+j33 MVA shed | Stable, no load shed |
| 4 | Collapse at 144 s, 590+j190 MVA shed | Collapse at 220 s, 533.0+j168.7 MVA shed |
| 5 | Stable, 224+j68 MVA shed | Stable, 208+j63 MVA shed |
| 6 | Stable, 60+j20 MVA shed | Stable, 60+j20 MVA shed |
| 7 | Stable, no load shed | Stable, no load shed |
| 8 | Stable, 424+j139 MVA shed | Stable, 377+j122 MVA shed |

Table E.2: Simulation Results with the Local SPS.

| Case # | CSPS1 | CSPS2 |
|--------|---------------------------|---------------------------|
| 1 | Stable, 160+j49 MVA shed | Stable, no load shed |
| 2 | Stable, no load shed | Stable, no load shed |
| 3 | Stable, 115+j37 MVA shed | Stable, no load shed |
| 4 | Stable, 570+j185 MVA shed | Stable, 500+j161 MVA shed |
| 5 | Stable, 160+j46 MVA shed | Stable, 75+j22 MVA shed |
| 6 | Stable, no load shed | Stable, no load shed |
| 7 | Stable, no load shed | Stable, no load shed |
| 8 | Stable, 494+j155 MVA shed | Stable, 270+j75 MVA shed |

Table E.3: Simulation Results with the Coordinated SPS.

armature current constraints of the limited generators. The CSPS2 decreases the voltage setpoints of the generators at buses N1043 and N4042, taking these out of their armature current limits. Generators at N2032, N4021, N4041 and N4047 have reactive capability to spare and are used to support the weak central-south region from the outside. Subsequently, the tap changers are used to restore the controlled voltages at nodes where this can be done without violating transmission voltage constraints.

E.6.2 Summary of Simulation Results

Tables E.2–E.3 list the system responses with the two versions of the local and coordinated SPS respectively. The local schemes stabilize the system in all cases except case 4, in which the collapse is due to instability of the short-term dynamics, not modelled in the system model used by the coordinated schemes. Nevertheless, the coordinated schemes keep a more even voltage profile than the local schemes and thereby keep the system within the (short-term) stability region even though the short-term dynamics are not explicitly modelled in the system model used by these schemes. Surprisingly, in case 3 the LSPS1

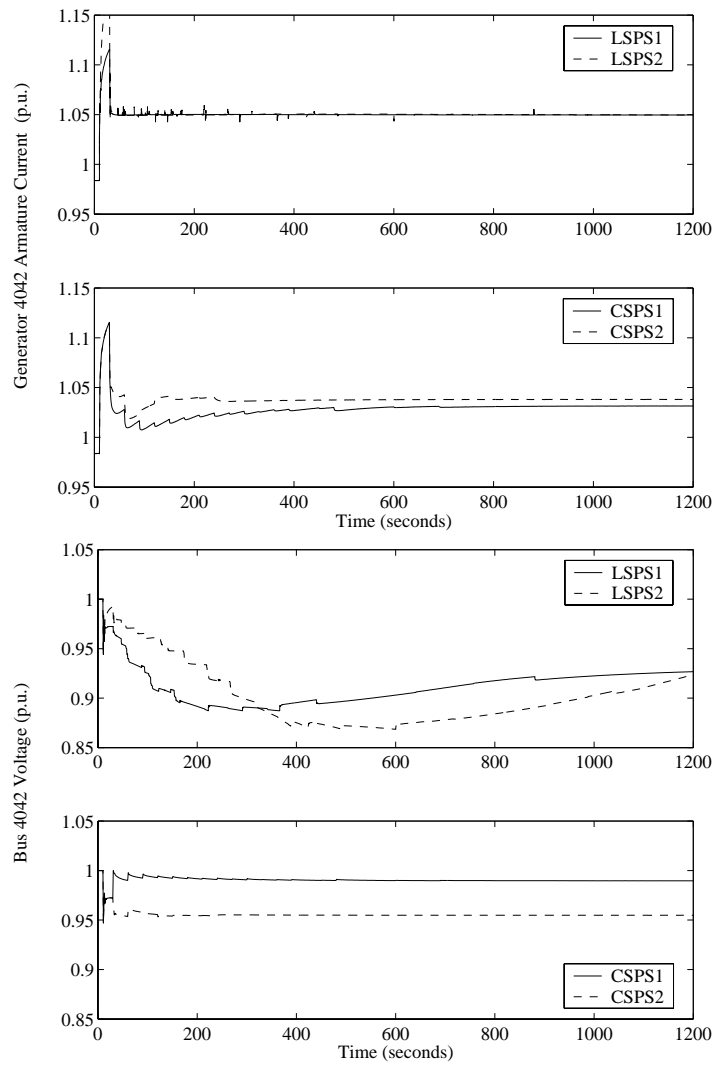


Figure E.3: Voltage at bus N4042 and armature current of generator 4042 following tripping of the generator at bus N4062 with the different protection schemes.

| CSPS1 | | | CSPS2 | | |
|----------|----------------|-----------|----------|---------------|----------|
| Time (s) | Control | | Time (s) | Control | |
| 30 | tap T4044-1044 | +1 step | 30 | tap T4041-41 | +1 step |
| 30 | tap T4043-43 | -6 steps | 30 | tap T4042-42 | +1 step |
| 30 | tap T4051-51 | -2 steps | 30 | tap T4061-61 | +1 step |
| 30 | load 1044 | shed 5 % | 30 | tap T4062-62 | +1 step |
| 30 | load 43 | shed 15 % | 30 | Gen 1043 s.p. | -3 steps |
| 60 | tap T4043-43 | +1 step | 30 | Gen 2032 s.p. | +1 step |
| 60 | tap T4046-46 | -1 step | 30 | Gen 4021 s.p. | +1 step |
| 60 | tap T4051-51 | -2 steps | 30 | Gen 4041 s.p. | +1 step |
| 60 | tap T4063-63 | -1 step | 30 | Gen 4042 s.p. | -2 steps |
| 90 | tap T4046-46 | -1 step | 30 | Gen 4047 s.p. | +2 steps |
| 120 | tap T4063-63 | -1 step | 60 | tap T4041-41 | +1 step |
| 150 | tap T4042-42 | -1 step | 60 | tap T4042-42 | +1 step |
| 180 | tap T4061-61 | -1 step | 60 | tap T4047-47 | -1 step |
| 210 | tap T4063-63 | -1 step | 60 | tap T4061-61 | +1 step |
| 240 | tap T4047-47 | -1 step | 60 | Gen 2032 s.p. | +1 step |
| 270 | tap T4062-62 | -1 step | 60 | Gen 4021 s.p. | +1 step |
| 300 | tap T4046-46 | -1 step | 60 | Gen 4041 s.p. | +1 step |
| 300 | tap T4063-63 | +1 step | 60 | Gen 4047 s.p. | +1 step |
| 330 | tap T4061-61 | +1 step | 90 | Gen 4021 s.p. | +1 step |
| 330 | tap T4063-63 | -1 step | 120 | Gen 4041 s.p. | +1 step |
| 360 | tap T4061-61 | -1 step | 150 | Gen 2032 s.p. | +1 step |
| 360 | tap T4062-62 | +1 step | 300 | tap T4047-47 | -1 step |
| 390 | tap T4062-62 | -1 step | 330 | tap T4046-46 | -1 step |
| 480 | tap T4041-41 | -1 step | | | |
| 480 | tap T4062-62 | +1 step | | | |
| 600 | tap T4062-62 | -1 step | | | |

Table E.4: Control response in case 1 - CSPS.

| LSPS1 | | | LSPS2 | | |
|----------|----------------|----------|----------|----------------|----------|
| Time (s) | Control | | Time (s) | Control | |
| 47 | tap T4044-1044 | +1 step | 47 | tap T4044-1044 | +1 step |
| 56 | tap T4041-41 | +1 step | 56 | tap T4041-41 | +1 step |
| 57 | tap T4061-61 | +1 step | 57 | tap T4061-61 | +1 step |
| 58 | tap T4045-1045 | +1 step | 80 | tap T4042-42 | +1 step |
| 58 | tap T4042-42 | +1 step | 80 | tap T4045-1045 | +1 step |
| 60 | tap T4043-43 | +1 step | 94 | tap T4044-1044 | +1 step |
| 60 | tap T4062-62 | +1 step | 126 | tap T4041-41 | +1 step |
| 62 | tap T4046-46 | +1 step | 126 | tap T4043-43 | +1 step |
| 88 | load 1041 | shed 5 % | 128 | tap T4042-42 | +1 step |
| 93 | tap T4047-47 | +1 step | 141 | tap T4044-1044 | +1 step |
| 94 | tap T4044-1044 | +1 step | 172 | tap T4061-61 | +1 step |
| 102 | tap T4041-41 | +1 step | 173 | tap T4062-62 | +1 step |
| 103 | tap T4061-61 | +1 step | 174 | tap T4046-46 | +1 step |
| 103 | tap T4041-41 | block | 174 | tap T4045-1045 | +1 step |
| 104 | tap T4044-1044 | block | 176 | tap T4042-42 | +1 step |
| 104 | tap T4042-42 | block | 219 | tap T4043-43 | +1 step |
| 104 | tap T4061-61 | block | 220 | tap T4041-41 | +1 step |
| 106 | tap T4045-1045 | +1 step | 220 | tap T4044-1044 | +1 step |
| 106 | tap T4043-43 | +1 step | 223 | tap T4042-42 | +1 step |
| 107 | tap T4062-62 | +1 step | 230 | tap T4042-42 | blocked |
| 110 | tap T4046-46 | +1 step | 230 | tap T4044-1044 | blocked |
| 116 | tap T4043-43 | block | 266 | tap T4061-61 | +1 step |
| 122 | load 1042 | shed 5 % | 267 | tap T4043-43 | +1 step |
| 147 | load 1042 | shed 5 % | 267 | tap T4045-1045 | +1 step |
| 153 | tap T4051-51 | +1 step | 268 | tap T4046-46 | +1 step |
| 154 | tap T4045-1045 | +1 step | 276 | tap T4041-41 | blocked |
| 157 | tap T4046-46 | +1 step | 277 | tap T4043-43 | blocked |
| 164 | tap T4046-46 | block | 281 | tap T4046-46 | blocked |
| 165 | load 1046 | shed 5 % | 282 | tap T4061-61 | blocked |
| 169 | tap T4047-47 | +1 step | 292 | tap T4047-47 | +1 step |
| 183 | tap T4045-1045 | block | 316 | tap T4045-1045 | +1 step |
| 215 | tap T4047-47 | +1 step | 338 | tap T4047-47 | +1 step |
| 223 | load 1044 | shed 5 % | 363 | tap T4062-62 | +1 step |
| 262 | tap T4047-47 | +1 step | 366 | tap T4045-1045 | blocked |
| 291 | load 1042 | shed 5 % | 384 | tap T4047-47 | +1 step |
| 341 | tap T4062-62 | +1 step | 387 | tap T4047-47 | blocked |
| 366 | load 1044 | shed 5 % | 388 | load 46 | shed 5 % |
| 392 | tap T4045-1045 | release | 424 | load 46 | +1 step |
| 440 | tap T4045-1045 | +1 step | 487 | load 1041 | shed 5 % |
| 450 | tap T4045-1045 | block | 600 | load 1042 | shed 5 % |
| 487 | tap T4045-1045 | release | 624 | tap T4047-47 | released |
| 641 | tap T4047-47 | -1 step | 670 | tap T4047-47 | +1 step |
| 664 | tap T4046-46 | release | 716 | tap T4047-47 | +1 step |
| 757 | tap T4047-47 | -1 step | 758 | tap T4045-1045 | released |
| 834 | tap T4043-43 | release | 906 | tap T4047-47 | -1 step |
| 881 | tap T4043-43 | +1 step | 988 | tap T4046-46 | released |
| 891 | tap T4043-43 | block | 988 | tap T4047-47 | -1 step |
| 920 | tap T4043-43 | release | 1035 | tap T4046-46 | +1 step |
| | | | 1074 | tap T4061-61 | released |
| | | | 1103 | tap T4047-47 | -1 step |
| | | | 1121 | tap T4043-43 | released |
| | | | 1168 | tap T4041-41 | released |
| | | | 1186 | tap T4047-47 | -1 step |

Table E.5: Control response in case 1 - LSPS.

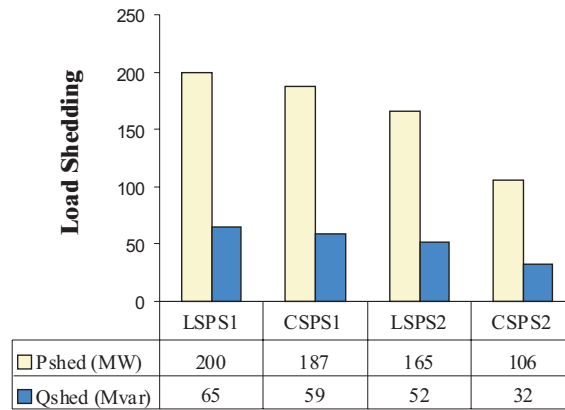


Figure E.4: Average load shedding over the eight scenarios. Nominal load is 10940 MW and 3358 Mvar.

sheds less load than the CSPS1. The voltage at bus N4042 is allowed to decrease below the voltage constraint of 0.92 p.u. with the local schemes since there is no undervoltage load shedding relay at this bus. On the other hand, the CSPS1 has the option of shedding load at neighbouring buses in order to avoid this violation. Therefore, the amount of load shedding can be higher with the coordinated scheme. Case 6 is another interesting case, which illustrates misoperation of the local schemes—both LSPS1 and LSPS2 sheds load. The simulation of the same scenario with CSPS1 and CSPS2 shows that load shedding is not necessary to avoid collapse.

Figure E.4 shows a comparison of the amount of load shedding executed by the different schemes. The amount of load shedding by the LSPS2 compared to the LSPS1 is about 17% lower, since the generator reactive capabilities are better utilized.

Although the simulation results are slightly biased towards the LSPS1 because of less stringent handling of voltage constraints than with the CSPS1, the benefits of coordinated control when only load shedding is allowed seems to be small. The reduction in the amount of load shedding required is only reduced by 6% with the CSPS1 compared to the LSPS1. This reduction can be ascribed to better control of the tap changers and is presumably not due to the coordination of load shedding in different geographical locations.

However, with the CSPS2, which has generator setpoint voltages included as control variables, remote generators can be used to support weak regions as an alternative to load shedding and the load shedding reduction is about 47 % compared to the LSPS1 and 35 % compared to the LSPS2. Also, because of better management of voltage constraints by both coordinated schemes, they are more likely to keep the trajectories of the system in a region where the short-term dynamics are stable.

E.7 Conclusions

A coordinated system protection scheme for voltage control in the emergency state, capable of coordinating dissimilar and discrete controls such as generator, tap changer and load shedding controls using heuristic tree search, has been presented. Eight scenarios, some of which leads to voltage collapse unless emergency control measures are taken, has been used to evaluate system protection schemes based on local as well centralized measurements. Simulation results indicate that load shedding based on local measurements is near optimal when load shedding is the only emergency control considered. Another conclusion is that the reactive capability of generators is somewhat better utilized when generators use line-drop compensation.

On the other hand, the results indicate that the protection scheme based on centralized measurements can use remote generators to support a weak region as an alternative to load shedding. The reduction in the amount of load shedding required is about 35 % compared to the best local strategy. Also, the centralized scheme maintains a more even voltage profile than the local schemes and may therefore avoid short-term voltage instability that occurs with the local scheme, even though the short-term dynamics are not explicitly modelled.

E.8 Acknowledgements

The authors gratefully acknowledge the contributions from Professor Gustaf Olsson of Lund University and Professor David J. Hill at Sydney University, and the financial support from Sydkraft AB, Sweden.

Appendix: Controller Tuning

The coordinated SPS has been tuned according to the tuning criteria in Larsson et al. (2000), aiming to ensure that load shedding is not used unless there will be a constraint violation or singularity-induced bifurcation during the prediction interval that cannot be relaxed by any of the other controls. Furthermore the tuning allows the full range of all control to be used in order to relax a constraint violation. The tuning procedure yields $\mathbf{Q} = \text{diag}([1 \dots 1])$ and $\mathbf{R} = \text{diag}([r_1 \dots r_m])$ with its elements given by $r_i=1$ for tap changer and voltage setpoint controls and $r_i = 1000$ for load shedding controls. All penalties are calculated in p.u. and control penalties are scaled by the squared step size of the control, i.e., the penalty for a 4 p.u. load is $(4 * 0.05)^2$. The penalties for constraint violations and singularity-induced bifurcations in the penalty term P is 1000 and 10000, respectively.

Using a Matlab implementation on a 350 MHz Pentium II processor, the search is successively broadened allowing 60 s computation time in each control determination. The aim of this paper is to show the applicability of the method, not a practical implementation. The Matlab code is somewhat inefficient, especially the transposition table and iterative broadening implementations, and execution on a faster processor or C-coding of the search method will surely improve performance by at least a factor 2. The sample time has therefore been chosen to 30 s. The prediction time is 120 s and the maximum search depth is 15.

Paper F

ObjectStab—A Modelica Library for Power System Stability Studies

Mats Larsson

Modelica 2000, Modelica Workshop
Lund, Sweden

Abstract: *Traditionally, the simulation of transient and voltage stability in power systems has been constrained to domain-specific tools such as Simpow, PSS/E, ETMSP and Eurostag. While being efficient and thereby able to simulate large systems, their component models are often encapsulated and difficult or impossible to examine and modify. Also, these simulators often require substantial training and are therefore unsuitable for normal classroom use. For academic and educational use, it is more important that the component modelling is transparent and flexible, and that users can quickly get started with their simulations. This paper describes a freely available power system library called **ObjectStab** intended for voltage and transient stability analysis and simulation written in Modelica, a general-purpose object-oriented modelling language. All component models are transparent and can easily be modified or extended. Power system topology and parameter data are entered in one-line diagram form using a graphical editor. The component library has been validated using comparative simulations with Eurostag.*

F.1 Introduction

The simulation of power systems using special-purpose tools is now a well-established area and several commercial tools are available, e.g., Simpow, PSS/E and Eurostag. While most of these tools are computationally very efficient and reasonably user-friendly they have a closed architecture where it is very difficult or impossible to view or change most of the component models. Some tools, e.g., Eurostag, provide the possibility of modelling controllers such as governors and exciters using block diagram representation but this is often cumbersome. Moreover, these constructs do not enable the user to modify any of the generator or network models. The Power System Toolbox (Chow and Cheung, 1992) is a set of Matlab program files capable of dynamic simulation of power systems. Here the component models are accessible, but the modification of these requires a proper understanding of the interaction of the model files in this specific environment. Graphical editing of the models is not possible. Some of the above mentioned tools have the capability of exporting a linearized representation of the system for further analysis but the full nonlinear representation remains hidden to the user. Also, most of the industrial-grade tools require substantial training before they can be used productively.

Modelica (ModelicaDef, 1999, ModelicaTut, 1999) is an object-oriented general-purpose modelling language that is under development in an international effort to define a unified language for modelling of physical systems. Modelica supports object-oriented modelling using inheritance concepts taken from computer languages such as Simula and C++. It also supports acausal modelling, meaning that a model's terminals do not necessarily have to be assigned an input or output role. While object-oriented concepts enable proper structuring of models, the capability of acausal modelling makes it easy to model for example power lines that are very cumbersome to model using block-oriented languages such as Simulink.

Causality is generally not defined in electrical systems (Åström et al., 1998). For example, when modelling a resistor, it is not evident ahead of time, whether an equation of the type

$$u = R i \quad (\text{F.1})$$

will be needed, or one of the form:

$$i = \frac{u}{R} \quad (\text{F.2})$$

It depends on the environment in which the resistor is embedded. Consequently, the modelling tool should relax the causality constraint that has been imposed on the modelling equations in the past. Using causal modelling as in Simulink, that does not have the capability of relaxing such constraints, is illustrated in Hiyama et al. (1999) where a model for transient stability simulation is described. With this approach, the network has to be modelled using the traditional admittance matrix method and the power system topology cannot be visualized in the graphical editor.

In Modelica, models can be entered as ordinary or differential-algebraic equations, state graphs and block diagrams etc. Modelica also supports discrete-event constructs for hybrid modelling. Object-oriented modelling of power systems using general-purpose simulation languages has previously been described in Mattsson (1992), where a block library was developed using the modelling language Omola. However, the Omola project is now discontinued and the experiences from this have been brought into the Modelica project.

At the time of publication, the simulation tool Dymola (Elmqvist et al., 2000) was the only tool supporting the Modelica language although some other producers of general-purpose simulators have announced that future versions of their programs will support Modelica. There is already a number of Modelica libraries for various application domains such as; 3-dimensional multibody systems, rotational and translational mechanics, hydraulics, magnetics, thermodynamical systems and chemical processes.

This paper describes a component library written in Modelica for the simulation of transient and voltage stability in power systems. It is designed for use by undergraduate and graduate students in the teaching of power system dynamic stability and for rapid testing of research ideas. All component models are transparent and can easily be modified or extended. Emphasis has been given to keeping the component models transparent and simple. Power system topology and parameter data are entered in one-line diagram form using a graphical editor. Using the Dymola simulator, the full hybrid nonlinear or linearized equation system can be exported for use as a block in Simulink simulations and the full range of Matlab tools for visualization and control design can then be used. The component library has been validated using comparative simulations with Eurostag (Deuse and Stubbe, 1993).

F.2 The Component Library

The **ObjectStab** library presently contains the following component models:

- Generators with constant frequency and voltage as slack or PV nodes, or using 3rd or 6th order dq-models with detailed models of excitation and governor control systems, or as quasi-steady state equivalents according to Van Cutsem and Vournas (1998).
- Transmission lines in pi-link or series impedance representation.
- Reactive power compensation devices; shunt reactors, shunt capacitances and series capacitances.
- Fixed ratio transformers.
- On-load tap changing transformers (OLTC) modelled as detailed discrete models or using their corresponding continuous approximations according to Sauer and Pai (1994).
- Static and dynamic loads, including generic exponential recovery loads (Karlsson and Hill, 1994).
- Buses.
- Faulted lines and buses with fault impedance.

Standard assumptions for multi-machine power system stability simulations are made, i.e., generator stator and network time constants are neglected and voltages and currents are assumed to be sinusoidal and symmetrical. Except where other references are given, the components are modelled according to the guidelines given in Machowski et al. (1997). Furthermore each generator's set of equations is referred to an individual dq-frame and the stator equations are related to the system (common) reference frame through the so-called Kron's transformation (Machowski et al., 1997).

All models can be modified and extended through inheritance. New models or extensions of old ones can be entered as differential and algebraic equations, block diagrams or state graphs. Voltages and currents are described by their phasor representation:

$$\mathbf{I} = i_a + j i_b \quad (\text{F.3})$$

$$\mathbf{V} = 1 + v_a + j v_b \quad (\text{F.4})$$

Using this representation a connection point for power system components can be defined by the following Modelica connector definition

```
connector Pin
  Real va;
  Real vb;
  flow Real ia;
  flow Real ib;
end Pin;
```

By definition all `Pins` use a p.u. system based on the system reference of 100 MVA, although the generator models support parameter entry on their own individual base.

F.2.1 Modelling example: Impedance line model

The inheritance hierarchy for the impedance transmission line model is given below:

```
partial model TwoPin
  Pin T1;
  Pin T2;
end TwoPin;
```

The definition implies that a `TwoPin` is a model with two pins named `T1` and `T2` that will be used as external connectors for the line. The `Impedance` model is defined using the `TwoPin` as a base class and thereby inherit its attributes. Furthermore equations defining the real and imaginary voltage drop on the line have to be given:

```
model Impedance
  extends Base.TwoPin;
  parameter Base.Resistance R=0.0 "Resistance";
  parameter Base.Reactance X=0.1 "Reactance";
equation
  [T1.va-T2.va; T1.vb-T2.vb] = [R, -X;
                               X,  R]*[T1.ia; T1.ib];
  [T1.ia; T1.ib] + [T2.ia; T2.ib] = [0; 0];
end Impedance;
```

F.2.2 Modelling example: 3rd order Generator Model

The dynamic generator models inherit from the `OnePin` class and its declarations are split into three classes in order to simplify the implementation of

new generator models. The class DetGen defines the swing equation and the coordinate transformations as follows:

```

partial model Partial.DetGen
  extends Base.OnePin;
  parameter Base.Voltage V0=1;
  parameter Base.ActivePower Pg0=1;
  parameter Base.VoltageAngle theta0=0;
  parameter Boolean isSlack=true;
  parameter Base.ApparentPower Sbase=100;
  parameter Base.InertiaConstant H=6;
  parameter Base.DampingCoefficient D=0;
  Base.AngularVelocity w(start=1);
  Base.VoltageAngle delta;
  Base.MechanicalPower Pm;
  Base.VoltageAmplitude Efd;
  Base.Current id,iq;
  Base.Voltage vd,vq;
  Base.Current Iarm=sqrt(id^2 + iq^2);
  Base.ActivePower Pe;
equation
  // swing equations
  der(w) = 1/(2*H)*(Pm-Pe-D/Base.ws*(w-Base.wref));
  der(delta) = Base.ws*(w - Base.wref);
  // Kron's transformation
  -[T.ia; T.ib] = [-sin(delta), cos(delta);
                  cos(delta), sin(delta)]*[id; iq];
  // Load-flow initialization equation
  if initial() then
    if isSlack then
      1 + T.va = V0*cos(theta0);
      T.vb = V0*sin(theta0);
    else
      V = V0;
      Pg = Pg0;
    end if;
  else
    [1 + T.va; T.vb]=[-sin(delta), cos(delta);
                    cos(delta), sin(delta)]*[vd;vq];
  end if;
end DetGen;

```

During the initialization, which is equivalent to a load-flow calculation, generators are represented as either PV-nodes or Slack nodes (Machowski et al., 1997) depending on the attribute `isSlack`. It is declared as a partial class, i.e., a non-instantiable class, since it lacks equations for the stator and EMF equations that are dependent on the type of generator model used. For the 3rd order generator model with a single transient EMF in the q-axis the definition is as follows:

```
partial model ObjectStab.Generators.Partial.DetGen3
  extends DetGen;
  parameter Base.Resistance ra=0;
  parameter Base.Reactance xd=0.8948;
  parameter Base.Reactance xq=0.84;
  parameter Base.Reactance xdp=0.30;
  parameter Base.Time Td0p=7;
  Base.Voltage Eqp(start=1);
equation
  // Transient EMF equation
  Td0p*der(Eqp) = Efd - Eqp + id*(xd - xdp);
  // stator equations
  vd = -ra*id - xq*iq;
  vq = Eqp + xdp*id - ra*iq;
  // electrical power
  Pe = Eqp*iq + (xdp - xq)*id*iq;
end DetGen3;
```

Also `DetGen3` is declared as a partial class since it does not contain equations for the governor and excitation system. These are provided in the instantiable class `GovExc3rdGen` which contains models of the governor and excitation system.

```
model GovExc3rdGen
  extends Partial.DetGen3;
  replaceable Controllers.ConstPm Gov;
  replaceable Controllers.ConstEfd Exc;
equation
  // connection equations for governor and exciter
  Gov.u = w;
  Pm = Gov.y;
  Exc.u1 = sqrt(vd^2 + vq^2);
  Exc.u2 = w - Base.wref;
  Efd = Exc.y;
  // initialization
```

```

when initial() then
  reinit(w, Base.wref);
  reinit(delta, atan2(T.vb-ra*T.ib-xq*T.ia,
                    1.0+T.va-ra*T.ia+xq*T.ib));
  reinit(id, -(-sin(delta)*T.ia+cos(delta)*T.ib));
  reinit(iq, -(cos(delta)*T.ia+sin(delta)*T.ib));
  reinit(Eqp, (Pg+ra*(id^2+iq^2)-
              id*iq*xdp+id*iq*xq)/iq);
  reinit(Gov.Pm0, Pg + ra*(id^2 + iq^2));
  reinit(Exc.Ef0, (Pg+ra*(id^2+iq^2)+
                 id*iq*xq-id*xd*iq)/iq);
  reinit(Exc.Vref, V + Exc.Ef0/Exc.K);
end when;
end GovExc3rdGen;

```

This model also contains equations for the initialization of the generator dynamic states from the values given by the `Pin` variables. The values of the `Pin` variables are automatically calculated in the initialization that precedes every simulation. Since the governor and exciter models have been declared using the modifier `replaceable`, they can be replaced for models taken from a controller library or for user-defined models in instantiations of the `GovExc3rdGen` class.

F.3 Extending the Library

The goal has been to provide a framework with the basic models necessary for power system stability studies. However, such a library can never be complete and users can create their own models inheriting from the (partial) base classes and providing the equations given below:

- Generic current injector models `OnePin` and `TwoPin`—equations for the real and imaginary currents or voltages of each connector (`Pin`).
- Loads—equations for active and reactive load.
- Generators—equations for active and reactive production.
- Governing and excitation systems—equations for the mechanical shaft power or the field voltage must be given, respectively.

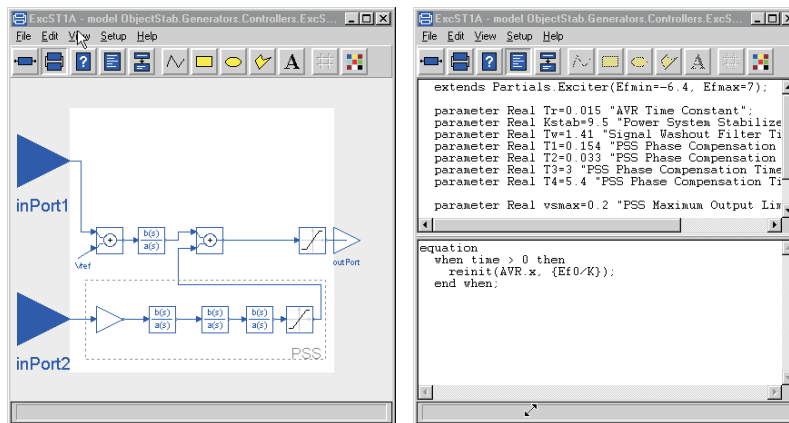


Figure F.1: Diagram and equation windows for the IEEE ST1A Excitation system model (Kundur, 1994).

The equations in user-defined models can be defined by block diagrams, state graphs or differential or algebraic equations. Internal dynamic states in user-defined models should be initialized from their terminal variables, similarly to the generator model in Section F.2.2.

F.3.1 Extension Example: Exciter IEEE ST1A

New exciter models can be constructed by creating a new class that inherits from the partial class `Exciter`. This partial class contains the declarations necessary for communication with the generator models and calculation of the initial values of the field voltage and voltage reference. The block diagram can then be drawn using components from the Modelica standard block libraries as shown in Figure F.1 (left), or alternatively, the corresponding differential or algebraic equations can be entered in the equation window of the new model. The design of new governor system is analogous. Note that also initialization equations for dynamic blocks which at the start of the simulation have nonzero output must be given as shown in Figure F.1 (right).

F.4 Case Study: Four-Generator Test System

The following steps must be carried out to simulate a power system using the `ObjectStab` library and the `Dymola` simulator:

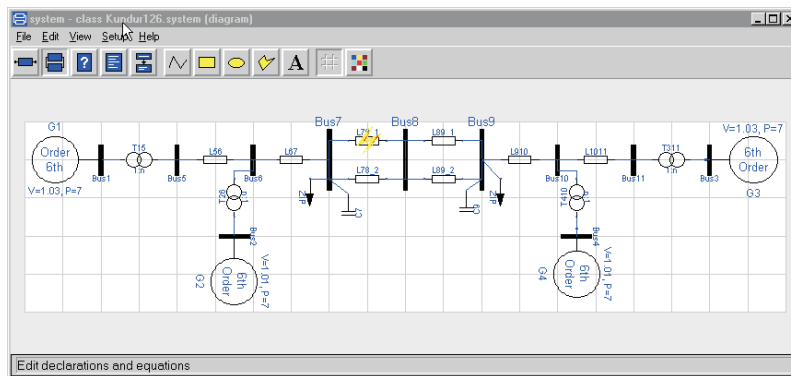


Figure F.2: The four-generator test system from Kundur (1994).

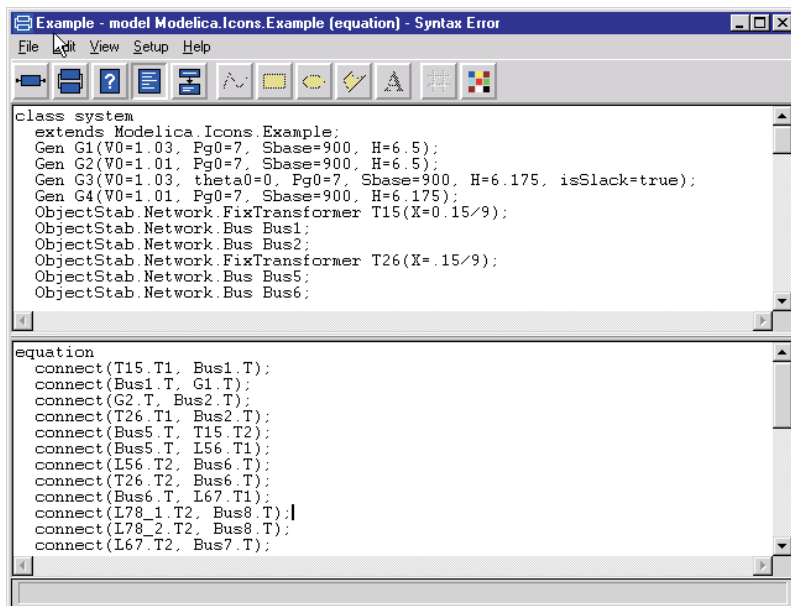


Figure F.3: Textual representation of the four-generator test system.

1. Create a new model window, and make the system model a subclass of `ObjectStab.Base.System`.
2. Draw the power system in the model window as shown in Figure F.2 using the graphical model editor. New components are created by dragging them from a library window into the model window. By double-clicking on a component in the model window, a dialog window appears and the parameters can be entered.
3. Compile the model by choosing 'Translate' in the 'File' menu of the model editor.
4. Simulate the system by choosing 'Simulate' from the 'Simulation' menu of the simulator window. If desired, parameter values can be adjusted using a dialog window prior to starting the simulation.

As an alternative to steps 1-2, the model can be entered in the textual format illustrated in Figure F.3. If the system is built using the graphical editor, parameter values are entered using dialog windows and the corresponding textual representation is automatically generated. Figure F.2 shows the graphical display of the four-generator test system (Kundur, 1994) used for validation of the library. Figure F.4 shows simulation results obtained using the **ObjectStab** library and results from simulation results obtained using Eurostag (Deuse and Stubbe, 1993). At simulation time 2 s, a ground fault occurs close to bus 7. The faulted line is disconnected at both ends at 2.07 s, and later at 3.5 s the fault has cleared and the line is reconnected. In the figure we can see that there is a near-perfect agreement between the results of the two programs.

F.5 Further Work

The current version (4.1) of the Dymola simulator does not exploit the sparse structure of the differential-algebraic equation system that results from a large power system model. The simulation of large systems is therefore very slow with Dymola compared to domain-specific tools such as PSS/E or Eurostag. As an example, the simulation of a ground fault with the four node system takes about 10 s with Eurostag and 15 s with Dymola on a 150 MHz SUN UltraSparc, which is comparable. The corresponding times for the same simulation with the Nordic 32 test system (CIGRE, 1995b), which contains 41 buses and 23

generators, are 20 s with Eurostag and 1330 s with Dymola. Thus, Dymola is a factor 66 slower than Eurostag on the large test system. Integration algorithms using sparse matrix techniques may be included in a later version of Dymola and will hopefully make the simulation times comparable with industrial-grade tools even for large systems. Currently, the generator and transformer models do not contain saturation modelling. This may be included in a later version of the library.

F.6 How To Get ObjectStab Running

The **ObjectStab** library was constructed for use with the simulation tool Dymola, which runs on Microsoft Windows as well as SUN Solaris and Linux platforms. In addition to the component models, the library includes models of the four-generator test system used in this paper and the Nordic 32 test system from CIGRE (1995b). A demo version of Dymola for Windows can be downloaded from the Dynasim website¹. The library itself can be downloaded from the **ObjectStab** website², and is free for educational use.

F.7 Conclusions

A component library called **ObjectStab** for power system transient and voltage stability simulations has been presented. Using the library, users can quickly enter their power system in one-line diagram form using a graphical editor, without having to type cryptic data files in text format or entering parameter data in countless dialog windows. The library has an open structure and all models can be modified or extended using various Modelica constructs, such as state machines, block diagrams or plain algebraic or differential equations. The models also have reasonable default parameter values defined such that users can play around with the models even before they have full understanding of the meaning of all system parameters. It is primarily intended as an educational tool, which can be used to experiment with and observe the effect of the different levels of modelling or trying out new types of controllers. Because of some drawbacks described in Section F.5 it cannot yet compete with special-purpose tools such as Eurostag in terms of computational efficiency, and is therefore at present most suitable for analysis of small systems.

¹<http://www.dynasim.se/>

²<http://www.iea.lth.se/~ielmatsl/ObjectStab/>

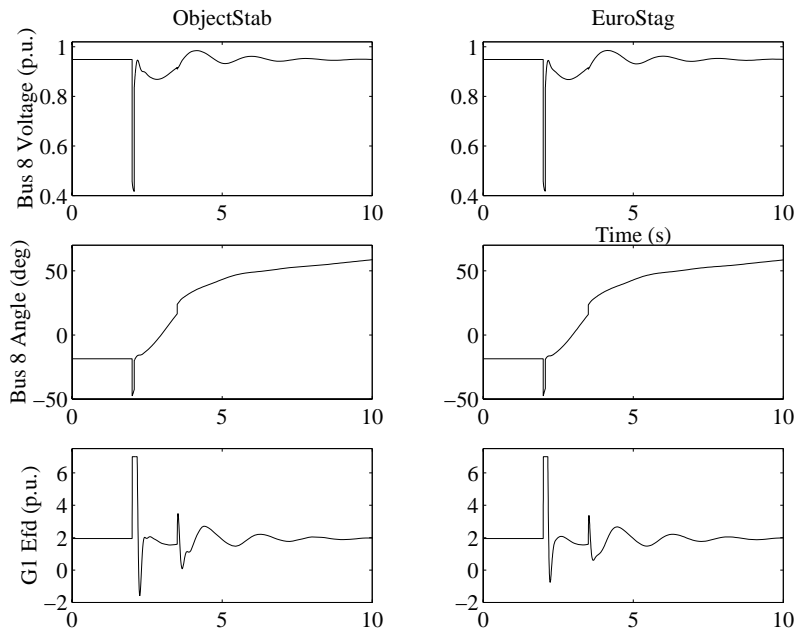


Figure F.4: Simulation results obtained using the **ObjectStab** library and Eurostag.

F.8 Acknowledgements

Parts of the library are based on models developed in a master's project (Romero Navarro, 1999). A special thank goes to Inés Romero Navarro for her dedicated work in the masters project. Also, the contributions from Professor Gustaf Olsson and the financial support from the Sydkraft Research Foundation are gratefully acknowledged. Thanks also to the development crew at Dynasim AB, especially Hans Olsson and Sven-Erik Mattsson for modelling help and quick bug fixes.

Part III

Bibliography

Bibliography

- Abe, S., Fukunaga, Y., Isono, A. and Kondo, B. (1982). Power system voltage stability. *IEEE Transactions on Power Apparatus and Systems*, vol. PAS-101, no. 10, pp. 3830–40.
- Abed, A. (1999). WSCC voltage stability criteria, undervoltage load shedding strategy, and reactive power reserve monitoring methodology. In *Power Engineering Society Summer Meeting*, vol. 1, pp. 191–7. IEEE.
- Altsjö, K. (1993). *Modellering av spänningsregulator för lindningskopplare*. Master's thesis, Electrical and Computer Engineering, Chalmers Institute of Technology, Sweden. Examensarbete 92/93:02 (in Swedish).
- Amin, M. (2000). Modeling and control of electric power systems and markets. *IEEE Control Systems Magazine*, vol. 20, no. 4, pp. 20–4.
- Arnborg, S. (1997). *Emergency Control of Power Systems in Voltage Unstable Conditions*. Ph.D. thesis, Royal Institute of Technology, Sweden.
- Arnborg, S., Andersson, G., Hill, D. J. and Hiskens, I. A. (1998). On influence of load modelling for undervoltage load shedding studies. *IEEE Transactions on Power Systems*, vol. 13, no. 2, pp. 395–400.
- Bachmann, B. and Wiesmann, H.-J. (2000). Advanced modeling of electromagnetic transients in power systems. *Modelica Workshop 2000, Lund University, Lund, Sweden*.
- Balanathan, R., Pahalawaththa, N. C. and Annakkage, U. D. (1998a). A strategy for undervoltage load shedding in power systems. In *POWERCON '98*, vol. 2, pp. 1494–8. IEEE.

- Balanathan, R., Pahalawaththa, N. C., Annakkage, U. D. and Sharp, P. W. (1998b). Undervoltage load shedding to avoid voltage instability. *IEEE Proceedings Generation, Transmission and Distribution*, vol. 145, no. 2, pp. 175–81.
- Bauer, P. and de Haan, S. W. H. (1998). Electronic tap changer for 500 kva/10 kv distribution transformers: design, experimental results and impact in distribution networks. In *Conference Record of 1998 Industry Applications Conference*, vol. 2, pp. 1530–7. IEEE.
- Berizzi, A., Finazzi, P., Dosi, D., Marannino, P. and Corsi, S. (1998). First and second order methods for voltage collapse assessment and security enhancement. *IEEE Transactions on Power Systems*, vol. 13, no. 2, pp. 543–51.
- Borghetti, A., Caldon, R., Mari, A. and Nucci, C. A. (1997). On dynamic load models for voltage stability studies. *IEEE Transactions on Power Systems*, vol. 12, no. 1, pp. 293–303.
- Breuker, D. (1998). *Memory versus Search in Games*. Ph.D. thesis, Department of Computer Science, Maastricht University, The Netherlands.
- Cañizares, C. A., De Souza, A. C. Z. and Quintana, V. (1996). Comparison of performance indices for detection of proximity to voltage collapse. *IEEE Transactions on Power Systems*, vol. 11, no. 3, pp. 1441–1450.
- Ćalović, M. S. (1984). Modelling and analysis of under-load tap-changing transformer control system. *IEEE Transactions on Power Apparatus and Systems*, vol. PAS-103, no. 7, pp. 1909–15.
- Campbell, M. (1999). Knowledge discovery in Deep Blue. *Communications of the ACM*, vol. 42, no. 11, pp. 65–67.
- Carbone, F., Castellano, G. and Moreschini, G. (1996). Coordination and control of tap changers under load at different voltage level transformers. In *MELECON '96*, vol. 3, pp. 1646–8. IEEE.
- Carpentier, J. (1962). Contribution a l'étude de dispatching économique. *Bulletin de la Société Française des Electriciens*, vol. 3, pp. 431–337. (in French).

- Chang, C. S. and Huang, J. S. (1999). Centralized control of transformer tap changing for voltage stability enhancement. *Electric Machines And Power Systems*, vol. 27, no. 10, pp. 1041–54.
- Chang, C. S. and Hui, K. C. (1988). Electrical power system dynamic stability evaluation using a knowledge-based approach. In *Proceedings of the 1988 IEEE International Conference on Systems, Man, and Cybernetics*, vol. 2, pp. 1384–8. IEEE.
- Cheng, S. J., Malik, O. P. and Hope, G. S. (1988). An expert system for voltage and reactive power control of a power system. *IEEE Transactions on Power Systems*, vol. 3, no. 4, pp. 1449–55.
- Chow, J. H. and Cheung, K. W. (1992). A toolbox for power system dynamics and control engineering education and research. *IEEE Transactions on Power Systems*, vol. 7, no. 4, pp. 1559–64.
- CIGRE (1995a). *Indices predicting voltage collapse including dynamic phenomena*. Tech. rep., CIGRE Task Force 38.02.11.
- CIGRE (1995b). *Long Term Dynamics Phase II*. Tech. rep., CIGRE Task Force 38.02.08.
- CIGRE (1998). *Protection against Voltage Collapse*. Tech. rep., CIGRE Task Force 34.08.
- CIGRE (2000). *System Protection Schemes in Power Networks*. Tech. rep., CIGRE Task Force 38.02.19. (final draft).
- Cooke, G. H. and Williams, K. T. (1992). New thyristor assisted diverter switch for on load transformer tap changers. *IEE Proceedings-Electric Power Applications*, vol. 139, no. 6, pp. 507–11.
- Corsi, S. (2000). The secondary voltage regulation in Italy. In *Power Engineering Society Winter Meeting*, vol. 1, pp. 296–304. IEEE.
- Deuse, J. and Stubbe, M. (1993). Dynamic simulation of voltage collapses. *IEEE Transactions on Power Systems*, vol. 8, no. 3, pp. 894–904.
- Dommel, H. W. and Tinney, W. F. (1968). Optimal power flow solutions. *IEEE Transactions on Power Apparatus and Systems*, vol. PAS-87, no. 10, pp. 1866–76.

- Dovan, T., Dillon, T. S., Berger, C. S. and Forward, K. E. (1987). A micro-computer based on-line identification approach to power system dynamic load modelling. *IEEE Transactions on Power Systems*, vol. PWRS-2, no. 3, pp. 529–536.
- Elmqvist, H., Brück, D. and Otter, M. (2000). *Dymola, Users Manual*. Dynasim AB, Sweden. <http://www.dynasim.se>.
- Feng, Z., Ajjarapu, V. and Maratukulam, D. J. (1998). A practical minimum load shedding strategy to mitigate voltage collapse. *IEEE Transactions on Power Systems*, vol. 13, no. 4, pp. 1285–90.
- Gao, B., Morison, G. K. and Kundur, P. (1992). Voltage stability evaluation using modal analysis. *IEEE Transactions on Power Systems*, vol. 7, no. 4, pp. 1529–42.
- Garcia, C. E., Prett, D. M. and Morari, M. (1989). Model predictive control: theory and practice—a survey. *Automatica*, vol. 25, no. 3, pp. 335–48.
- Ginsberg, M. L. and Harvey, W. D. (1992). Iterative broadening. *Artificial Intelligence*, vol. 55, no. 2–3, pp. 367–83.
- Glover, J. D. and Sarma, M. (1994). *Power System Analysis and Design*. PWS Publishing Company. ISBN 0-53493-960-0.
- Godart, T. F. and Puttgen, H. B. (1991). A reactive path concept applied within a voltage control expert system. *IEEE Transactions on Power Systems*, vol. 6, no. 2, pp. 787–93.
- Gomez, A., Martinez, J. L. et al. (1996). Benefits of using an operational tool for reactive power scheduling. In *Proceedings 12th Power Systems Computation Conference, Dresden, Germany*.
- Grainger, J. J. and Civanlar, S. (1985). volt/var control on distributions systems with lateral branches using shunt capacitors and voltage regulators: Parts I–III. *IEEE Transactions on Power Apparatus and Systems*, vol. PAS-104, no. 11, pp. 3287–97.
- Granville, S., Mello, J. C. O. and Melo, A. C. G. (1996). Application of interior point methods to power flow unsolvability. *IEEE Transactions on Power Systems*, vol. 11, no. 2, pp. 1096–103.

- Hamilton, S. and Garber, L. (1997). Deep Blue's hardware-software synergy. *Computer*, vol. 30, no. 10, pp. 29–35. Discussion by J. Wilson.
- Häring, H. (1995). Developments of on-load tapchangers: Current experience and future. In *European Seminar on On-load tap changers current experience and future developments*, pp. 2/1–2/5. IEE.
- Harsan, H., Hadjsaid, N. and Pruvot, P. (1997). Cyclic security analysis for security constrained optimal power flow. *IEEE Transactions on Power Systems*, vol. 13, no. 2, pp. 948–53.
- Hiskens, I. A. and Hill, D. J. (1993). Dynamic interaction between tapping transformers. In *Proceedings of 11th Power Systems Computation Conference, Avignon, France*.
- Hiyama, T., Fujimoto, Y. and Hayashi, J. (1999). Matlab/Simulink based transient stability simulation of electric power systems. In *Power Engineering Society Winter Meeting*, vol. 1, pp. 249–53. IEEE.
- Hsu, F.-H. (1999). IBM's Deep Blue chess grandmaster chips. *IEEE Micro*, vol. 19, no. 2, pp. 70–81.
- Hsu, J. C. and Meyer, A. U. (1968). *Modern Control Principles and Applications*. Mc-Graw Hill.
- IEEE (1995). Standard load models for power flow and dynamic performance simulation. *IEEE Transactions on Power Systems*, vol. 10, no. 3, pp. 1302–1313.
- Ilic, M. D., Liu, X., Leung, G., Athans, M., Vialas, C. and Pruvot, P. (1995). Improved secondary and new tertiary voltage control. *IEEE Transactions on Power Systems*, vol. 10, no. 4, pp. 1851–62.
- Engelsson, B., Lindström, P.-O., Karlsson, D., Runvik, G. and Sjödin, J.-O. (1997). Wide-area protection against voltage collapse. *IEEE Computer Applications in Power*, vol. 10, no. 4, pp. 30–5.
- Janssens, N. (1993). Tertiary and secondary voltage control for the Belgian HV system. In *Colloquium on International Practices in Reactive Power Control*, pp. 8/1–4. IEE, London, UK.

- Jantzen, J. (1991). *Fuzzy Control*. Technical University of Denmark. Publ. no. 9109.
- Johansson, S. G. (1999). Mitigation of voltage collapse caused by armature current protection. *IEEE Transactions on Power Systems*, vol. 14, no. 2, pp. 591–9.
- Johansson, S. G. and Daalder, J. E. (1997). Maximum thermal utilization of generator rotors to avoid voltage collapse. In *IPEC '97. Proceedings of the International Power Engineering Conference.*, vol. 1, pp. 234–9. Nanyang Technol. Univ, Singapore.
- Ju, P., Handschin, E. and Karlsson, D. (1996). Nonlinear dynamic load modelling: model and parameter estimation. *IEEE Transactions on Power Systems*, vol. 11, no. 4, pp. 1689–1697.
- Junghanns, A. (1999). *Pushing the Limits: New Developments in Single-Agent Search*. Ph.D. thesis, Department of Computing Science, University of Alberta, Canada.
- Kahlil, H. K. (1992). *Nonlinear Systems*. Macmillan Publishing Company. ISBN 0-02-946336-X.
- Karlsson, D. (1992). *Voltage Stability Simulations using Detailed Models Based on Field Measurements*. Ph.D. thesis, Electrical and Computer Engineering, Chalmers Institute of Technology, Sweden. Tech. Report no. 230.
- Karlsson, D. (1993). *Kaskadkopplade llningskopplare, inledande registreringar*. Tech. rep. Internal Report PTS-9309-62, Sydkraft AB, Malmö, Sweden (in Swedish).
- Karlsson, D. and Hill, D. J. (1994). Modelling and identification of nonlinear dynamic loads in power systems. *IEEE Transactions on Power Systems*, vol. 9, no. 1, pp. 157–63.
- Kolluri, S., Tinnium, K. and Stephens, M. (2000). Design and operating experience with fast acting load shedding scheme in the Entergy system to prevent voltage collapse. In *Power Engineering Society Winter Meeting*, vol. 2, pp. 1489–94. IEEE.

- Kundur, P. (1994). *Power System Stability and Control*. Power System Engineering Series. McGraw-Hill, New York. ISBN 0-07-035958-X.
- Lai, L. L. (1988). Development of an expert system for power system protection coordination. In *Fourth International Conference on Developments in Power Protection.*, pp. 310–4. IEEE.
- Lakervi, E. and Holmes, E. J. (1989). *Electricity Distribution Network Design*. Peregrinus Books. ISBN 0-86341-309-9.
- Larsson, M. (1997). *Coordinated Tap Changer Control - Theory and Practice*. No. ISBN 91-88934-07-1. Department of Industrial Electrical Engineering and Automation, Lund University, Sweden. Licentiate Thesis.
- Larsson, M. (1999). Emergency state voltage control using a tree search method. In *Power Engineering Society Summer Meeting*, vol. 2, pp. 1312–17. IEEE.
- Larsson, M. (2000a). A Modelica library for power system stability studies. *Modelica Workshop 2000, Lund University, Lund, Sweden*.
- Larsson, M. (2000b). Thesis website. <http://www.iea.lth.se/~ielmatsl/Publications/thesis.html>.
- Larsson, M., Hill, D. J. and Olsson, G. (2000). Emergency voltage control using search and predictive control. *Accepted by International Journal of Power and Energy Systems.*
- Larsson, M. and Karlsson, D. (1995). Coordinated control of cascaded tap changers in a radial distribution network. In *Stockholm Power Tech International Symposium on Electric Power Engineering*, vol. 5, pp. 686–91. IEEE.
- Larsson, M., Popović, D. H. and Hill, D. J. (1998). Limit cycles in power systems due to OLTC deadbands and load-voltage dynamics. *Electric Power Systems Research*, vol. 47, no. 32, pp. 181–8.
- Larsson, T., Innanen, R. and Norstrom, G. (1997). Static electronic tap-changer for fast phase voltage control. In *International Electric Machines and Drives Conference Record*, pp. 4.1–3. IEEE.

- le Dous, G. (1999). *Voltage Stability in Power Systems - Load Modelling based on 130 kV Field Measurements*. Tech. Rep. 324L, Chalmers University of Technology, Sweden. Licentiate Thesis.
- Löf, P.-A., Smed, T., Andersson, G. and Hill, D. J. (1992). Fast calculation of a voltage stability index. *IEEE Transactions on Power Systems*, vol. 7, no. 1, pp. 54–64.
- Lind, R. and Karlsson, D. (1996). Distribution system modelling for voltage stability studies. *IEEE Transactions on Power Systems*, vol. 11, no. 4, pp. 1677–82.
- Liu, C.-C. and Tomsovic, K. (1986). An expert system assisting decision-making of reactive power/voltage control. *IEEE Transactions on Power Systems*, vol. PWRS-1, no. 3, pp. 195–201.
- Liu, C.-C. and Vu, K. T. (1989). Analysis of tap-changer dynamics and construction of voltage stability regions. *IEEE Transactions on Power Systems*, vol. 36, no. 4, pp. 575–90.
- Liu, W.-H. E., Papalexopoulos, A. D. and Tinney, W. F. (1992). Discrete shunt controls in a newton optimal power flow. *IEEE Transactions on Power Systems*, vol. 7, no. 4, pp. 1509–16.
- Machowski, J., Bialek, J. W. and Bumby, J. R. (1997). *Power System Dynamics and Stability*. John Wiley, New York. ISBN 0471956430.
- Makarov, Y. V., Popović, D. H. and Hill, D. J. (1998). Stabilization of transient processes in power systems by an eigenvalue shift approach. *IEEE Transactions on Power Systems*, vol. 13, no. 2, pp. 382–8.
- Mattsson, S.-E. (1992). Modelling of power systems in Omola for transient stability studies. In *IEEE Symposium on Computer-Aided Control System Design*, pp. 30–6. IEEE.
- Mayne, D. Q., Rawlings, J. B., Rao, C. V. and Scaert, P. O. M. (2000). Constrained model predictive control: Stability and optimality. *Automatica*, vol. 36, no. 6, pp. 789–814.

- Medanić, J., Ilić-Spong, M. and Christensen, J. (1987). Discrete models of slow voltage dynamics for under load tap-changing transformer coordination. *IEEE Transactions on Power Systems*, vol. 2, no. 4, pp. 873–82.
- ModelicaDef (1999). *Modelica - A Unified Object-Oriented Language for Physical Systems Modeling, Language Specification*. Modelica Design Group. <http://www.modelica.org/documents.shtml>.
- ModelicaTut (1999). *Modelica - A Unified Object-Oriented Language for Physical Systems Modeling, Tutorial and Rationale*. Modelica Design Group. <http://www.modelica.org/documents.shtml>.
- Moors, C., Lefebvre, D. and Van Cutsem, T. (2000). Design of load shedding schemes against voltage instability. In *Power Engineering Society Winter Meeting*, vol. 2, pp. 1495–500. IEEE.
- Morari, M. and Lee, J. H. (1999). Model predictive control: past, present and future. *Computers & Chemical Engineering*, vol. 23, no. 4–5, pp. 667–82.
- Morelato, A. L. and Monticelli, A. J. (1989). Heuristic search approach to distribution system restoration. *IEEE Transactions on Power Delivery*, vol. 4, no. 4, pp. 2235–41.
- Nanba, M., Huang, Y., Kai, T. and Iwamoto, S. (1998). Studies on VIPI based control methods for improving voltage stability. *International Journal of Electrical Power & Energy Systems*, vol. 120, no. 2, pp. 141–6.
- Nord Pool (1999). Nord pool annual report. <http://www.nordpool.com/>.
- Nordel (1999). Nordel annual report. <http://www.nordel.org/>.
- Ohtsuki, H., Yokoyama, A. and Sekine, Y. (1991). Reverse action of on-load tap changer in association with voltage collapse. *IEEE Transactions on Power Systems*, vol. 6, no. 2, pp. 300–6.
- Overbye, T. J. and Klump, R. P. (1998). Determination of emergency power system voltage control actions. *IEEE Transactions on Power Systems*, vol. 13, no. 1, pp. 205–10.
- Pal, M. K. (1992). Voltage stability conditions considering load characteristics. *IEEE Transactions on Power Systems*, vol. 7, no. 1, pp. 243–9.

- Pal, M. K. (1995). Assessment of corrective measures for voltage stability considering load dynamics. *International Journal of Electrical Power & Energy Systems*, vol. 17, no. 5, pp. 325–34.
- Pessi, E., Gallanti, M. and Cicoria, R. (1990). SELF: an expert system application to power system planning. In *Tenth International Workshop. Expert Systems and their Applications. Specialized Conference: Artificial Intelligence and Electrical Engineering.*, pp. 217–31.
- Plaat, A. (1996). *Research Re: search & Re-search*. Ph.D. thesis, Erasmus University, Rotterdam, The Netherlands. Tinbergen Series no. 117.
- Popović, D. H., Hill, D. J. and Hiskens, I. A. (1996a). Oscillatory behaviour of power supply systems with single dynamic load. In *Proceedings 12th Power Systems Computation Conference, Dresden, Germany.*
- Popović, D. H., Hill, D. J. and Wu, Q. (1998). Coordinated static and dynamic voltage control in large power systems. In L. Fink and C. Vournas, eds., *Proceedings Bulk Power System Voltage Phenomena - IV: Restructuring*, pp. 391–405. Tech. Univ. Athens., Greece.
- Popović, D. H., Hiskens, I. A. and Hill, D. J. (1996b). Investigations of load-tap changer interaction. *International Journal of Electrical Power and Energy Systems*, vol. 18, no. 2, pp. 81–97.
- Popović, D. S., Levi, V. A. and Gorecan, Z. A. (1997). Co-ordination of emergency secondary-voltage control and load shedding to prevent voltage instability. *IEE Proceedings. Generation, Transmission & Distribution*, vol. 144, no. 3, pp. 293–300.
- Ramos, J. L. M., Exposito, A. G., Cerezo, J. C., Ruiz, E. M. and Salinas, F. C. (1995). A hybrid tool to assist the operator in reactive power/voltage control and optimization. *IEEE Transactions on Power Systems*, vol. 10, no. 2, pp. 760–8.
- Romero Navarro, I. (1999). *Object-oriented Modelling and Simulation of Power Systems using DYMOLA*. Master's thesis, Department of Industrial Electrical Engineering and Automation, Lund University.

- Roytelman, I. and Ganesan, V. (2000). Coordinated local and centralized control in distribution management systems. *IEEE Transactions on Power Delivery*, vol. 15, no. 2, pp. 718–24.
- Roytelman, I., Wee, B. K. and Lugtu, R. L. (1995). Volt/var control algorithm for modern distribution management system. *IEEE Transactions on Power Systems*, vol. 10, no. 3, pp. 1454–60.
- Roytelman, I., Wee, B. K., Lugtu, R. L., Kalas, T. M. and Brossart, T. (1998). Pilot project to estimate the centralized volt/var control effectiveness. *IEEE Transactions on Power Systems*, vol. 13, no. 3, pp. 864–9.
- Russell, S. J. and Norvig, P. (1995). *Artificial Intelligence - A Modern Approach*. Prentice-Hall. ISBN 0-13-360124-2.
- Sahba, M. (1988). A method for plausibility checks and data validation in power systems. *IEEE Transactions on Power Systems*, vol. 3, no. 1, pp. 267–71.
- Samuelsson, O. (2000). *Wide Area Measurements of Power System Dynamics*. Tech. Rep. 99:50, Elforsk, Sweden.
- Sancha, J. L., Fernandez, J. L., Cortes, A. and T, A. J. (1996). Secondary voltage control: analysis, solutions and simulation results for the spanish transmission system. *IEEE Transactions on Power Systems*, vol. 11, no. 2, pp. 630–8.
- Sauer, P. W. and Pai, M. A. (1994). A comparison of discrete vs. continuous dynamic models of tap-changing-under-load transformers. In *Proceedings Bulk Power System Voltage Phenomena - III : Voltage Stability, Security and Control, Davos, Switzerland*.
- Schaeffer, J. and Plaat, A. (2000). Unifying single-agent and two-player search. In H. Hamilton, ed., *AI'00: Advances in Artificial Intelligence*, pp. 1–12. Springer-Verlag.
- Shannon, C. E. (1950). Programming a computer for playing chess. *Philosophical Magazine*, vol. 41, no. 314, pp. 256–75. Reprinted in: Claude Elwood Shannon collected papers edited by N.J.A. Sloane, Aaron D. Wyner, IEEE Press, ISBN 0-7803-0434-9.

- Shuttleworth, R., Tian, X., Fan, C. and Power, A. (1996). New tap changing scheme. *IEE Proceedings-Electric Power Applications*, vol. 143, no. 1, pp. 108–12.
- Spence, G. and Hall, A. C. (1995). On-load tap-changers current experience and future development: Users experience and perspective. In *European Seminar on On-load tap changers current experience and future developments*, pp. 1/1–1/7. IEE.
- SS 421 18 11 (1989). *Spänningsgodhet i lågspänningsnät för allmän distribution*. Tech. rep., Svenska Elektriska Kommissionen. (in Swedish).
- Stewart, B. S., Liaw, C.-F. and White III, C. C. (1994). A bibliography of heuristic search research through 1992. *IEEE Transactions on Systems, Man & Cybernetics*, vol. 24, no. 2, pp. 268–93.
- Sun, Y., Wang, Z. and Yao, X. (1999). Study on secondary voltage control of power system. *Automation of Electric Power Systems*, vol. 23, no. 9, pp. 9–14. (in Chinese).
- SVK (2000). *Effektbalansutvecklingen - Rapport till näringslivsdepartementet*. Tech. rep., Svenska Kraftnät. (in Swedish), <http://www.svk.se/>.
- Tamura, Y., Ogata, T., Motoyoshi, T., Tayama, Y. and Nakanishi, Y. (1989). Interactions between regulating equipments in voltage instability environment. In *Proceedings of the 28th Conference on Decision and Control*, vol. 1, pp. 326–31. IEEE.
- Taylor, C. W. (1994). *Power System Voltage Stability*. McGraw-Hill. ISBN 0-07-063184-0.
- Taylor, C. W. (2000a). Line drop compensation, high side voltage control, secondary voltage control- why not control a generator like a static var compensator. In *Power Engineering Society Summer Meeting*, vol. 1, pp. 307–10. IEEE.
- Taylor, C. W. (2000b). Minutes of preliminary meeting of Cigre TF 38.02.23 on coordinated voltage control in transmission networks, Seattle, USA.

- Tuan, T., Fandino, J., Hadjsaid, N., Sabonnadiere, J. and Vu, H. (1994). Emergency load shedding to avoid risks of voltage instability using indicators. *IEEE Transactions on Power Systems*, vol. 9, no. 1, pp. 341–51.
- Van Cutsem, T. (1995). An approach to corrective control of voltage instability using simulation and sensitivity. *IEEE Transactions on Power Systems*, vol. 10, no. 2, pp. 616–22.
- Van Cutsem, T. (2000). Voltage instability: phenomena, countermeasures, and analysis methods. *Proceedings of the IEEE*, vol. 88, no. 2, pp. 208–27.
- Van Cutsem, T. and Vournas, C. (1998). *Voltage Stability of Electric Power Systems*. Power Electronics and Power Systems Series. Kluwer Academic Publishers. ISBN 0-7923-8139-4.
- van den Bosch, P. P. J. and Honderd, G. (1985). A solution of the unit commitment problem via decomposition and dynamic programming (power systems). *IEEE Transactions on Power Apparatus and Systems*, vol. PAS-104, no. 7, pp. 1684–90.
- Vournas, C. D. and Van Cutsem, T. (1995). Voltage oscillations with cascaded load restoration. In *Stockholm Power Tech International Symposium on Electric Power Engineering*, vol. 5, pp. 173–8. IEEE.
- Vu, H., Pruvot, P., Launay, C. and Harmand, Y. (1996). An improved voltage control on large-scale power system. *IEEE Transactions on Power Systems*, vol. 11, no. 3, pp. 1295–1303.
- Vu, K., Begovic, M. M., Novosel, D. and Saha, M. M. (1997). Use of local measurements to estimate voltage-stability margin. In *20th International Conference on Power Industry Computer Applications*, pp. 318–323. IEEE.
- Vu, K. T. and Liu, C.-C. (1992). Shrinking stability regions and voltage collapse in power systems. *IEEE Transactions on Circuits & Systems I-Fundamental Theory & Applications*, vol. 39, no. 4, pp. 271–89.
- Vu, K. T., Liu, C.-C., Taylor, C. W. and Jimma, K. M. (1995). Voltage instability: mechanisms and control strategies. *Proceedings of the IEEE*, vol. 83, no. 11, pp. 1442–55.

- Walve, K. (1986). Modelling of power system components at severe disturbances. In *International Conference on Large High Voltage Electric Systems*, vol. 2, pp. 1–9. CIGRÉ.
- Wang, X., Ejebe, G. C., Tong, J. and Waight, J. G. (1998). Preventive/corrective control for voltage stability using direct interior point method. *IEEE Transactions on Power Systems*, vol. 13, no. 3, pp. 878–83.
- WSCC (1996). *Disturbance Report - For the Power System Outages that occurred on July 2 and July 3, 1996.* Tech. rep., Western Systems Coordinating Council, USA. <http://www.wsc.com>.
- Wu, J. S., Tomsovic, K. L. and Chen, C. S. (1991). A heuristic search approach to feeder switching operations for overload, faults, unbalanced flow and maintenance. *IEEE Transactions on Power Delivery*, vol. 6, no. 4, pp. 1579–86.
- Wu, Q., Popović, D. H. and Hill, D. J. (2000). Avoiding sustained oscillations in power systems with tap changing transformers. *International Journal of Electrical Power & Energy Systems*, vol. 22, no. 8, pp. 597–605.
- Wu, Q., Popović, D. H., Hill, D. J. and Larsson, M. (1999a). Tap changing dynamic models for power systems voltage behaviour analysis. In *1999 Power Systems Computation Conference, Trondheim, Norway*.
- Wu, Q., Popović, D. H., Hill, D. J. and Parker, C. J. (1999b). System security enhancement against voltage collapse via coordinated control. In *Power Engineering Society Winter Meeting*, vol. 1, pp. 755–60. IEEE.
- Xu, W. and Mansour, Y. (1994). Voltage stability analysis using generic dynamic load models. *IEEE Transactions on Power Systems*, vol. 9, no. 1, pp. 479–93.
- Xu, W., Vaahedi, E., Mansour, Y. and Tamby, J. (1997). Voltage stability load parameter determination from field tests on B.C. Hydro's system. *IEEE Transactions on Power Systems*, vol. 12, no. 3, pp. 1290–7.
- Yorino, N., Danyoshi, M. and Kitagawa, M. (1997). Interaction among multiple controls in tap change under load transformers. *IEEE Transactions on Power Systems*, vol. 12, no. 1, pp. 430–6.

- Yorino, N., Shuto, T., Nshimoto, H., Sasaki, H., Sugihara and Nakanishi, Y. (1999). A distributed autonomous control method for TCUL transformers using fuzzy adaptive control scheme. *Transactions of the Institute of Electrical Engineers of Japan*, vol. 119B, no. 12, pp. 1455–61. (in Japanese).
- Åström, K. J., Elmqvist, H. and Mattson, S. E. (1998). Evolution of continuous-time modeling and simulation. In *The 12th European Simulation Multiconference, ESM'98, June 16-19, 1998, Manchester, UK*.